Dissertation

zur Erlangung des Doktorgrades

der Naturwissenschaften

der Fakultät für Biologie

der Ludwig-Maximilian Universität München

Regulation of AMPA receptor function

and synaptic localization

by stargazin and PSD-95

vorgelegt von

Barbara Cokić

München, Februar 2009

Erstgutachter: Prof. Dr. Tobias Bonhoeffer

Zweitgutachter: Prof. Dr. Andreas Herz

Tag der mündlichen Prüfung: 30.03.2009

To my beloved family

Die vorliegende Arbeit wurde zwischen September 2005 und Januar 2009 unter der Leitung von Dr. Valentin Stein am Max-Planck Institut für Neurobiologie in Martinsried durchgeführt.

Ehrenwörtliche Versicherung:

Ich versichere hiermit ehrenwörtlich, dass ich die Dissertation mit dem Titel "Regulation of AMPA receptor function and synaptic localization by stargazin and PSD-95" selbständig und ohne unerlaubte Beihilfe angefertigt habe. Ich habe mich dabei keiner anderen als der von mir ausdrücklich bezeichneten Hilfen und Quellen bedient.

Erklärung:

Hiermit erkläre ich, dass ich mich nicht anderweitig einer Doktorprüfung ohne Erfolg unterzogen habe. Die Dissertation wurde in ihrer jetzigen oder ähnlichen Form bei keiner anderen Hochschule eingereicht und hat noch keinen sonstigen Prüfungszwecken gedient.

München, im Februar 2009

Barbara Cokic

Contents

Contents

xii

List of Figures

1 Summary

The majority of excitatory transmission in the brain is mediated by glutamatergic synapses. Rapid synaptic signaling is mediated by AMPA and kainate receptors, whereas NMDA receptors mediate slow synaptic currents. Pathophysiological activation of glutamatergic neurons can lead to excitotoxicity and neuronal death, for example in ischaemia and neurodegenerative disorders. Therefore, studying the structure and function of AMPA receptors is important for understanding general mechanisms of synaptic transmission as well as for the development of new therapies.

AMPA receptors are associated with auxiliary subunits called Transmembrane AMPA Receptor Regulatory Proteins (TARPs). The first identified member of this family was stargazin. Given the structural similarity to the $\gamma 1$ subunit of skeletal muscle voltage-gated Ca^{2+}-channels, stargazin is also called $\gamma 2$. The *stargazer* mouse is a spontaneous mutant that lacks AMPA receptors in granule cells of cerebellum and suffer from ataxia. In addition to stargazin, the family includes $\gamma 3$, $\gamma 4$ and $\gamma 8$. TARPs regulate all aspects of AMPA receptor function - from early steps of synthesis and trafficking to the cell surface, to synaptic localization and biophysical properties. TARPs interact with PSD-95, a main scaffolding protein of excitatory synapses that belongs to the Membrane-Associated Guanylate Kinases (MAGUK) family. Via this interaction AMPA receptors are localized to the synapse. PSD-95 clusters many other synaptic proteins and organizes signaling complexes in the synapse.

The goal of this thesis was to investigate the role of stargazin in regulating the antagonism of AMPA receptors. I focused on the commonly used antagonists CNQX, GYKI-53655 (GYKI) and CP-465,022 (CP) and explored how stargazin changes the inhibition of AMPA receptors by these drugs. The second goal was to assess the role of PSD-95 in synaptic function. More specifically, I aimed to investigate how an increased level of PSD-95 in a neuron affects AMPA and NMDA currents, as well as the presynaptic function of a neuron.

In the first part of my thesis I used the heterologous Xenopus oocyte expression system to express AMPA receptor subunits alone or with stargazin. Using the two-electrode voltage clamp, I measured the glutamate-evoked currents and obtained dose-response curves for CNQX, GYKI and CP. I found that stargazin decreases the affinity of GluR1 for CNQX, which was explained by the partial agonistic effect of CNQX in the presence of stargazin. In contrast, stargazin increases the affinity for GYKI, and has only a small effect on CP. I also tested the effect of stargazin on recently described GYKI-insensitive receptors and found that inhibition of these receptors is restored by co-expression with stargazin. My data strongly suggest that the identified residues do not constitute the full GYKI-binding site. I could also show that the ectodomain of stargazin controls the changes in antagonist sensitivity of the receptors.

In the second part of my thesis I used cultured hippocampal slices and Semliki Forest virus to overexpress PSD-95:GFP in CA1 region of hippocampus. I recorded simultaneously from a cell overexpressing PSD-95 and a neighboring control cell and compared their AMPA and NMDA currents. I confirmed the finding that overexpression of PSD-95 robustly increases currents mediated by AMPA receptors. In contrast to other studies, I observed that PSD-95 increases NMDA currents, although to smaller extent. I addressed the debated role of PSD-95 in regulating the presynatic release probability and found that overexpression of PSD-95 did not change glutamate release probability. Importantly, I observed that cells overexpressing PSD-95 have a lower rectification index of synaptic AMPA receptors, strongly suggesting that PSD-95 overexpression led to an increased fraction of AMPA receptors that lack GluR2 subunit.

In conclusion, the work presented in this thesis gives further insights into AMPA receptor physiology, both from the aspect of pharmacology and synaptic trafficking. The results of co-expression of stargazin with the previously described GYKI-insensitive GluR1 mutants strongly indicate that TARP interacts with the linker domains of AMPA receptors. This finding is of great importance for understanding the molecular mechanism of AMPA-TARP interaction. Furthermore, this thesis shows that PSD-95 regulates both AMPA and NMDA synaptic currents by increasing the number of synaptic receptors. In addition, my data suggest that PSD-95 enriches the number of GluR2-lacking receptors in the synapse. Given the Ca^{2+}-permeability of GluR2-lacking receptors and their implication in plasticity and

excitotoxicity, this finding is important for understanding how the synaptic localization of these receptors is regulated.

2 Abbreviations

2-ClAd	2-chloroadenosine
ABP	AMPA receptor-binding protein
ACSF	artificial cerebro-spinal fluid
APV	amino-5-phosphonopentanoate
AMPA	α-amino-3-hydroxyl-5-methyl-4-isoxazole-propionate
AMPA-R	AMPA receptor
BHK	baby hamster kidney
CA1	Cornu ammonis 1
CA3	Cornu ammonis 3
Cdk5	Cyclin-dependent kinase 5
CI	Ca^{2+}-impermeable
CNQX	6-cyano-7-nitroquinoxaline-2,3-dione
CNS	central nervous system
CP	Ca^{2+}-permeable
CP-465,022	3-(2-chloro-phenyl)-2-[2-(6-diethylaminomethyl-pyridin-2-yl) -vinyl]-6-fluoro-3H-quinazolin-4-one
CTZ	cyclothiazide
DIV	days in vitro
DMSO	dimethyl sufoxide
DNQX	6,7-dinitroquinoxaline-2,3-dione
EPSC	excitatory postsynaptic current
GFP	green fluorescent protein
GK	guanylate kinase
GRIP	glutamate receptor-interacting protein

GYKI-53655	1-(4-aminophyl)-4-methyl-7,8-methylendioxy-5H-2,3-benzodiazepine
LBD	ligand-binding domain
LTD	long-term depression
LTP	long-term potentiation
MAGUK	membrane-associated guanylate kinase
NBQX	2,3-dioxo-6-nitro-1,2,3,4-tetrahydrobenzo[f]quinoxaline-7-sulfonamide
NMDA	N-methyl-D-aspartate
NMDA-R	NMDA receptor
NSF	N-ethylmaleimide-sensitive factor
PDZ	PSD95/disc large/zona occludens 1
PEPA	4-[2-(phenylsulfonylamino)ethylthio]-2,6-difluorophenoxyacetamide
PICK1	protein interacting with C-kinase
PSD	postsynaptic density
PSD-93	postsynaptic density protein of 93 kDa
PSD-95	postsynaptic density protein of 95 kDa
SAP102	synapse-associated protein of 102 kDa
SAP97	synapse-associated protein of 97 kDa
SFV	Semliki Forest Virus
SH3	Src-homology 3
Stg	stargazin
TARP	transmembrane AMPA receptor regulatory proteins
TCM	trichlormethiazide
TEVC	two-electrode voltage clamp
TTX	tetrodotoxin

3 Introduction

The majority of excitatory synapses in the central nervous system (CNS) is glutamatergic. Glutamate acts on two classes of glutamate receptors: ionotropic and metabotropic. Ionotropic receptors are ligand-gated ion channels, whereas metabotropic receptors act by activating a second messenger cascade. The focus of this study will be on the ionotropic receptors. Ionotropic glutamate receptors are divided into three subfamilies: AMPA (α-amino-3-hydroxyl-5-methyl-4-isoxazole-propionate), NMDA (N-methyl-D-aspartate) and kainate receptors. All three receptor subfamilies are cation-channels, selective for Na^+ and K^+. Subpopulation of AMPA receptors, as well as all NMDA and kainate receptors are also permeable for Ca^{2+}. Rapid synaptic transmission is mediated by AMPA and kainate receptors. In contrast, NMDA receptors mediate slow synaptic currents and they are involved in initiation of some forms of synaptic plasticity. AMPA and NMDA receptors are discussed in more details in the following sections. Kainate receptors mediate synaptic responses only in some brain regions and they are not in the scope of this study.

This study is an effort to understand both the regulation of AMPA receptor biophysical properties and synaptic localization. Under normal physiological conditions the strength of a glutamatergic synapse is modulated to adapt to local or global changes in neuronal activity. This "plasticity" of the synapses can be expressed as a change in the receptor number and also receptor properties. In addition, pathophysiological activation of glutamatergic neurons can lead to a large increase in intracellular Ca^{2+}, excitotoxicity and neuronal death, for example in ischaemia and neurodegenerative disorders. Taken together, there is growing interest in understanding the AMPA receptor pharmacology.

3.1 Excitatory synapses

Chemical synapses are functional connections between neurons. The information is passed uni-directionally from a presynaptic cell to a postsynaptic cell and therefore the chemical synapses are asymmetric in structure and function. The presynaptic terminal, or synaptic bouton, is a specialized area within the axon that contains synaptic vesicles filled with neurotransmitter. Juxtaposed to the presynapse is a region of the postsynaptic cell containing neurotransmitter receptors. In excitatory synapses the receptors are often found in specialized protrusions from the dendrites called dendritic spines.
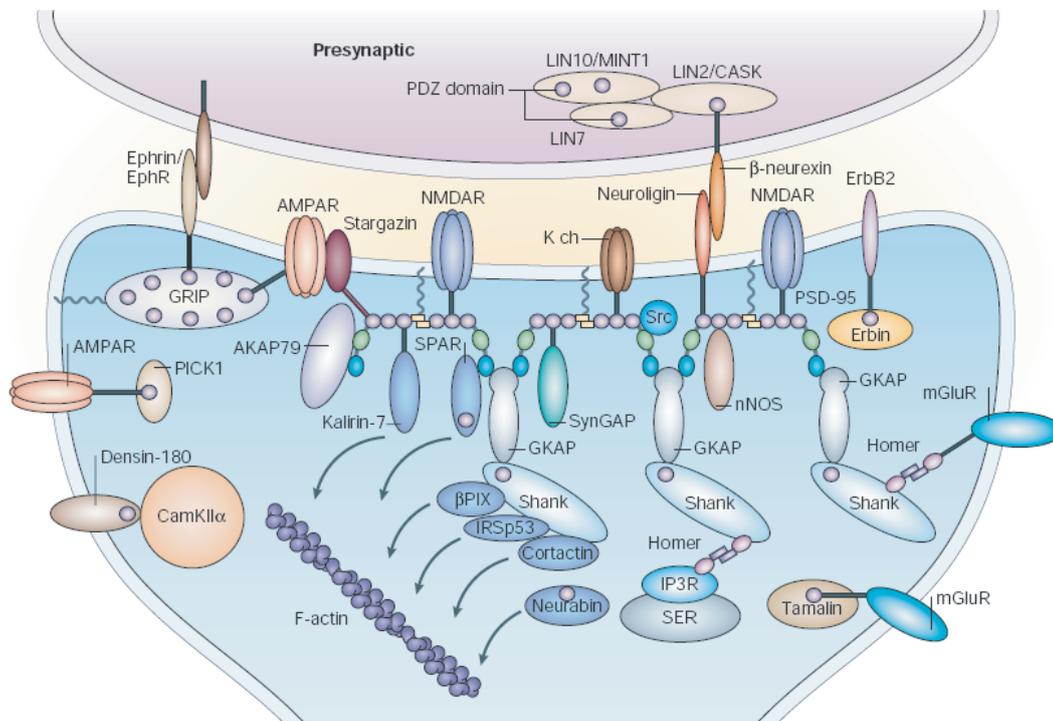
Figure 3.1: Mammalian excitatory synapse with a focus on the postsynaptic side. Cytoplasmic C-terminal tails of proteins are indicated by black lines. Adopted from (Kim and Sheng, 2004).

An excitatory synapse is a synapse in which an action potential in the presynaptic cell increases the probability of an action potential occurring in the postsynaptic cell. Activation of the postsynaptic receptors generates excitatory postsynaptic currents (EPSCs), a depolarization of the postsynaptic membrane caused by the flow of positively charged ions into

the cell.

A scheme of a glutamatergic synapse is given in figure 3.1, illustrating the complexity of proteins that take part in synaptic function. AMPA and NMDA receptors are localized in the postsynaptic membrane and they mediate glutamate binding. AMPA receptors have associated auxiliary subunits, transmembrane proteins of the TARP family with stargazin being the first member identified. TARPs are discussed in more details in a following section. Beside AMPA and NMDA receptors, other channels and transmembrane proteins are localized in the postsynaptic membrane that are involved in different aspects of regulation of synaptic function.

On the intracellular side of the postsynaptic membrane is a complex of interlinked proteins called the postsynaptic density (PSD). Proteins of the PSD are involved in trafficking and localization of synaptic receptors and also in organizing the postsynaptic signaling pathways. They are cytoplasmic proteins often containing multiple PDZ (PSD95/disc large/zona occludens 1) domains. The main scaffolding protein of the excitatory synapses is PSD-95. PSD-95 is a PDZ protein that belongs to the MAGUK family, which is the subject of another section of the Introduction.

3.2 AMPA receptors

Structure. AMPA receptors are tetrameric complexes composed of four different subunits, GluR1-4 (Hollmann and Heinemann, 1994). Each subunit has three transmembrane domains and one re-entrant loop (Fig. 3.3A). These loops form the pore of the receptor. The extracellular domains of the receptor form a ligand-binding domain (LBD), a clamshell-like structure containing the glutamate binding sites.

AMPA receptor subunits are alternatively spliced in a region preceding the fourth membrane domain, giving flip and flop splice variants of each subunit (Sommer et al., 1990). This region regulates some of the receptor properties, e.g. the flop versions desensitize and deactivate more rapidly than the flip versions (Mosbacher et al., 1994). Flip and flop splice variants affect also AMPA receptor trafficking, with flop isoforms being largely retained in endoplasmic reticulum (Coleman et al., 2006). These two splice variants are differentially expressed. Adult pyramidal CA1 neurons of hippocampus express mainly flop variants,

whereas flip isoforms dominate prior to birth (Monyer et al., 1991).

An interesting finding followed the AMPA receptor subunits cloning: the genomic GluR2 subunit sequence was different from the GluR2 cDNA sequence in a single amino acid in the pore region (Sommer et al., 1991). Namely, the GluR2 subunit is edited on RNA level in the pore domain: glutamine at position 607 is edited into arginine (Q/R editing site). All the other subunits have unchanged glutamine at this position. Edited GluR2 subunits are largely unassembled and retained in endoplasmatic reticulum, whereas GluR1 and GluR2Q subunits readily tetramerize (Greger et al., 2002; Greger et al., 2003). These effects on tetramerization and retention in the ER ensure that GluR2 subunit is available for co-assembly with other subunits.
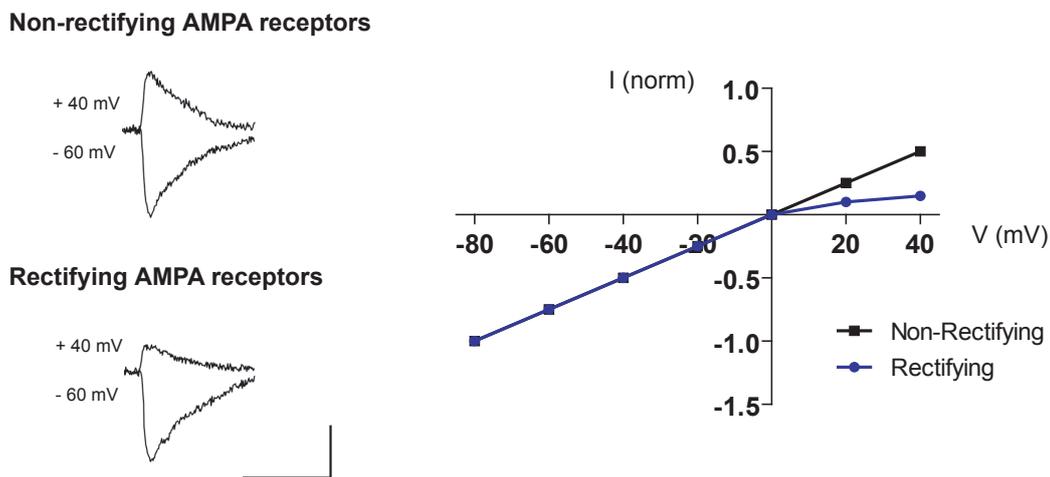
Figure 3.2: Traces of mean evoked AMPA currents recorded at -60 mV and +40 mV mediated by rectifying and non-rectifying AMPA receptors (left). Scale bars: 40 pA, 25 ms. The current traces are taken from (Steiner et al., 2005). I-V curve of rectifying receptors show smaller currents at positive voltages compared to non-rectifying receptors (right).

RNA editing of GluR2 has a large impact on AMPA receptor function. The presence of edited GluR2 subunit controls the biophysical properties of the receptors, such as Ca^{2+}-impermeability and linear current-voltage (I-V) curve. GluR2-lacking receptors are Ca^{2+}-permeable, have high single-channel conductance and are blocked by endogenous polyamines at positive voltages and therefore exhibiting inwardly rectifying I-V relationship. The example of I-V curves of GluR2-containing (non-rectifying) and Glu2-lacking (rectifying) receptors

are shown in figure 3.2. Rectifying receptors allow only small outward current due to the polyamine block at positive voltages.

AMPA receptors can be subdivided into two groups based on their cytoplasmic tail: GluR2 and GluR3 have short cytoplasmic domain whereas GluR1 and GluR4 have long cytoplasmic domain. The C-terminus of each subunit interacts with specific cytoplasmic proteins, many of which are proteins with multiple PDZ domains. For example, GluR1 interacts with SAP97 (synapse-associated protein of 97 kDa), the only member of MAGUK family shown to interact directly with AMPA receptors (Leonard et al., 1998). GluR2 and GluR3 interact with GRIP (glutamate receptor-interacting protein), ABP (AMPA receptor-binding protein) and PICK1 (protein interacting with C-kinase). In addition to the PDZ proteins, cytoplasmic tail of GluR2 interacts with NSF (N-ethylmaleimide-sensitive factor), a protein involved in vesicles exocytosis. These interactions of AMPA receptor subunits play important roles in controlling their trafficking and stabilization at the synapse.

In the adult hippocampus, two populations of AMPA receptors predominate: receptors composed of GluR1/GluR2 and GluR2/GluR3 (Wenthold et al., 1996). Although the majority of AMPA receptors in the CNS are GluR2-containing, significant expression of GluR2-lacking receptors in various brain regions has been observed. Since GluR2-lacking receptors are Ca^{2+}-permeable, they have been implicated in the processes of synaptic plasticity and excitotoxicity.

Gating. AMPA receptors are activated upon agonist binding to the LBD, which includes two polypeptide segments, D1 and D2 (Fig. 3.3B). Glutamate binding leads to the rotation of the D2 domain towards the D1 by $\approx 21°$ and closure of the "clamshell"-like structure. This conformational change leads to the channel pore opening (Armstrong and Gouaux, 2000). Beside glutamate which acts as a full agonist on AMPA receptors, there are also partial agonists of AMPA receptors. For example, kainate binds to the LBD but only leads to a partial opening of the pore. Deactivation is a process opposite to the activation: the clamshell re-opens, pore closes and glutamate is released from the LBD.

Receptors are in the open-state only briefly given that closed clamshell is a high energy conformation. Therefore the receptors are rapidly desensitized. Desensitization is a conformational change of a receptor that leads to the pore closure in the continued presence of glutamate. It involves a $\approx 14°$ rotation of D1 toward D2 that leads to the pore closure
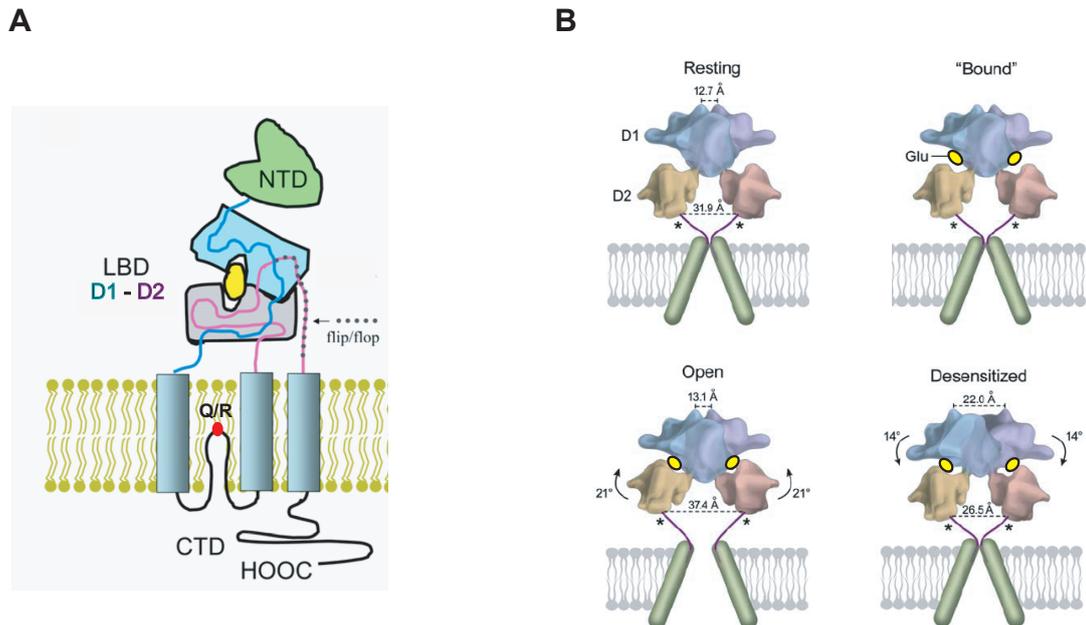
Figure 3.3: A, Schematic diagram of AMPA receptor subunit. Depicted are N- and C- terminal domain (NTD and CTD), ligand-binding domain (LBD) with segments D1 and D2, flip/flop splicing region and Q/R editing site. Modified from (Ziff, 2007). **B**, Two subunits of AMPA receptor tetramer with their D1 and D2 domains. Binding of glutamate (yellow circles) to the receptor is followed by a conformational change leading to open and desensitized state. Modified from (Armstrong et al., 2006).

(Armstrong et al., 2006). Conformation of desensitized receptors is very stable and receptors have large preference for this state.

AMPA receptors and synaptic plasticity. Postsynaptic changes in AMPA receptor function are an important contribution to the expression of long-term potentiation (LTP) and long-term depression (LTD), cellular correlates of learning and memory. The main feature of LTP and LTD is that a short period of synaptic activity can trigger persistent changes of synaptic transmission lasting at least several hours. The main question in understanding the mechanism of synaptic plasticity is whether the changes in synaptic strength originate from the postsynaptic or the presynaptic modification. The answer to this question was the identification of postsynaptically "silent synapses". These synapses contain only NMDA receptors and upon LTP they can be converted into active synapses through a recruitment of AMPA receptors (Malinow and Malenka, 2002). Several studies showed using different

techniques that GluR1-containing receptors were delivered into synapses upon LTP induction (Shi et al., 1999; Hayashi et al., 2000; Kakegawa et al., 2004). On the other hand, removal of GluR2-containing AMPA receptors from the synapses underlies LTD.

How does the AMPA receptor number change during synaptic plasticity? Both receptor endo/exocytosis and lateral diffusion in the membrane seem to be involved. The favored model is that AMPA receptors do not directly exchange between the PSD and cytosolic compartments. Instead, exocytosis and endocytosis occur at extrasynaptic membrane sites from which AMPA receptors laterally diffuse into or out of the synapse.

Another evidence that activity influences the number of synaptic AMPA receptors comes from experiments with chronic pharmacological manipulations of network activity. Increasing network activity causes decrease in synaptic AMPA receptor number, while chronic application of AMPA receptor antagonists causes the receptor number increase (Turrigiano and Nelson, 1998; O'Brien et al., 1998). These are the processes of homeostatic synaptic scaling, a form of synaptic plasticity that scale the strength of all of a neuron excitatory synapses up or down to stabilize neuronal firing.

3.3 Pharmacology of AMPA receptors

Agonists. The binding of an agonist to AMPA receptor leads to a conformational change of the LBD that spreads to the membrane spanning domains to open the channel. Glutamate is a full agonist of AMPA receptors and its binding to the receptor leads to the complete conformational change of the LBD. Besides glutamate, AMPA and quisqualate also act as full agonist of AMPA receptors. Kainate and propionic acid are partial AMPA receptor agonists and they lead to the incomplete conformational change of the LBD and therefore partial opening of the pore. AMPA has a high selectivity for AMPA receptors over kainate receptors (10-20 fold higher affinity for GluR1-4 over a GluR5 kainate subunit), whereas kainate shows high selectivity for kainate receptors. AMPA receptors mediate rapidly desensitizing responses to AMPA, quisqualate and glutamate, but non-desensitizing responses to kainate. The structure of AMPA and glutamate are shown in figure 3.4.

Antagonists. Two classes of antagonists act on AMPA receptors: competitive and non-competitive. Competitive antagonists bind to AMPA receptors in the same binding pocket

Agonists
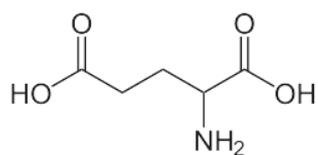
glutamate
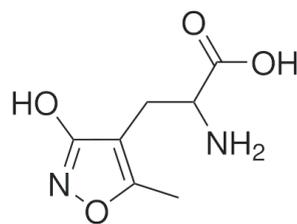
AMPA

Non-competitive Antagonists
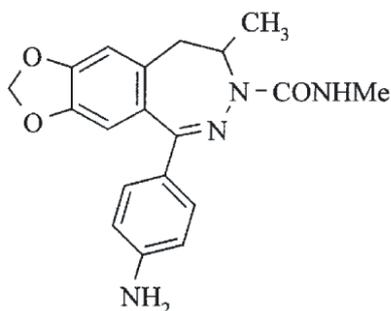
GYKI-53655
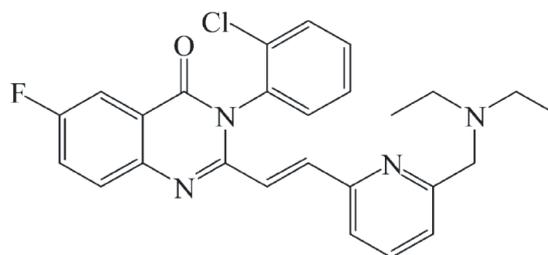
CP-465,022

Competitive Antagonist　　　　　　　**Positive modulator**
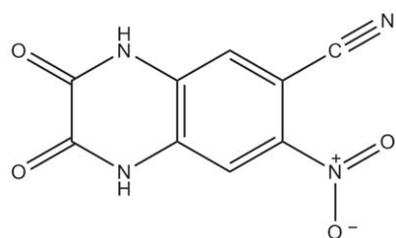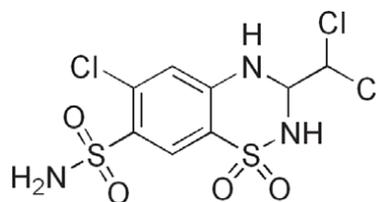
CNQX

TCM

Figure 3.4: Structures of AMPA receptor agonists: AMPA and glutamate, antagonists: GYKI, CP and CNQX, and positive modulator TCM.

as agonists, thereby occluding agonist binding. On the other hand, non-competitive antagonsits (also termed negative modulators or allosteric antagonists) bind outside of the agonist binding site and interfere with the conformational change that leads to the channel opening.

The quinoxalinediones family of the competitive AMPA and kainate receptor antagonist was first developed. The family consists of 6-cyano-7-nitroquinoxaline-2,3-dione (CNQX),

6,7-dinitroquinoxaline-2,3-dione (DNQX), and 2,3-dioxo-6-nitro-1,2,3,4-tetrahydrobenzo[f]-quinoxaline-7-sulfonamide (NBQX). However, given the recent finding that CNQX and DNQX can act also as partial agonists on AMPA receptors (Menuz et al., 2007), as well as their poor pharmaceutical properties in clinical development, there has been a need for developing new antagonists.

Changing the position of the nitrogen atoms in the structure of 1,4-benzodiazepines led to the discovery of a 2,3-benzodiazepines, a family of non-competitive AMPA receptor antagonists. The 2,3-benzodiazepine derivative GYKI-52466 was first found to exhibit anticonvulsant potency and neuroprotection (Tarnawa et al., 1989). Later more selective and potent analogs have been developed by the substitution at the N-3 position, e.g. GYKI-53655 (1-(4-aminophyl)-4-methyl-7,8-methylendioxy-5H-2,3-benzodiazepine, Fig. 3.4). GYKI-53655 has the advantage of being a selective antagonist for AMPA receptors over kainate receptors and more potent than GYKI-52466.

Another non-competitive AMPA receptor antagonist, CP-465,022 (3-(2-chloro-phenyl)-2-[2-(6-diethylaminomethyl-pyridin-2-yl)-vinyl]-6-fluoro-3H-quinazolin-4-one, Fig. 3.4) was developed from the efforts to increase the potency and selectivity of previously known piriqualone. CP-465,022 is an AMPA receptor selective derivative of piraquilone and is about 100-fold more potent on AMPA receptors than GYKI-53655.

Positive modulators. AMPA receptor-mediated synaptic currents are very brief (1-2 ms) because of the rapid inactivation of AMPA receptors by the processes of deactivation and desensitization. There is a class of drugs that block desensitization and slow deactivation of AMPA receptors, therefore promoting excitatory transmission. They are also called positive allosteric modulators and are typified by cyclothiazide (CTZ) and trichlormethiazide (TCM). The structure of TCM is shown in figure 3.4. CTZ and TCM bind within LBD and stabilize the dimer interface. CTZ shows a preference for the flip variants of AMPA receptors (Partin et al., 1996), whereas the potentiator 4-[2-(phenylsulfonylamino)ethylthio]-2,6-difluorophenoxyacetamide (PEPA) acts specifically on flop isoforms (Sekiguchi et al., 1997).

3.4 Transmembrane AMPA receptor regulatory proteins (TARPs)

Until recently trafficking of AMPA receptors was thought to be regulated solely by the interactions of their C-termini with proteins like PICK1, GRIP, SAP97 and others. The fact that PSD-95, a scaffolding protein that clusters synaptic proteins, does not interact directly with AMPA receptor subunits implied the existence of some link-protein between AMPA receptor and PSD-95. Stargazin was found to be that link protein.

The *stargazer* mouse is a spontaneous mutant that shows characteristic behavior of frequently tipping its head back to stare upward (Noebels et al., 1990). These mice suffer from epileptic discharges in the neocortex and ataxic gait (Noebels et al., 1990). The gene disrupted in stargazer mice, *Cacng2*, encodes a 36-kD protein, stargazin, with structural similarity to the $\gamma 1$ subunit of skeletal muscle voltage-gated Ca^{2+}-channels and it is also called $\gamma 2$ (Letts et al., 1998). *Stargazer* mice lack AMPA receptors in cerebellar mossy fiber to granule cell synapses, indicating a role of stargazin in synaptic targeting of AMPA receptors (Chen et al., 2000).

The TARP family consists of stargazin and stargazin-related proteins with a role in regulating AMPA receptors, including $\gamma 3$, $\gamma 4$ and $\gamma 8$ (Tomita et al., 2003) (Fig. 3.5B). TARPs are members of a large superfamily of four pass transmembrane proteins that include the $\gamma 1$ subunit of the skeletal muscle calcium channel and claudin family tight junction proteins (Fig. 3.5A). Proteins in the TARP family share 60 % sequence homology and are differentially expressed in the brain, $\gamma 2$ being preferentially expressed in the cerebellum, $\gamma 3$ in the cortex, $\gamma 4$ in scattered cells in white matter of cerebellum and corpus callosum and $\gamma 8$ in the hippocampus (Tomita et al., 2003).

A family of type II TARPs has been recently described, comprising of $\gamma 5$ and $\gamma 7$ (Kato et al., 2008). $\gamma 5$ modulates only receptors containing edited GluR2 subunit and regulates channel properties in a different way from canonical TARPs: it increases rates of GluR2 deactivation and desensitization and decreases glutamate potency, with no effect on receptors trafficking (Kato et al., 2008).

As auxiliary subunits of AMPA receptors, TARPs control both the receptor trafficking and channel properties of AMPA receptors. Distinct domains of stargazin are involved in these function: the C-terminal tail regulates trafficking of AMPA receptors whereas ectodomain of
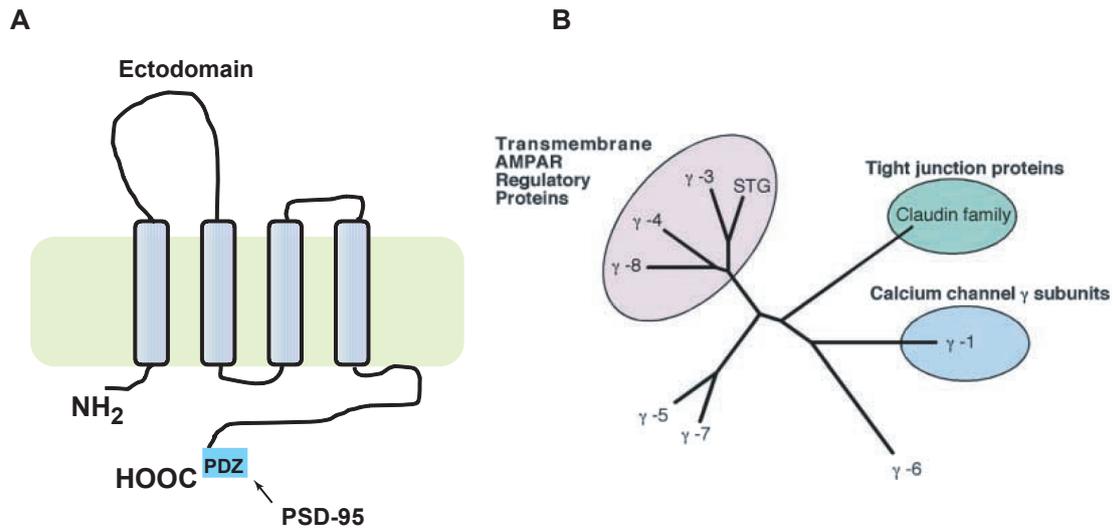
Figure 3.5: A, Scheme of stargazin structure. Depicted are cytoplasmic N- and C- terminus and the first ectodomain that modulates biophysical properties of AMPA receptors. The PDZ domain at the very end of the C-terminus intracts with PSD-95. **B**, Phylogenetic tree of TARPs and related proteins. Adopted from (Tomita et al., 2003).

stargazin controls biophysical properties of AMPA receptors (Tomita et al., 2005). Stargazin delivers AMPA receptors to the cell surface and regulates receptor synaptic localization through an interaction with PSD-95 (Chen et al., 2000). It slows AMPA receptor activation, deactivation and desensitization and increases the efficacy of partial agonist kainate (Tomita et al., 2005; Priel et al., 2005; Turetsky et al., 2005). In addition, stargazin increases the efficacy of CTZ on AMPA receptors (Tomita et al., 2006) and attenuates the rectification of AMPA receptors (Soto et al., 2007).

It seems that all AMPA receptors are associated with TARPs, given the current lack of evidence for "TARP-less" receptors. However, many aspects of the AMPA receptor-TARP interaction are not fully understood. The interacting sites of both TARP and AMPA receptor are not identified yet. Furthermore, the number of TARP molecules per AMPA receptor tetramer is not known, as well as whether this number is constant or dynamically regulated. Whether TARP binding is AMPA receptor subunit-dependent is yet another mystery.

3.5 NMDA receptors

NMDA receptors contribute to the excitatory synaptic transmission and have a critical role in synaptic plasticity. They have some unique functional features, which include block by extracellular Mg^{2+} at negative voltages, high permeability to Ca^{2+} and slow current kinetics. NMDA receptors are released from the Mg^{2+}-block during membrane depolarization that is mediated by activation of AMPA receptors. The synapses with only NMDA receptors are referred as "silent". Ca^{2+} influx trough NMDA receptors can lead to different forms of NMDA receptor-dependent synaptic plasticity. Depending on the pattern of synaptic stimulation, synapses can undergo LTP or LTD.

Gating of NMDA receptors is modulated by several ligands and modulators: the co-agonist glycin must bind in addition to glutamate for the channel to open. Extracellular Zn^{2+} and polyamines also modify the behavior of the receptor.

NMDA receptors are tetramers composed of three subunit types, NR1, NR2(A-D) and NR3. In the hippocampus, the NR1 subunit can assemble as heterodimers containing NR1/NR2A or NR1/NR2B or as heterotrimers containing NR1/NR2A/NR2B. NR2B-containing NMDA receptors are expressed early in development, while the expression of NR2A-containing receptors increases during development (Monyer et al., 1994). Importantly, NR2B-containing receptors have a slower decay compared to NR2A-containing receptors. The glycine-binding site is located in NR1 subunit, whereas NR2 binds glutamate.

NMDA receptor subunits interact with various intracellular scaffolding and signaling molecules within postsynaptic density, for example PSD-95, S-SCAM and CIPP (Cantallops and Cline, 2000). However, their trafficking to the cell surface and regulation of their synaptic localization is not well establish. Their mobility in the membrane is generally smaller than of AMPA receptors and changes in neuronal activity affect mainly AMPA receptor but not NMDA receptor mobility (Groc et al., 2004). However, the subunit composition of synaptic NMDA receptors can quickly change in an activity-dependent manner in neonatal synapses, which is thought to regulate the requirement for evoking LTP or LTD (Bellone and Nicoll, 2007).

Inappropriate activation of NMDA receptors is implicated in several diseases. In particular, excessive Ca^{2+} influx through NMDA receptors can cause excitotoxic neuronal death.

Therefore NMDA receptors are potential therapeutic targets for treating stroke and seizures.

3.6 Membrane-associated guanylate kinases (MAGUKs)

MAGUK proteins have been shown by genetic, electrophysiological and morphological studies to be essential for controlling the structure, strength and plasticity of glutamatergic synapses. Modifications of MAGUK protein function in the glutamatergic synapse has been already described in several neurological disorders such as Alzheimer's disease, Parkinson's disease, Huntington's disease, ischemia, schizophrenia and neuropathic pain, reviewed by (Gardoni, 2008).

MAGUKs comprise a family of scaffolding molecules at excitatory synapses. The prototypical member of the family is postsynaptic density protein of 95 kDa, PSD-95. The family includes also PSD-93, SAP-102 and SAP-97 (Funke et al., 2005). All MAGUKs share a common domain structure organization with three N-terminal PDZ domains, a Src-homology 3 (SH3) domain and C-terminal catalytically inactive guanylate kinase (GK) domain (Fig. 3.6). The N-terminal region of PSD-95 and PSD-93 contains two cysteines that undergo palmitoylation, whereas SAP-97 contains the L27 domain instead.

MAGUK proteins are expressed in all regions of the brain, but their relative abundance changes during development. SAP102 is expressed in the hippocampus in the early postnatal period and decreases with age, whereas PSD-95 and PSD-93 expression increases by one month of age (Sans et al., 2000).

PSD-95 is located in the postsynaptic density in close proximity to the postsynaptic membrane. Given its location and multiple PDZ domains it has potential of clustering synaptic receptors and channels. PSD-95 interacts with AMPA receptors via TARPs, and directly with NR2 subunit of NMDA receptors and K^+ channel. Beside clustering and stabilization of the receptors at the synapse, PSD-95 modulates the activity of the proteins it binds to. For example, it reduces single-channel conductance of the inward-rectifying K^+ channel (Nehring et al., 2000) and regulates NMDA receptor desensitization (Sornarajah et al., 2008). Another important role of PSD-95 is to organize signaling complexes at the PSD. For instance PSD-95 interacts with neuronal nitric oxide synthase (nNOS), an enzyme that produces nitric oxide implicated in retrograde signaling in synapses. Also, PSD-95 binds to
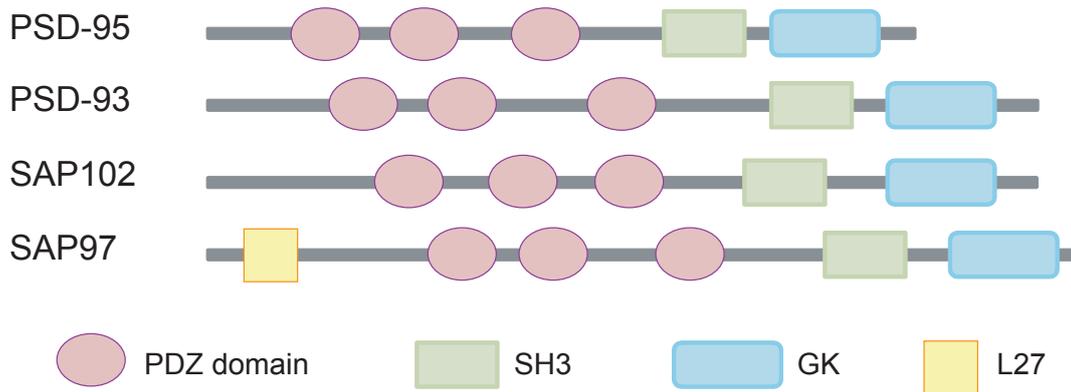
Figure 3.6: Members of MAGUK family: PSD-95, PSD-93, SAP102 and SAP97 with their PDZ, SH3 and GK domains. SAP97 contains L27 domain in its N-terminus.

kalirin-7, a protein involved in spine formation (Penzes et al., 2001).

Synaptic abundance of PSD-95 is regulated by neuronal activity. Neuronal activity promotes the dispersal of PSD-95 from the synapses by depalmitoylation of PSD-95 N-terminus (El-Husseini Ael et al., 2002) and also through the ubiquitin-proteasome pathway (Colledge et al., 2003). The function of PSD-95 is also regulated by phosphorylation. CamKII phosphorylates PSD-95 at Ser73 that destabilizes PSD-95 in the PSD (Steiner et al., 2008). It seems that phosphorylation of PSD-95 by CamKII is not important for basal synaptic transmission mediated by AMPA and NMDA receptors, but for spine growth and LTP expression. Phosphorylation of another serine in PSD-95, Ser295, is important for the synaptic accumulation of PSD-95. This phosphorylation is mediated by Rac1-JNK1 signaling pathway and enhances synaptic accumulation of PSD-95 and the ability of PSD-95 to recruit AMPA receptors to the synapse (Kim et al., 2007). Cyclin-dependent kinase 5 (Cdk5) phosphorylates N-terminal domain of PSD-95 and inhibits its multimerization (Morabito et al., 2004). Cdk5-dependent phosphorylation of PSD-95 was proposed to dynamically regulate the clustering of PSD-95/NMDA receptor complexes at the synapse.

As the main component of the excitatory PSD, PSD-95 has been studied by many labs. The main findings are reviewed by (Elias and Nicoll, 2007). The conclusion that emerged from these studies is that PSD-95 regulates the number of synaptic AMPA receptors, whereas the number of synaptic NMDA receptors seems not to depend on PSD-95. The possible role

of PSD-95 in presynaptic neurotransmitter release is not well established in the field. There are still many open questions regarding the roles of PSD-95 in the synapse and how different mechanisms orchestrate together to control the abundance of different MAGUKs at the synapse.

3.7 Hipppocampal preparation

The hippocampus is located inside the medial temporal lobe of the cerebral cortex. It belongs to the limbic system and plays a major role in memory and spatial navigation. The hippocampus came in the focus of neuroscience when Scoville and Milner published the study on H.M., a patient who had his two hippocampi surgically removed for treatment of epilepsy. The patient had severe memory deficits (Scoville and Milner, 1957). Since that finding, hippocampus became the favorite brain region to study neuronal plasticity, a cellular correlate of memory. This led to the discovery of "place cells", hippocampal neurons that are activated selectively when an animal moves through a particular location in space (O'Keefe and Dostrovsky, 1971). Therefore the hippocampus has been proposed to function as a spatial map of the brain.

The hippocampus has the shape of a curved tube, named a ram's horn (Cornu Ammonis). Pyramidal cells, principal cell of the hippocampus, account for 85-90% of the total cell number. There are also various interneurons identified in the hippocampus, but their number is small compared to the pyramidal cells. The CA3 and CA1 (Cornu ammonis 3 and 1) regions of hippocampus contain populations of pyramidal cells that are similar in many aspects but they differ in some of their physiological properties and connectivity (Fig. 3.7). CA3 cells receive inputs from the granule cells of the dentate gyrus. This synapse is also called mossy fiber synapse due to the numerous and large presynaptic terminals. Dentate gyrus is a region of adult neurogenesis. Neuronal stems cells proliferate and produce new cells which are important for normal learning and memory and their dysfunction is involved in some diseases. Pyramidal neurons of CA3 region project their axons, also called Schaffer collaterals, to CA1 pyramidal cells and also other CA3 cells (Fig. 3.7).

Given its anatomical features, e.g. laminal structure and simple connectivity pattern, hippocampus has been used to study synaptic plasticity, seizure activity and ischemia. The
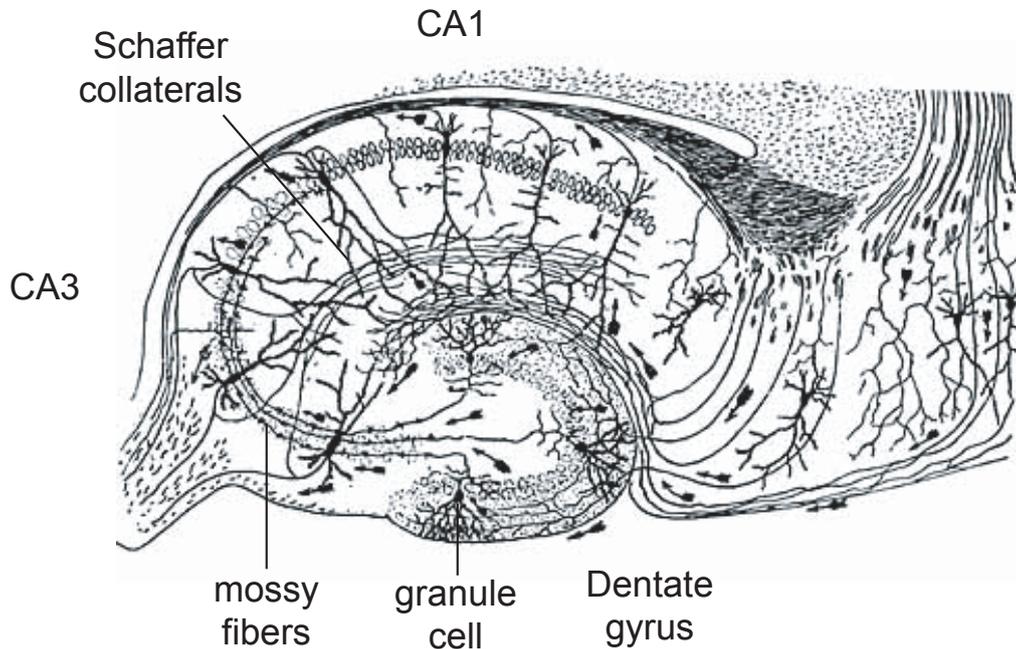
Figure 3.7: Neuronal organization in a hippocampal slice. CA3 and CA1 regions are depicted as well as Schaffer collaterals pathway. Granule cell from dentate gyrus project their mossy fibers to the CA3 region. Modified from Cajal, 1911.

Schaffer collateral-CA1 synapse has been a favorite model synapse to study basal synaptic transmission and LTP. The capacity of hippocampal synapses to change with activity comes from the intrinsic properties of hippocampal neurons, for example high expression level of NMDA receptors (Malenka and Nicoll, 1993).

Organotypic slice cultures have the main advantage of a fairly intact histotypic organization (Stoppini et al., 1991), i.e. hippocampal laminal structure is well preserved. The slices can be cultured for several weeks and it has been shown that neuronal development in the slices resembles development *in vivo*. Cultured hippocampal slices allow for various experimental manipulations. For example, neurons can be cultured under different biochemical conditions or single cells can be altered using different molecular biology methods.

3.8 Summary of aims

AMPA receptors mediate the fast component of excitatory transmission in the brain. By now many aspects of AMPA receptor function, like structure, assembly, trafficking and gating, have been well understood. A new chapter in AMPA receptor physiology was opened when it was found that AMPA receptors are associated with auxiliary subunits, named TARPs. Since that finding the main goal of many studies dealing with the AMPA receptors was to understand the role of TARPs in AMPA receptor function. It is clear by now that TARPs are involved in almost every aspect of AMPA receptor function. Importantly, TARPs are shown to be the link between AMPA receptors and the synaptic scaffolding molecule, PSD-95. PSD-95 is a member of MAGUK family and has been studied by many laboratories as a synaptic "slot" candidate which could determine the number of synaptic receptors and therefore the synaptic strength.

However, there is still a long list of open questions regarding the TARP-AMPA receptor interaction and the role of PSD-95 in regulating synaptic transmission. The goal of this study was to further explore the effect of TARP association on AMPA receptor function, focusing on stargazin, the prototypical TARP. The second goal was to assess the role of PSD-95 in the synapse and to understand the origin of some conflicting results obtained in different laboratories.

In the first part of my thesis, I investigated the effect of stargazin on AMPA receptor pharmacology. To that end, I employed the Xenopus oocyte heterologous expression system to study isolated AMPA receptor-mediated currents. I measured dose-response curves of GluR1 for different AMPA receptor antagonists in the presence and absence of stargazin. The focus was on commonly used antagonists CNQX, GYKI-53655 and CP-465,022.

In the second part of this study, I explored how PSD-95 regulates synaptic transmission. I virally overexpressed PSD-95 in cultured hippocampal slices and measured AMPA and NMDA currents from infected and neighboring control cells. By use of various experimental paradigms I assessed the presynaptic function, as well as AMPA and NMDA receptor subunit-composition in cells overexpressing PSD-95.

4 Material and Methods

4.1 Material

All the chemicals and media used in this study are listed in the following two tables. Chemicals were dissolved either in distilled water or dimethyl sufoxide (DMSO).

4.1.1 Chemicals

Chemical	Supplier
(+)MK-801 hydrogen maleate	Sigma
(2R)-amino-5-phosphonopentanoate (APV)	BioTrend
2,3-Dioxo-6-nitro-1,2,3,4-tetrahydrobenzo(f)quinoxaline-7-sulfonamide (NBQX)	BioTrend
2-Amino-2-hydroxymethyl-propane-1,3-diol (Tris, Trizma base)	Sigma
2-chloroadenosine	Sigma
6-cyano-7-nitroquinoxaline-2,3-dione (CNQX)	Tocris
6x gel loading buffer	Fermentas
Adenosine 5'-triphosphate magnesium salt (MgATP)	Sigma
Agarose	Inivitrogen
Aprotinin	Sigma
Bovine albumin powder	Sigma
Calcium chloride dihydrate ($CaCl_2$)	Merck
Calcium nitrate tetrahydrate ($Ca(NO_3)_2$)	Merck
Cesium chloride (CsCl)	Sigma
Cesium methane-sulfonate ($CsMeSO_4$)	Sigma
Collagenase Type 3	Worthington
CP-465,022	Pfizer
D(+)Glucose monohydrate	Merck
Dimethyl sufoxide (DMSO)	Merck
Ethidiumbromide Solution	Fluka Chemie
Ethyl-3-aminobenzoate methanesulfonate salt	Sigma

Chemical	Supplier
Fetal bovine serum	Biochrom
Gel Mount I M Aqueous Mounting Medium	Sigma
GeneRuler 1kb DNA-ladder	Fermentas
Gentamycin	Sigma
Glacial acetic acid	Merck
Guanosine 5'-triphosphate sodim salt hydrate (NaGTP)	Sigma
GYKI-53655	Taros
Horse serum	Gibco
L-Glutamic acid sodium salt hydrate	Sigma
L-Glutamin	Gibco
Magnesium chloride hexahydrate ($MgCl_2$)	Merck
Magnesium sulfate heptahydrate ($MgSO_4$)	Merck
Mineral oil	Sigma
N-2-Hydroxyethylpiperazine-N'-2-ethane sulfonic acid (HEPES)	Biomol
Paraformaldehyde (PFA)	Merck
Penicillin	Gibco
Phosphocreatine disodium salt hydrate enzymatic (Na P-creatine)	Sigma
Picrotoxin	Sigma
Potassium chloride (KCl)	Merck
Restriction enzymes	Fermenatas
Potassium dihydrogen phosphate (KH_2PO_4)	Merck
RiboRuler RNA ladder, High Range	Ambion
Sodium chloride (NaCl)	Merck
Sodium dihydrogen phosphate monohydrate (NaH_2PO_4)	Merck
Sodium hydrogen carbonate ($NaHCO_3$)	Merck
Spermine	Fluka Chemie
Streptomycin	Gibco
Tetrodoxin citrate (TTX)	BioTrend
Titriplex II (EDTA)	Merck
Titriplex VI (EGTA)	Merck
Trichlormethiazide (TCM)	Sigma
Trypsin/EDTA	Gibco
α-chymotrypsin	Sigma

4.1.2 Media and solutions

Name	Recipe
BHK cells medium	Glasgow MEM BHK-21 medium (Gibco), 10 % Fetal bovine serum, 1 % Penicilin/Streptomycin
Slice-preparation medium	MEM medium (Gibco), 1 % Penicilin/Streptomycin, 1 % 1M Tris/HCl pH 7.2
Slice-culturing medium	50 % MEM medium (Gibco), 25 % HBSS (Gibco), 25 % Horse serum, 0.5 % L-Glutamine 200 mM
PBS (10x)	100 mM Na_2HPO_4, 20 mM KH_2PO_4, 1.37 M NaCl, 27 mM KCl
TAE (50x)	in 1 l: 242 g Tris, 57.1 ml glacial acetic acid, 100 ml 0.5M EDTA (pH 8.0)
ORII	in mM: 100 NaCl, 2 KCl, 1 $MgCl_2$, 5 HEPES, pH 7.5
Barth's solution	in mM: 88 NaCl, 1 KCl, 0.41 $CaCl_2$, 0.82 $MgSO_4$, 0.32 Ca $(NO_3)_2$, 10 HEPES, pH 7.6
ND96	in mM: 96 NaCl, 2 KCl, 1 $MgCl_2$, 1.8 $CaCl_2$, 5 HEPES, pH 7.4
Oocytes recording solution	in mM: 90 NaCl, 1 KCl, 1.8 $MgCl_2$, 10 HEPES, pH 7.4
ACSF	in mM: 119 NaCl, 2.5 KCl, 1.3 $MgSO_4$, 1 NaH_2PO_4, 26.2 $NaHCO_3$, 4 $CaCl_2$, 4 $MgCl_2$, 11 glucose
Internal recording solution	in mM: 115 $CsMeSO_3$, 20 CsCl, 10 HEPES. 2.5 $MgCl_2$, 4 MgATP, 0.4 NaGTP, 10 Na P-creatine 0.6 EGTA, pH 7.2, 290 mOsm

4.2 Methods

4.2.1 General cloning methods

Digestion of DNA. 2-3 μg of DNA were digested with restriction enzymes to generate DNA fragments with desired "sticky" ends. DNA was cut with one or two enzymes. 1 μl of enzyme (concentration 10U/μl) was used in a recommended buffer in total reaction volume of 40-50 μl. The digestion time was at least 2h at recommended temperature. The efficiency of digestion was tested on 1 % agarose gel desolved in TAE buffer. The fragment of interest was cut from a gel and purified using the High Pure PCR Product Purification Kit (Roche).

Ligation. DNA fragments were ligated using T4 DNA ligase (Invitrogen) in 5x buffer provided by the manufacturer. The total ligation volume was 20 μl. Time of ligation was either 2 hours at room temperature or over the night at 17°C.

Electroporation of competent E. coli. 1-2 μl of ligation volume was mixed with 50μl of E. coli competent cells, strain XL1 blue, in a 1 cm cuvette. The settings of Bio-Rad Gene Pulser electroporator were: voltage 2.5 kV, resistance 400 ohms and capacitance 25 μFD. 1 ml of LB bacteria medium was added and cells were incubated at 37°C for 1 hour with constant agitation. The cells were collected by centrifugation (3 minutes at 800g) and plated on agar plate supplemented with the appropriate antibiotic.

Plasmid isolation from E.coli. For "mini-prep" of DNA one bacterial colony was inoculated with 3 ml of LB/antibiotic media and incubated overnight at 37°C. Cells were transfered in 1.5 ml Eppendorf tubes and centrifuged at 17500g for 1 minute. Plasmids were isolated using the QIAprep Spin Miniprep Kit (QIAGEN), based on the adsorption of DNA from the bacterial lysate on the selective silica membrane in combination with high-salt buffer.

Site-directed mutagenesis. Point-mutations were introduced in a DNA sequence using PCR and Phusion High-Fidelity DNA polymerase (Finnzymes). This method employs two pairs of primers. In the pair of mutagenic PCR primers one or more mutations were located in the middle of the primer with 10-15 bases of the original template DNA sequence on both sides. In two subsequent PCR reactions DNA fragment containing point mutations of interest was amplified and subcloned into an appropriate vector.

4.2.2 In vitro transcription

GluR1, GluR2, GYKI- and CP-insensitive mutants, stargazin and Ex1 chimera were subcloned into pTL vector (Lorenz et al., 1996) which contains SP6 RNA polymerase promoter site. For RNA production, the constructs were linearized using MluI restriction enzyme.

GFP, PSD-95, PSD-93, both PSD-95/93 chimeras and Cdk5-phosphorylation mutants of PSD-95 were cloned into pSFV vector for virus production, containing SP6 RNA polymerase promoter site. For transcription plasmids were linearized with SpeI restriction enzyme.

100-200 ng of linearized DNA was used as a template for transcription using mMessage

mMachine transcription kit (Ambion). The RNA was precipitated using LiCl precipitation solution provided by the manufacturer and resuspended in nuclease-free water.

4.2.3 Xenopus oocytes preparation and injection

Xenopus laevis frogs were anesthetized with 1g of ethyl 3-aminobenzoate methanesulfonate salt and 1g of $NaHCO_3$ dissolved in 1l of water. Frogs were kept in anesthetizing solution for 15-20 minutes. A 5-10 mm cut was made on one side of a frog abdomen and ovaries were pulled out. Ovaries were cut into smaller lobes, 20-30 oocytes each and single oocytes were isolated by collagenase treatment. 20 mg of collagenase type 3 (205 u/ml) was desolved in 20 ml of ORII solution. After 30 minutes of digestion with constant agitation, the collagenase solution was changed with fresh solution and oocytes were digested for additional 30 minutes. Oocytes were washed in Barth's solution and remaining connective tissue and cells follicle layers were removed manually with forceps. Stage V-VI oocytes were stored at 17°C in ND96 solution supplemented with 50 μg/ml gentamycin.

Oocytes were injected with 50 nl cRNA. Injecting pipettes (World Precision Instruments, Sarasota, FL) were filled with mineral oil and Nanoinjector II (Drummond Scientific Company) was used to inject the desired volume of RNA solution into oocytes. The amount of injected RNA, relative amount of co-injected stargazin and time of expression varied depending on the construct used (Fig. 5.9).

4.2.4 Two-electrode voltage clamp

After 1-2 days of expression glutamate-evoked currents were measured from oocytes using two-electrode voltage clamp (TEVC). Schematic presentation of TEVC is shown in figure 4.1. TEVC recordings were performed using a GeneClamp 500B amplifier connected to a Digidata 1322 controlled by pCLAMP 9.2 (Axon Instruments, Foster City, CA). Pipettes (World Precision Instruments, Sarasota, FL) had a resistance of 0.5 - 1.5 MΩ and were filled with 3 M KCl. Glutamate evoked currents were recorded at -70 mV. Oocytes were continuously perfused with the recording solution. Currents were evoked by 40 s applications of 200 μM glutamate supplemented with 500 μM TCM to block AMPA receptor desensitization.

Dose-inhibition curves were constructed by applying 4-5 concentrations per oocyte of an-
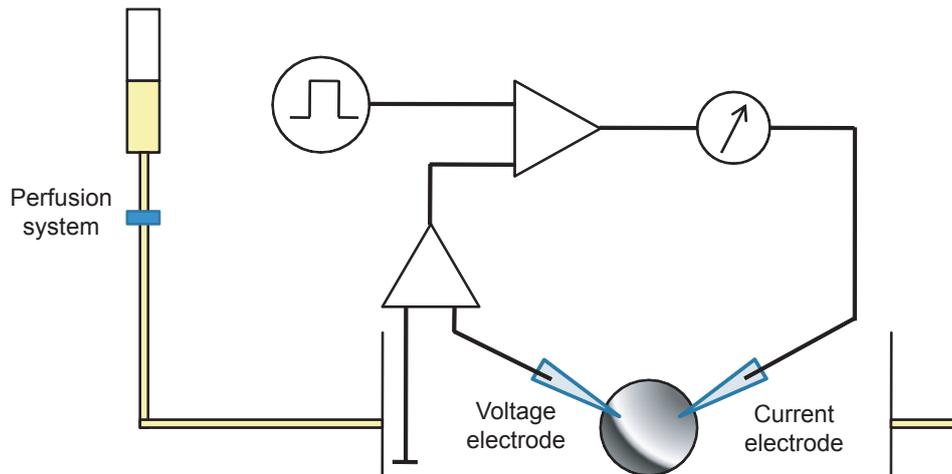
Figure 4.1: The principle of TEVC. The voltage electrode measures the resting potential of an oocyte. The resting membrane potential is compared to a command potential and resulting current is injected through a current electrode to clamp the cell at the command voltage. Glutamate and different antagonist were applied using the perfusion system.

tagonist mixed in agonist solution, and currents (I) were normalized to the current obtained with agonist alone (I_0). IC$_{50}$ values were determined by sigmoidal fits following the equation: $I/I_0 = 1/\left[1 + 10^{(Log(IC_{50})-x)\cdot HillSlope}\right]$. In the cases of imperfect fits we estimated IC$_{50}$ values from graphs. Data was analyzed with Prism 5.0 (GraphPad, San Diego, CA).

4.2.5 Surface labeling of oocytes

GluR1^{WT}, GluR1^{GYKI} and GluR1^{CP} were tagged by inserting the HA epitope (YPYD-VPDYA) three amino acids downstream from the signal peptide. Defolliculated oocytes were injected with 5 ng HA-tagged GluR1 alone or with 5 ng of HA-tagged GluR1 and 1 ng stargazin cRNA. Uninjected oocytes were used as a negative control. Surface receptor detection was performed two days after injection using chemiluminescence assay as described (Zerangue et al., 1999). Oocytes were blocked in ND96-1% BSA solution for half an hour and placed in a white flat-bottom 96-well plate, 5-7 oocytes per well. Oocytes were incubated for 1 h with 1 μg/ml rat anti HA antibody (3F10, Roche), followed by washing steps with ND96-1% BSA, 3x10 minutes. Washing was performed in 6 cm dish. Oocytes were transfered to 96-well plate and incubated for 1 h with horseradish peroxidase-coupled secondary anti-rat

IgG (Jackson Immuno Research), followed by 6x10 minutes washing steps. All washing and incubation steps were performed at 4°C. Oocytes were placed into 96-well plates with 50 μl SuperSignal ELISA Femto Maximum Sensitivity Substrate (Pierce, Rockford, IL) each. Chemiluminescence was quantified using Mithras LB 940 luminometer (Berthold Technologies, Bad Wildbad, Germany) and 10-20 oocytes were averaged for each condition. The signal of uninjected oocytes was substracted.

4.2.6 Organotypical hippocamapal slice preparation

Slices were prepared from 8 day old Wistar rats. Animals were decapitated and brains were placed in the slice-preparation medium on ice for 1 minute. Hippocampi were isolated under binocular and 400 μm thick slices were obtained using a McIlwain tissue culture chopper (The Mickle Laboratory Engineering). Single slices were separated by gentle shaking in a Falcon tube and undamaged slices were selected, transfered to fresh preparation medium and incubated at 4°C for 30 minutes to block the proteolytical processes in the slices.

Plate inserts were placed in 30 mm petri dishes with 1 ml of the slice-culturing medium. Biopore 0.4 μm membrane (Millipore Corporation) was cut into small square pieces ("confetti") and 3-4 pieces were placed on a single insert. Slices were transfered onto the membranes at the interface between air and culture medium and maintained at 35°C, 5% CO_2. The culture medium was changed every second day.

4.2.7 Preparation of Semliki Forest virus

Semliki Forest virus (SFV) is a single-stranded RNA virus with an envelope structure. The SFV genome is split into two vectors (Fig. 4.2). The expression vector contains the nonstructural genes (nsP1-4), subgenomic 26S promoter and multiple cloning site for introducing the gene of interest. The structural proteins are provided from the helper vector containing the capsid and envelope genes.

BHK cell preparation. To produce infectious virus particles, vector and helper RNA obtained by in vitro transcription were mixed and co-transfected into BHK 21 (Hamster Syrian Kidney) cells. BHK cells were transfered from a 90 % confluent 100 mm dish to a 150 mm dish in 1:10 dilution (2 ml of cell suspension in 18 ml BHK-medium). They were
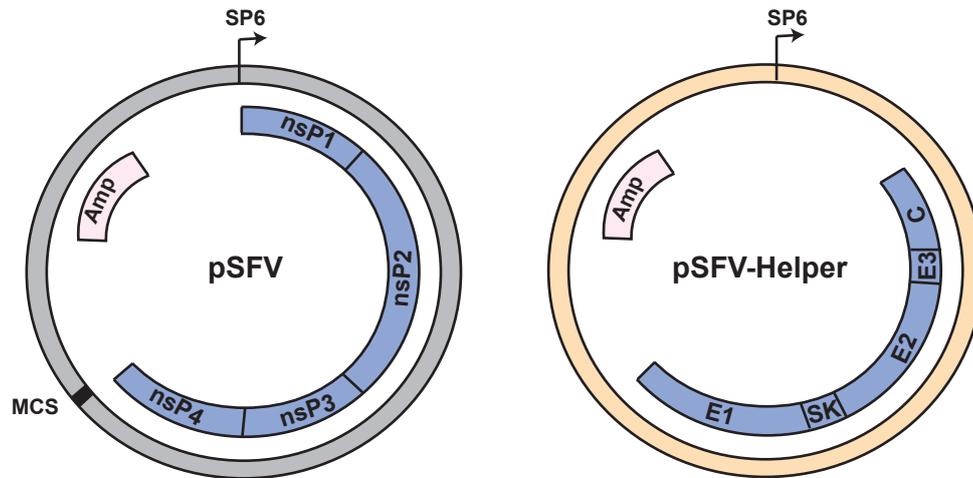
Figure 4.2: Maps of the pSFV and pSFV-helper plasmids used to generate recombinant SFV particles. Regions encoding the non-structural proteins (nsP1-4), the structural proteins (c, E3, E2, 6K and E1), the ampicillin resistance gene (Amp), SP6 promoter sites and multiple cloning site (MCS) are indicated.

cultured until they reached 60 % confluency (approximately 2 days); confluence higher than 60 % makes cells resuspension more difficult and clumps are more easily formed. To collect the cells for electroporation, 3 ml of trypsin/EDTA were added to a 150 mm dish and cells were incubated for 3 minutes (longer incubation time may lead to cell death). To inactivate trypsin, 17 ml of BHK-medium was added to the cells before the cells were transfered to a 50 ml Falcon tube and centrifuged for 3 minutes at 2500g. The supernatant was discarded by aspiration and cells were washed with 20 ml of RNase-free 1xPBS and centrifuged again for 3 minutes at 2500g. Supernatant was discarded and cell pellet was gently resuspended in 0.5 ml RNase-free 1xPBS to obtain single cells.

BHK cell electroporation. 0.5 ml of cells suspension was transfered to sterile 0.2 cm electroporation cuvette on ice. The RNA of pSFV containing gene of interest and pSFV-hleper ($\approx$20 μg each, i.e. total yield of both RNA reaction) were pre-mixed in the 1.5 ml Eppendorf tube and added to BHK cells. Cells were electroporated using Bio-Rad electroporator. The settings were: voltage 1.5 kV, capacitance 25 μF, infinity resistance. Cells were electroporated twice with an interval of 10-15 sec. Cells were mixed by finger flick-
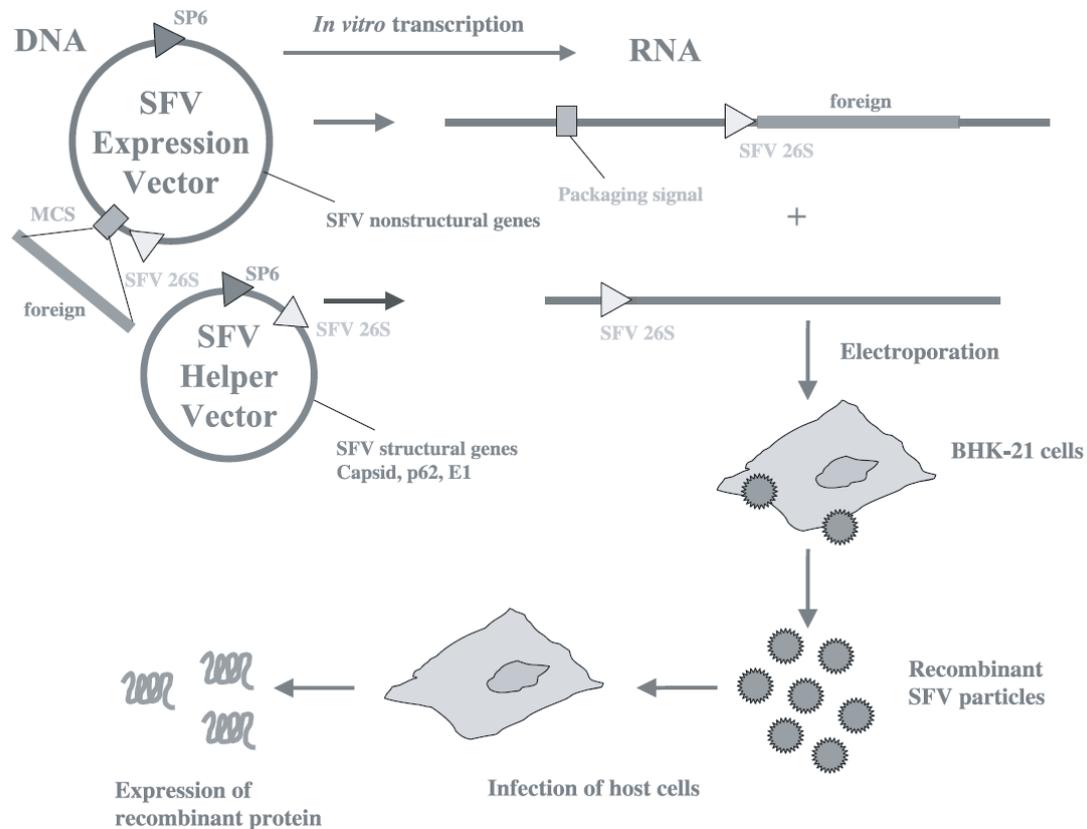
Figure 4.3: Schematic illustration of the production of replication-deficient SFV particles. Both vectors are in vitro transcribed and co-transfected into BHK cells. Generated viral particles are harvested and used to infect host cells. Adopted from (Lundstrom, 2003).

ing in between two electroporation. The time constant after each pulse was 0.7-0.8. After electroporation, cells were left to recover for ≈10 minutes in cuvette at room temperature. Electroporated BHK cells were added to 100 mm dish containing 9.5 ml BHK-medium, dish was mixed and kept at 37°C, 5% CO_2.

Collection of viral particles. Transcription and translation of pSFV and helper vectors via a BHK cell replication machinery results in formation of new infectious particles (Fig. 4.3). Since helper vector does not have packing signal, genes for structural proteins are not included in formed viral particles. After one round of infection, new viral particles cannot be formed, therefore the packed replicons are called "suicide vectors".

36 hours after electroporation the medium containing released viral particles was collected

(10 ml) and centrifuged to spin down cell debris at 2500g for 10 minutes at 4°C. Supernatant was collected and kept at 4°C. To concentrate viral particles, ultracentrifugation was performed the same day. The supernatant was spun for 2h at 76800g and 4°C using SW41 rotor. The supernatant was aspirated leaving 200-300 μl in the tube. Viral pellet was resuspended in this volume, split into 50 μl aliquots and stored at -80°C.

Activation of the virus. pSFV-helper plasmid contains three point mutations in the gene coding for structural protein that forms spikes necessary for the infection. Due to these mutations the spike-forming protein is insensitive to endogenous proteases that results in formation of nonfunctional spikes. Therefore the viral particles have to be activated, i.e. treated with exogenous proteases.

50 μl of viral solution was digested for 45 minutes at room temperature with 1:20 volumes of α-chymotripsin. α-chymotripsin was inactivated for 10 minutes at room temperature with 1:15 volumes aprotinin. Activated virus was aliquoted and stored at -80°C.

4.2.8 Infection of hippocampal cultured slices

Hippocampal slices (6-10 DIV) were infected one day before recording. Injecting pipettes (World Precision Instruments, Sarasota, FL) and Nanoinjector II (Drummond Scientific Company) were used similarly as for oocytes injection (see section **Xenopus oocytes preparation and injection**). 2-3 injections (23 nl each) of activated viral solution was injected into CA2-CA1 area of hippocampus. Infected cells were visualized using GFP (Fig. 4.4).

4.2.9 Electrophysiology in slice culture

Pyramidal cells of the hippocampal slices were visualized using differential interference contrast camera on a fixed-stage upright microscope (Olympus, BX51WI). Recordings were obtained from pairs of infected and uninfected cell simultaneously by stimulating Schaffer collaterals using 2-3 MΩ glass electrodes (World Precision Instruments) filled with external solution. Electrodes were pulled with P-97 micropipette puller (Sutter Instruments). External solution was ACSF (artificial cerebro-spinal fluid) saturated with 95 % O_2 and 5 % CO_2. To block inhibitory transmission 100 μM picrotoxin was added to external ACSF.
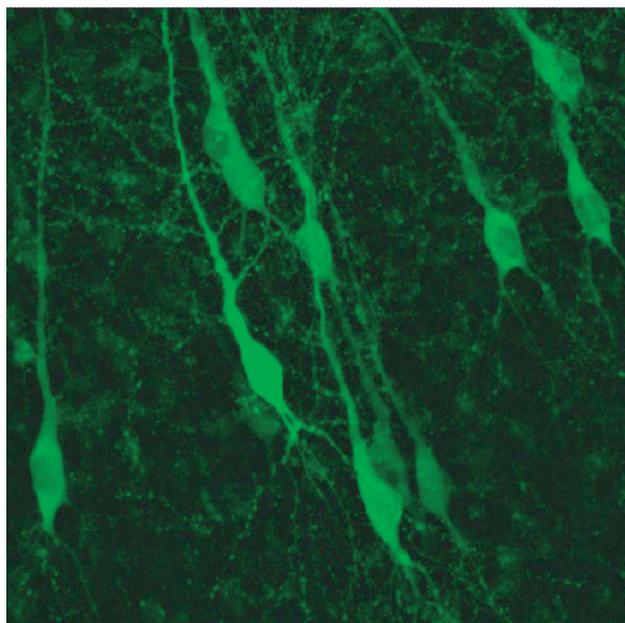
Figure 4.4: GFP-positive cells from CA1 pyramidal cell layer one day after infection with SVF vector expressing PSD-95:GFP.

Since spontaneous action potential firing in cultured hippocampal slices is very high, 20 μM 2-chloroadenosine was added to external solution to decrease presynaptic release probability of neurons and suppress epileptic activity. Only MK-801 experiments were done in the absence of 2-chloroadenosine. Isolated NMDA currents were measured in the presence of 10 μM NBQX and isolated AMPA currents in the presence of 100 μM APV in the external solution. Cell recordings were made using 2-3 MΩ glass electrodes filled with the internal solution. In the experiments where we measured rectification we included 0.1 mM spermine in the internal solution. Data were collected using Axopatch 700B amplifier (Axon Instruments) and digitized at 5 kHz with the Digidata 1322 controlled by pCLAMP 9.2. Membrane and series resistance were monitored by applying -5 mV test pulse to cells after obtainig the whole-cell configuration and only cells with input resistance lower than 20 MΩ and membrane resistance higher than 100 MΩ were analyzed.

AMPA receptor-mediated EPSCs were evoked at -70 mV and EPSCs were recorded after adjusting stimulation strength so that AMPA currents in control cells were 50-100 pA. The amplitude was determined by measuring the peak of response. After obtaining 20-30 sweeps, cells were depolarized to +40 mV, allowed to stabilize for 1 minute and another 40

sweeps were measured. NMDA EPSC amplitude was determined by measuring the current magnitude 70 ms after the stimulation artifact. Only sweeps 20-40 were taken for analysis. In both cases, stimulation pulses were delivered at 0.2 Hz. Decay kinetic of isolated NMDA currents was estimated as previously described (Cathala et al., 2005). Briefly, decay time (τ) was calculated from the area under the current from peak to 1.3 s after the peak and normalized to a peak amplitude.

4.2.10 Fixation and confocal microscopy

One day after infection slices were fixed with 4 % PFA in PBS for 20 minutes. Fixation was proceeded by washing steps with PBS 3x10 minutes. After washing, slices were placed on a microscope glass and maunted using maunting medium. Images were taken mainly the day after the fixation using Leica DM IRE 2 (Leica Microsystems) microscope equiped with 63x oil emersion objective. Z-stacks of images were made with 0.1 μm thick sections and maximal projections were obtained.

5 Results

5.1 Effect of stargazin on AMPA receptor antagonism

In neurons AMPA receptors are associated with their auxiliary subunits, TARPs. TARPs regulate both the trafficking and biophysical properties of AMPA receptors. In our study we focused on stargazin, the first TARP to be described as an auxiliary subunit of AMPA receptors. It was previously shown that stargazin dramatically increased the surface expression and glutamate evoked currents of AMPA receptors in Xenopus oocytes (Chen et al., 2003; Tomita et al., 2004). Here, we used this system to investigate the effects of stargazin on the antagonism of the competitive antagonist CNQX and the allosteric inhibitors GYKI-53655 and CP-465,022.

5.1.1 Effect of stargazin on GluR1 inhibition by CNQX, GYKI and CP

To study the inhibition of AMPA receptors, we injected the oocytes with GluR1 RNA alone or together with stargazin RNA. As co-expression with stargazin increases the glutamate evoked currents dramatically, we adjusted the amounts of injected RNA such that glutamate evoked currents had similar amplitudes. Absolute current level evoked in oocytes injected with 10 ng of GluR1 RNA alone was in the same order as when 0.1 ng of GluR1 RNA was co-injected with 0.1 ng of stargazin RNA (Fig. 5.1A).

We tested whether stargazin influenced the efficacy of CNQX on GluR1 homomeric receptors. Interestingly, GluR1 was less inhibited by CNQX when co-expressed with stargazin (Fig. 5.1A and B). Stargazin increased the IC_{50} for CNQX from 4.2 μM to 16.5 μM. What could cause the shift in apparent CNQX sensitivity? At the same time with our finding, it was shown that CNQX acts as a partial agonist at AMPA receptors co-expressed with stargazin, but not at GluR1 alone (Menuz et al., 2007). Indeed, in our hands 100 μM of
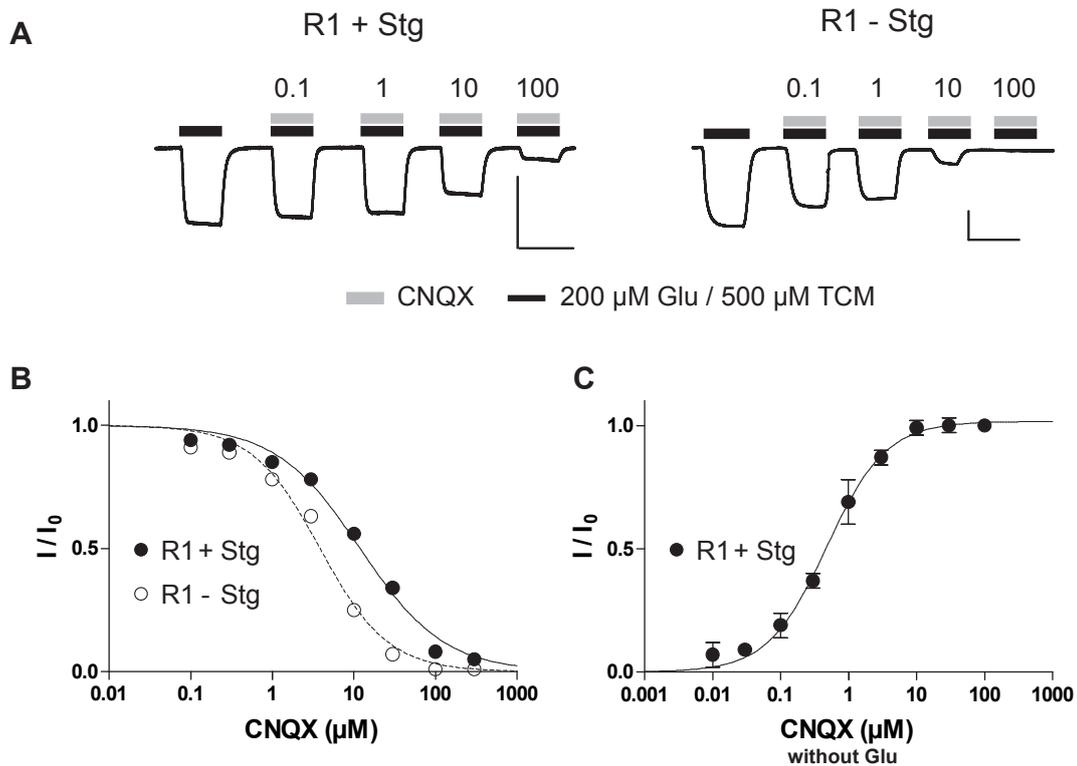
Figure 5.1: A, Representative traces of GluR1 glutamate-induced currents blocked by increasing concentrations of CNQX with (left panel) or without stargazin (right panel), scale bars 1 μA, 50 s. **B**, Dose-response curves for GluR1 with and without stargazin in the presence of CNQX and 200 μM glutamate. **C**, Dose-response curve for CNQX in the absence of glutamate, showing that CNQX is a partial agonist. Each data point represents mean ($\pm$SEM) of 5-40 oocytes.

CNQX alone evoked currents from GluR1 co-expressed with stargazin; these currents reached 9 % $\pm$ 1 % of the currents evoked by the full agonist glutamate (200 μM) (Fig. 5.2). This explains the shift of the IC_{50} towards higher concentrations of CNQX induced by stargazin. To further characterize the partial agonistic effect of CNQX we measured the dose-response curve of CNQX in the absence of glutamate. CNQX activated GluR1 receptors with an EC_{50} of 0.5 μM (Fig. 5.1C).

Next we asked the question which part of stargazin is responsible for the change in CNQX affinity. Tomita and co-workers showed that the first extracellular loop of stargazin controls gating, whereas the C-terminus is important for trafficking AMPA receptors to the surface
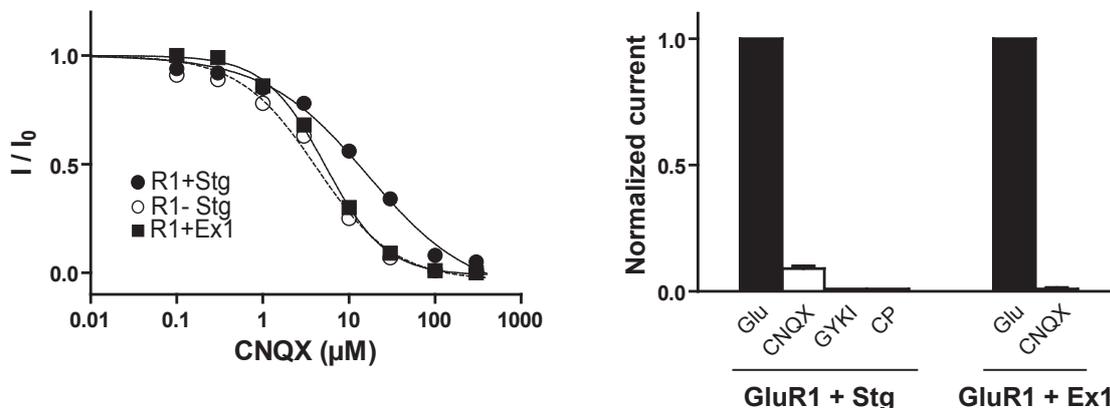
Figure 5.2: Dose-response curves of CNQX for GluR1 alone and upon co-expression with stargazin and Ex1. Bar graph shows that 100 μM CNQX alone evokes currents from GluR1 co-expressed with stargazin, but does not activate GluR1 co-expressed with Ex1. GYKI and CP alone did not evoke any currents. Each data point represents mean ($\pm$SEM) of 9-16 oocytes.

(Tomita et al., 2005). We took advantage of a construct where the ectodomain of stargazin is replaced by that of γ-5, the protein most similar in sequence to TARPs that does not regulate AMPA receptors. This γ-5-stargazin chimera (Ex1) mediates receptor trafficking but does not slow receptor desensitization and deactivation (Tomita et al., 2005).

The inhibiting effect of CNQX on GluR1 co-expressed with Ex1 was not different from GluR1 alone (Fig. 5.2). CNQX did not evoke detectable currents from GluR1 co-expressed with Ex1 (Fig. 5.2). This suggests that the ectodomain of stargazin is essential for the partial agonistic effect of CNQX.

We next focused on allosteric inhibitors, and compared their antagonism in the absence and presence of stargazin. We tested GYKI-53655 (in further text GYKI), a non-competitive inhibitor of 2,3-benzodiazepines family, and CP-465,022 (in further text CP), a quinazilonone derivative. Stargazin greatly increased the affinity of GluR1 for GYKI (IC$_{50}$: -Stg $\approx$100 μM; +Stg 38.5 μM) (Fig. 5.3A). In contrast the affinity for CP was only modestly affected by the presence of stargazin (IC$_{50}$ -Stg 1.1 μM; +Stg 0.6 μM) (Fig. 5.3B). To test whether GYKI and CP also have partial agonistic effect on GluR1 homomers associated with stargazin, we applied 300 μM GYKI or 30 μM CP in the absence of glutamate on GluR1 co-expressed with stargazin. No currents could be evoked by either GYKI or CP alone (Fig. 5.2).
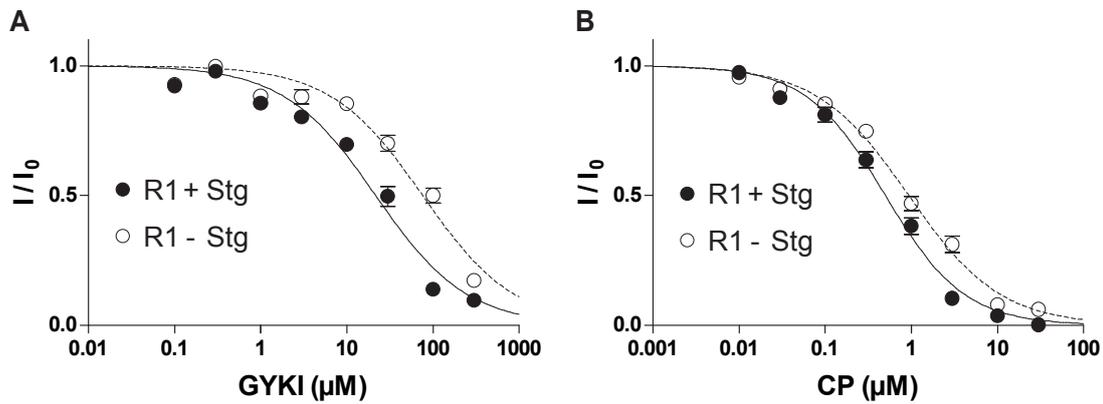
Figure 5.3: Dose-response curves of GYKI (**A**) and CP (**B**) for GluR1 and GluR1 + stargazin. Each data point represents mean (±SEM) of 5-40 oocytes.

5.1.2 Dependence of increased GluR1 sensitivity on the desensitization

It was debated in earlier studies that GYKI and the allosteric modulator cyclothiazide (CTZ) bind to the same domain of AMPA receptors (Donevan and Rogawski, 1993; Zorumski et al., 1993). Balannik and colleagues suggested that manipulations, which reduce AMPA receptor desensitization, decrease the inhibitory effect of GYKI and CP (Balannik et al., 2005). The increased affinity for GYKI in the presence of stargazin (Fig. 5.3A) could be an effect of blocked desensitization caused by TCM, a positive modulator structurally similar to CTZ (Mitchell and Fleck, 2007; Yamada and Tang, 1993). Therefore, we recorded glutamate evoked currents from GluR1^{WT} in the absence of TCM (fully desensitizing receptor) and from the non-desensitizing GluR1 mutant L497Y (GluR1^{LY}) (Stern-Bach et al., 1998) in the absence and presence of stargazin (Fig. 5.4A and B). Similarly as in the presence of TCM stargazin shifted the sensitivity of GluR1^{WT} to lower concentrations (IC$_{50}$: -Stg $\approx$ 200 μM; +Stg 28 μM), (Fig. 5.4A). This indicates that the change by stargazin is not an effect of altered desensitization.

In agreement with published data, GluR1^{LY} was less blocked by GYKI than GluR1^{WT} (Fig. 5.4B) (Balannik et al., 2005). However, there was no difference in the antagonism of GYKI on GluR1^{LY} when co-expressed with stargazin (IC$_{50}$: -Stg 300 μM; +Stg 300 μM). While stargazin enhanced the surface trafficking of GluR1^{LY}, it did not increase the glutamate evoked currents of GluR1^{LY} (Tomita et al., 2007). Together with our finding
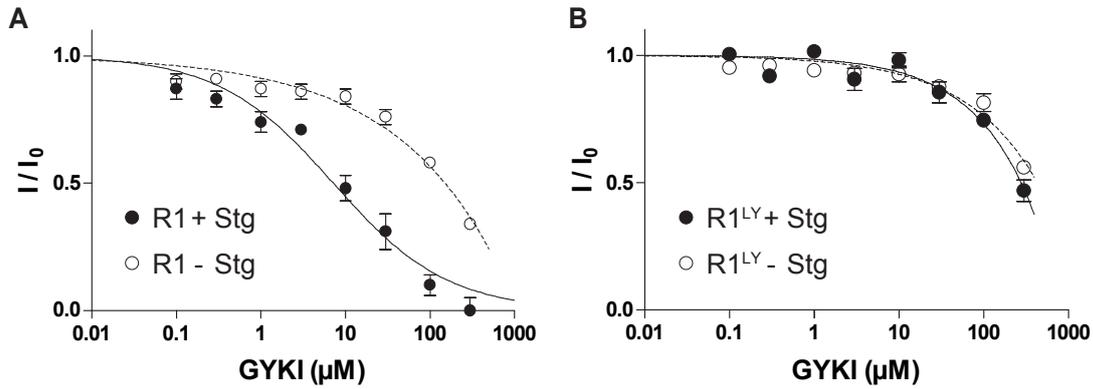
Figure 5.4: A, Dose-response curve of $GluR1^{WT}$ for GYKI in the absence of TCM. **B**, Dose-response curves of GYKI for $GluR1^{LY}$ in the presence and absence of stargazin. Each data point represents the mean ($\pm$SEM) of 14 oocytes.

this might suggest that LY mutation either alters the confirmation of the linker domains or changes the agonist efficacy occluding the effect of enhanced GYKI affinity in the presence of stargazin.

5.1.3 Effect of stargazin on GYKI- and CP-insensitive GluR1 mutants

Recently the binding sites for GYKI and CP were identified at the interface of the extracellular agonist-binding core and the transmembrane domains. The binding domains are located at the S1-M1 and S2-M4 linkers and comprise in total five changed residues (see Methods) (Balannik et al., 2005). The authors suggested that GYKI and CP interact with the S1-M1 and S2-M4 linkers, thereby disrupting the transduction of agonist binding into channel opening.

We used GYKI- and CP-insensitive variants of GluR1 ($GluR1^{GYKI}$ and $GluR1^{CP}$) to further investigate the effects of stargazin on the antagonism of the allosteric inhibitors. In agreement with published results $GluR1^{GYKI}$ and $GluR1^{CP}$ were not blocked by GYKI or CP (Fig. 5.5A and B). Surprisingly, the GYKI-insensitive mutant $GluR1^{GYKI}$ regained its sensitivity to GYKI in the presence of stargazin (IC_{50}: -Stg not determined; +Stg 100 μM, Fig. 5.5A). In contrast, the CP-insensitive mutant $GluR1^{CP}$ when co-expressed with stargazin was only modestly inhibited by higher concentrations of CP (Fig. 5.5B). Together with the finding that stargazin has only small effects on CP affinity (Fig. 5.3B), this suggests
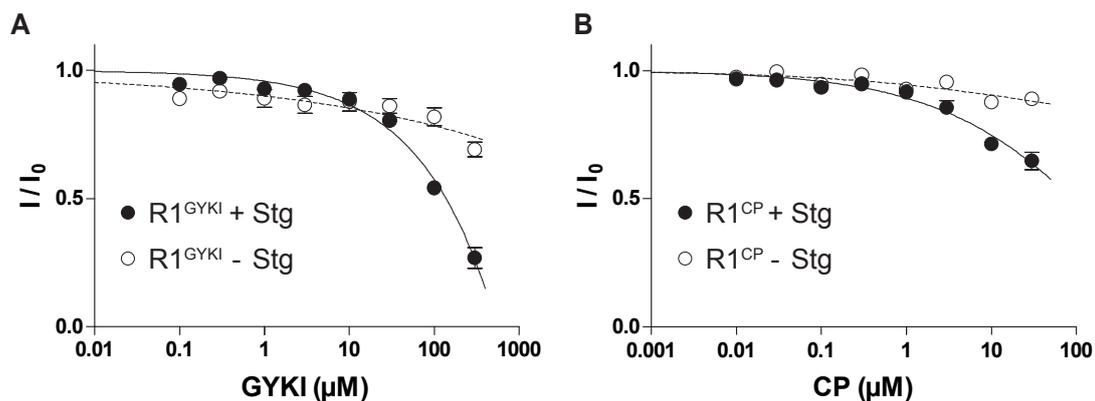
Figure 5.5: Dose-response curves of GYKI on GluR1^{GYKI} (**A**), and CP on GluR1^{CP} (**B**) in the presence and absence of stargazin.

that the binding sites for GYKI and CP might be distinct in GluR1 co-expressed with stargazin, and that stargazin only affects the GYKI site strongly.

We showed that CNQX partial agonistic effect, as well as the effect of stargazin on CNQX inhibition dose-response curve were fully abolished when GluR1 was co-expressed with Ex1 (Fig. 5.2). Does the same domain of stargazin control the effect on allosteric inhibitors? When co-expressed with Ex1, the dose response curve of GluR1^{WT} for GYKI was shifted toward higher concentrations compared to GluR1^{WT} alone (Fig. 5.6A). This suggests that mutated stargazin influences the efficacy of GYKI; however, Ex1 could have additional effects causing this shift. To further confirm that the ectodomain of stargazin modulates the antagonism of AMPA receptors, we co-expressed Ex1 with GluR1^{GYKI}. Here, the enhancing effect of stargazin was completely abolished with Ex1 (Fig. 5.6B).

5.1.4 Inhibition of GluR2^{WT} and GluR2 GYKI- and CP-insensitive mutants

To test the generality of the stargazin modulation of allosteric antagonism, we looked at the antagonism of GYKI and CP on GluR2 homomeric receptors. As the expression levels of GluR2 are extremely low without stargazin in heterologous expression systems, we only compared GluR2 to the insensitive mutants GluR2^{GYKI} and GluR2^{CP} when co-expressed with stargazin. First, we noticed that GluR2^{WT} has a lower affinity for GYKI compared to GluR1^{WT} (GluR1^{WT} + Stg: IC$_{50}$ = 38.5 μM; GluR2^{WT} + Stg: IC$_{50}$ = 100 μM) (Fig. 5.7). Similar to GluR1^{GYKI}, in the presence of stargazin GluR2^{GYKI} was sensitive to GYKI
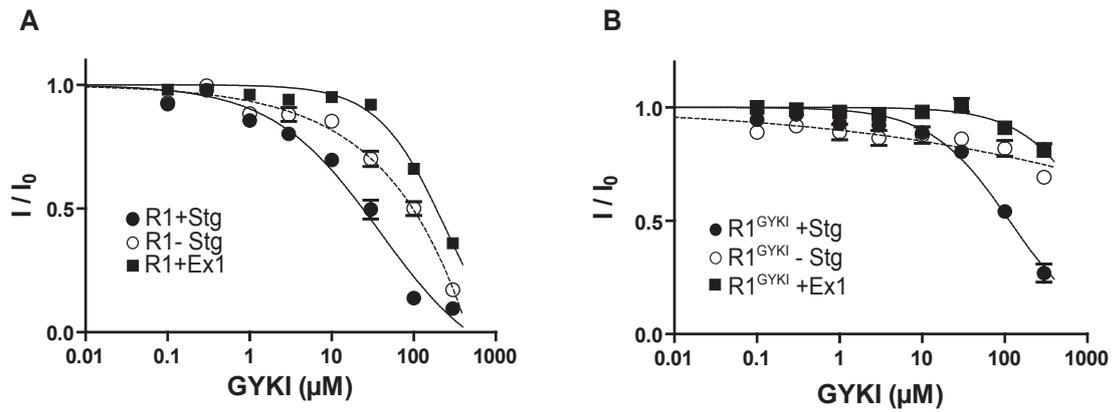
Figure 5.6: Dose-response curves of GYKI for GluR1^{WT} (**A**) and GluR1^{GYKI} (**B**) in the presence of stargazin and Ex1 chimera.
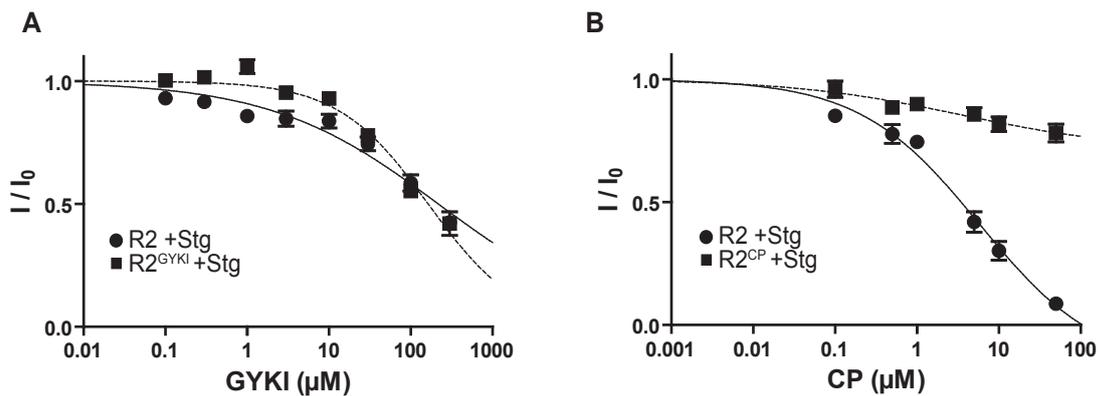
Figure 5.7: Dose-response curve of GYKI on GluR2^{GYKI} (**A**) and CP on GluR2^{CP} (**B**) compared to GluR2^{WT} response in the presence of stargazin. Each data point represents mean ($\pm$SEM) of 9-42 oocytes.

(Fig. 5.7A). In contrast, CP potently inhibited GluR2 co-expressed with stargazin, while the insensitive mutant GluR2^{CP} was not blocked by this drug (Fig. 5.7B). As the observed effects of the antagonists are qualitatively similar for GluR1 and GluR2, it seems that the mechanism of inhibition does not strongly depend on the subunit of AMPA receptors.

5.1.5 Glutamate-dose response of GluR1^{WT} and GluR1 insensitive mutants

During the course of our experiments we noticed significantly smaller glutamate evoked currents mediated by GluR1^{GYKI}, but similar current levels for GluR1^{CP} compared to GluR1^{WT}. What reduces the current of GluR1^{GYKI}? Either the efficacy of glutamate to activate the receptor is impaired such that the receptors are not fully activated by the glutamate concentration used, or the number of receptors at the surface is reduced.

First, we tested the glutamate affinity of the mutated receptors. As reported previously, stargazin increased the affinity for glutamate of GluR1^{WT} (Fig. 5.8) (Tomita et al., 2005). Interestingly, the EC$_{50}$ of GluR1^{GYKI} and GluR1^{CP} in the absence of stargazin was strongly increased to the level of GluR1^{WT} co-expressed with stargazin. Stargazin increased the gluta-
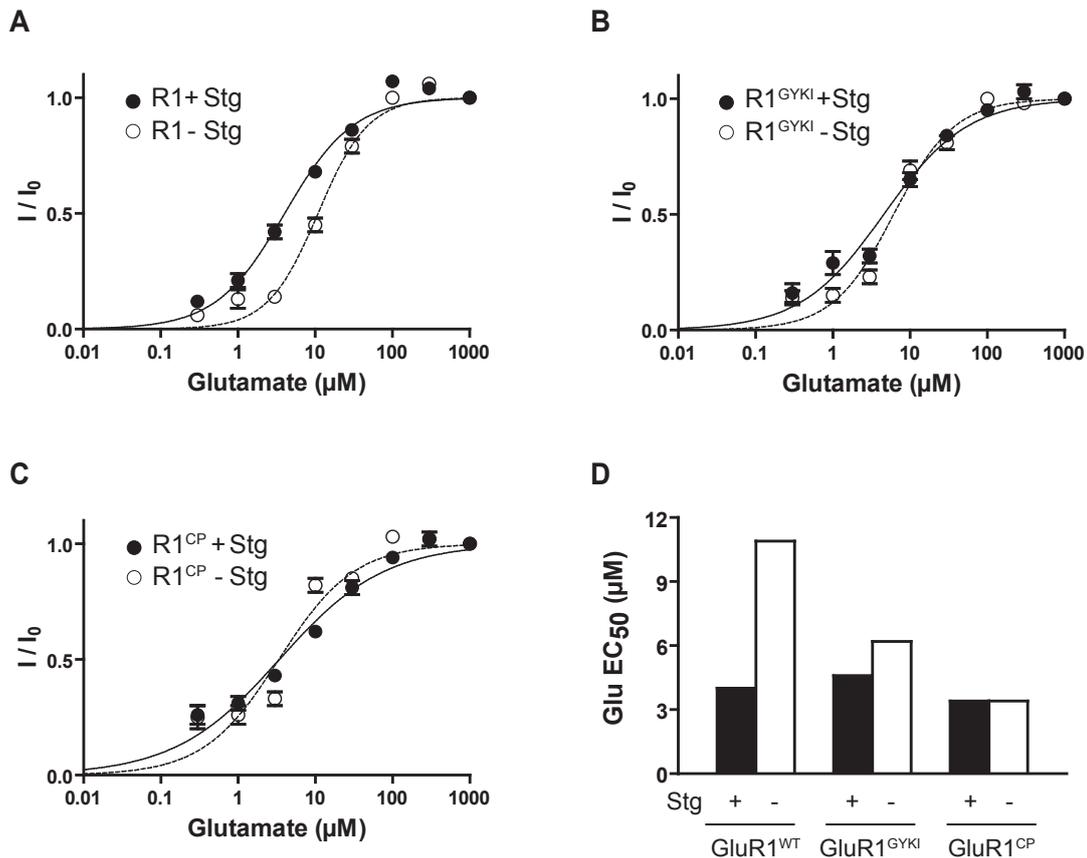
Figure 5.8: Glutamate-dose response curves for GluR1^{WT} (**A**), GluR1^{GYKI} (**B**) and GluR1^{CP} (**C**) in the presence and absence of stargazin. Each data point represents mean ($\pm$SEM) of 8-10 oocytes. **D**, EC$_{50}$ values obtained from the curves in **A**, **B** and **C**.

A

B
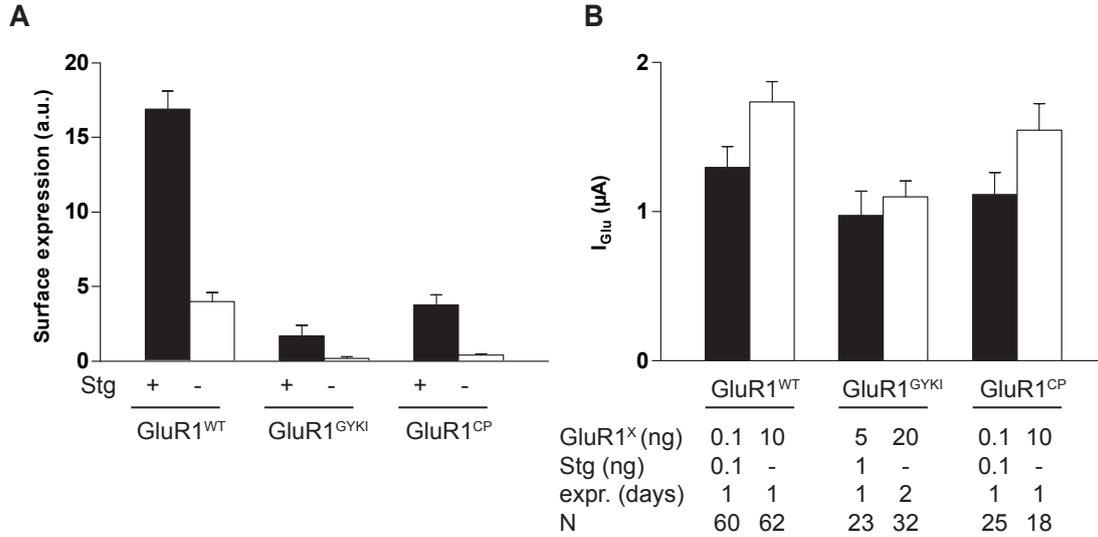
Figure 5.9: A, Surface expression of HA-tagged GluR1 receptors in the presence and absence of stargazin. Bars represent averages of 10-20 oocytes (±SEM). **B**, Oocytes expressing GluR1^{GYKI} show similar glutamate evoked currents as GluR1^{WT} and GluR1^{CP} when injected with the higher amounts of RNA and after longer expression time.

mate affinity of GluR1^{GYKI} only modestly and had no effect on GluR1^{CP} (EC$_{50}$: GluR1^{WT} - Stg = 10.94 μM, + Stg 4 μM; GluR1^{GYKI} - Stg = 6.2 μM, + Stg = 4.6 μM; GluR1^{CP} - Stg = 3.4 μM, + Stg = 3.4 μM). This shows that we fully activated all expressed receptors with the glutamate concentration used (200 μM).

5.1.6 Surface expression of GluR1 insensitive mutants

As an incomplete activation of the mutated receptors could not account for the current reduction we compared the surface expression of GluR1^{WT} to GluR1^{GYKI} and GluR1^{CP} expressed with and without stargazin. We used hemagglutinin (HA) tagged receptors to monitor the surface expression by chemiluminescence (Tomita et al., 2005; Zerangue et al., 1999). The tagging of GluR1^{WT} did not affect the current size compared to untagged receptors (data not shown). To compare surface expression we injected identical amounts of RNA. GluR1^{WT} homomeric receptors reached the surface, and coexpression with stargazin significantly increased the surface expression (GluR1 + Stg: 16.9 ± 1.2 a.u., n = 20; GluR1: 4.0 ± 0.6 a.u., n=19) (Fig. 5.9A). In contrast, GluR1^{GYKI} was found only in limited amounts

at the surface (GluR1^{GYKI} + Stg: 1.7 ± 0.7 a.u., n=10; GluR1^{GYKI} 0.2 ± 0.1 a.u., n=19). Surprisingly, trafficking of GluR1^{CP} to the surface was also impaired (GluR1^{CP} + Stg: 3.8 ± 0.7 a.u., n=19; GluR1^{CP} 0.4 ± 0.1 a.u., n=17). This indicates that the trafficking of the mutated receptors to the cell surface is impaired. We compensated for the lower expression levels of GluR1^{GYKI} by injecting higher amounts of RNA and longer expression times to obtain similar magnitudes of glutamate-evoked currents (Fig. 5.9B).

Together, these data indicate that the GYKI and CP mutations not only affect antagonist binding, but also change receptor trafficking and possibly also channel gating.

5.2 Regulation of synaptic function by PSD-95

Trafficking of AMPA and NMDA receptors controls the excitatory synaptic transmission. The synapses in the brain are highly plastic implying that synaptic receptors are dynamic and their trafficking, insertion, and internalization is tightly regulated. Insertion and removal of AMPA receptors are mechanisms underling synaptic plasticity. NMDA receptors are often regarded as a relatively stable complex in the postsynaptic membrane. However, recent studies suggest that they also move in the membrane via lateral diffusion (Zhao et al., 2008) and that subunit-composition switch of synaptic NMDA receptors is rapid in the neonatal synapses (Bellone and Nicoll, 2007). AMPA receptors are localized to synapses through binding of stargazin to PSD-95 (Schnell et al., 2002), whereas PSD-95 binds directly to the NR2 subunit of NMDA receptors. However the majority of the present data suggest that PSD-95 affects selectively AMPA currents with no effect on NMDA currents (Schnell et al., 2002; Stein et al., 2003; Beique and Andrade, 2003). Acute knockdown of PSD-95 in cultured brain slices decreases selectively AMPA currents (Elias et al., 2006), while in another study a smaller decrease in NMDA currents accompanied the AMPA currents decrease (Ehrlich et al., 2007).

Some studies reported that PSD-95 affected the presynaptic properties of a synapse. When overexpressed in dissociated hippocampal neurons, PSD-95 led to the presynaptic development since FM4-64 labeling was enhanced in presynaptic boutons opposing the PSD-95 overexpressing spines (El-Husseini et al., 2000). Futai and collegues reported that PSD-95 modulates the presynaptic release through retrograde signaling mediated by an interaction with neuroligin (Futai et al., 2007). However, PSD-95 has not been found to alter presynaptic release probability in cortical pyramidal neurons (Beique and Andrade, 2003).

Given this discrepancy in the published data about the effect of PSD-95 overexpression on synapse function, we infected CA1 hippocampal neurons with PSD-95:GFP fusion protein and investigated both presynaptic and postsynaptic changes in infected cells. In addition, we performed some experiments under different experimental conditions and addressed the question what could be the reason for different data obtained in different labs.

A

B

| -70 mV | +40 mV |

100 ms
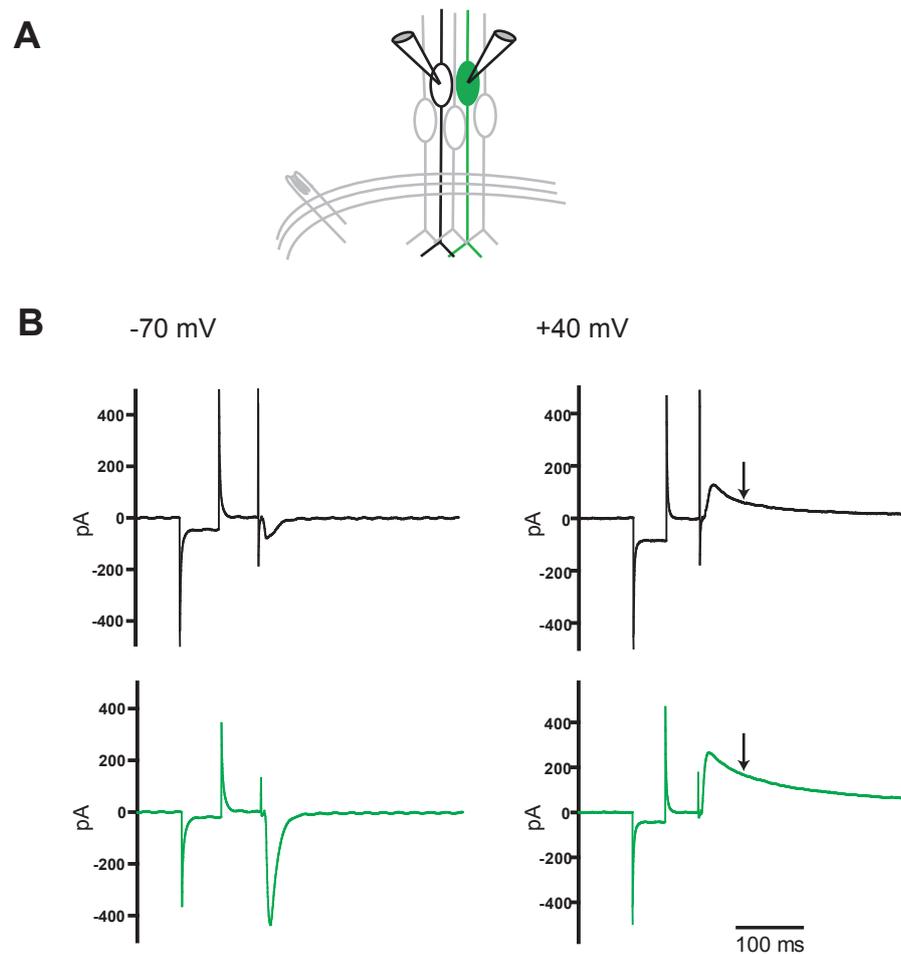
Figure 5.10: **A**, Illustration of the experimental approach used for the simultaneous recording from two cells in a slice. **B**, Example traces of non-infected (black) and infected cells (green) at -70 mV and +40 mV. AMPA currents are measured as peak currents at -70 mV and NMDA currents are measured at +40 mV, 70 ms after the stimulus (indicated by arrows). Membrane and series resistance were monitored by applying -5 mV test pulse before the stimulus.

5.2.1 Simultaneous recordings from two cells in slice

To assess the changes in synaptic function, we measured evoked AMPA and NMDA currents in infected cell and compared the amplitudes to a neighboring control, non-infected cell (Fig. 5.10A). AMPA currents were evoked by stimulating Schaffer collaterals at -70 mV. NMDA currents were measured at +40 mV, 70 ms after the stimulus artifact when AMPA currents have completely decayed. Figure 5.10B shows example current traces at -70 mV and +40

mV of a control and a PSD-95-overexpressing cell recorded simultaneously.

A Control / Control
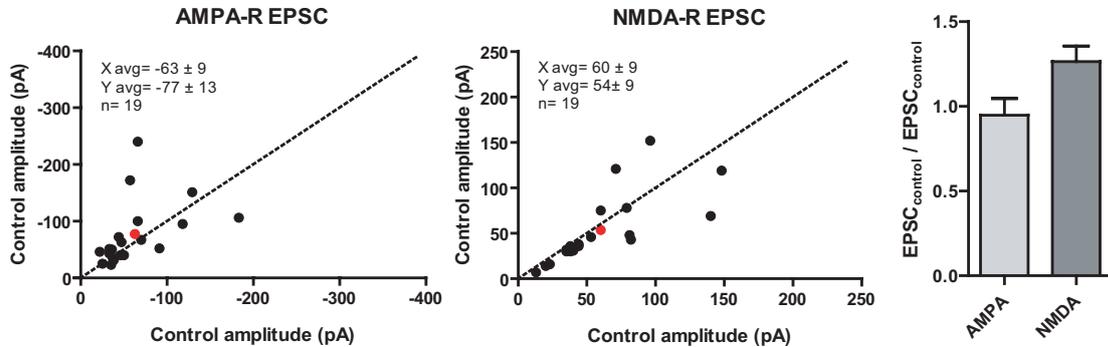
B Control / GFP
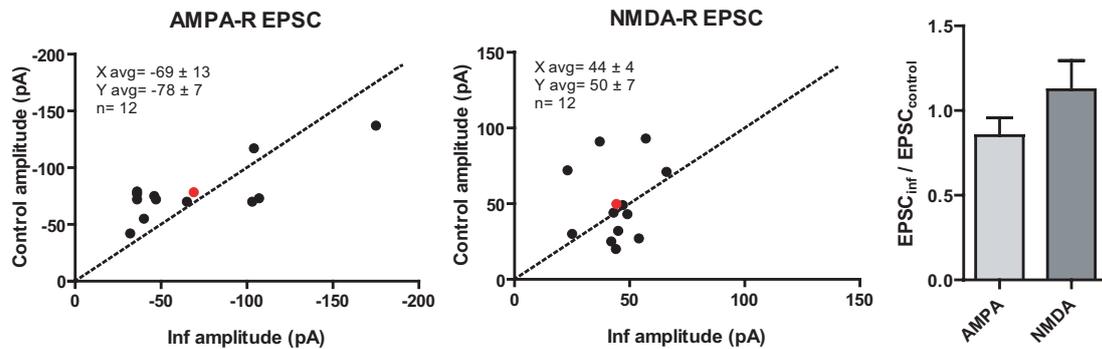
Figure 5.11: **A**, EPSC amplitudes distribution of two neighboring control cells. **B**, EPSC amplitudes distribution of GPF-infected and control cell. Each black dot on the scatter plots represents amplitudes for single pairs and red dot represents the mean.

First, we tested whether two neighboring control cells in a slice had same amplitudes given that they received same stimulus intensity. Two cells were recorded simultaneously in two different channels, 1 and 2. Measured currents were analyzed and presented in two different ways. In figure 5.11, scatter plots present the current amplitudes of cells in each pair (black dots). Cells recorded in channel 1 are plotted on X-axis and those recorded in channel 2 on Y-axis. The red dot represents the average amplitudes of each of the groups plotted as one pair. The dashed line in the scatter plots is included for the easiness of interpreting data in the graphs. When two cells of a pair have the same amplitude, the dot lays on the dashed line. The dots are shifted towards one of the axises when one group of the cells have larger

amplitudes.

Another way to present the data from paired recordings is to calculate the ratio between two cells (i.e. ratio = amplitude1 / amplitude2) and calculate the average ratio ± SEM. This is presented in the bar graphs in figure 5.11.

For both AMPA and NMDA currents of control cell pairs, the red dot was located close to the line, indicating that average amplitudes of the two cell groups were the same (Fig. 5.11A, scatter plots). However, the average ratio for AMPA currents was 0.9 ± 0.1 and for NMDA currents 1.3 ± 0.1 (Fig. 5.11A, bar graph). Given the distribution of NMDA amplitudes in the scatter plot, an average ratio of amplitudes of 1.3 ± 0.1 seems unexpected. This suggested that different ways of analyzing data, i.e. average ratio of amplitudes vs. ratio of average amplitudes could give different outcome.

The question remains whether 1.3-fold larger amplitudes in one cells group is significantly different from amplitudes in the second group. What would be the appropriate statistical test for this? The fact that current amplitudes vary significantly within the same cell from one sweep to another (which we did not take in consideration in our analysis) additionally complicates the interpretation of the data. Additional analysis, which are not in the scope of this study, will be necessary to address this problem. Throughout this study we presented both scatter plots and bar graphs.

PSD-95 used in this study was fused to GFP. To test whether GFP expression alone had some effect on the synaptic currents, we overexpressed GFP using the Semliki Forest virus system and recorded from infected and neighboring control cell (Fig. 5.11B). The average ratio between GFP overexpressing cell and control cell was 0.9 ± 0.1 for AMPA current and 1.1 ± 0.2 for NMDA current.

From these two control experiments we concluded that simultaneous recording from two neighboring cells in the slice was reliable approach to directly compare current size of the two cells.

5.2.2 Effect of PSD-95 overexpression on synaptic AMPA and NMDA currents

PSD-95 is a scaffolding protein located in the spines of glutamergic synapses (Cho et al., 1992). We tested whether the PSD-95:GFP fusion protein used in our study had normal spine

A GFP

B PSD-95:GFP
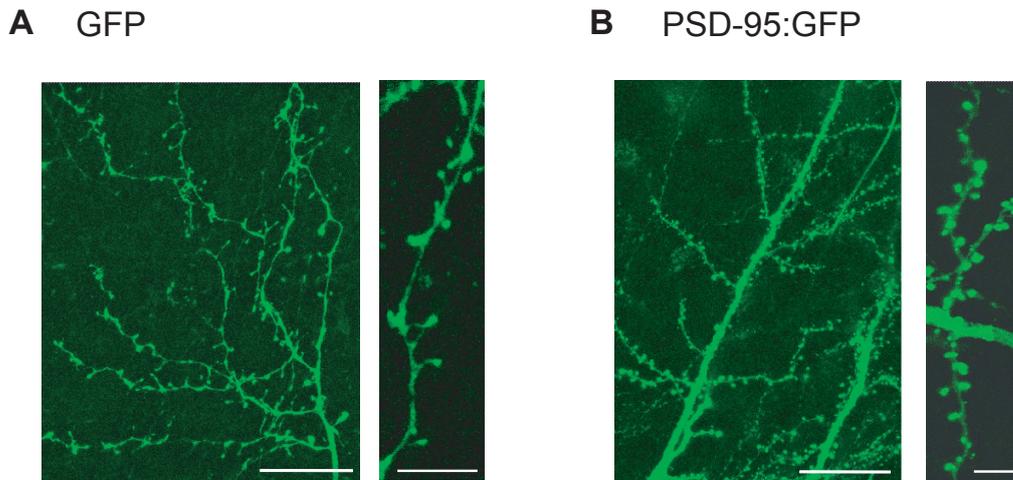
Figure 5.12: **A**, Confocal image of GFP infected CA1 cell in organotypical hippocampal slice. Scale bars: left panel 20.2 μm, right panel 6.4 μm. **B**, PSD-95 overexpressing cell showing PSD-95 localization to synaptic spines. Scale bars: left panel 27.7 μm, right panel 6.0 μm.

localization. Unlike GFP, which showed homogeneous distribution in both dendritic shafts and spines, CA1 hippocampal neurons overexpressing PSD-95:GFP showed a punctated GFP signal pattern, indicating that PSD:GFP was localized to spines (Fig. 5.12A and B).

As reported in previous studies (Schnell et al., 2002; Stein et al., 2003; Ehrlich et al., 2007; Beique and Andrade, 2003), we observed that the AMPA receptor component of excitatory currents was dramatically increased in the cells overexpressing PSD-95 (Fig. 5.13A and B). On average, the infected cell had 4.5 $\pm$ 0.4-fold larger AMPA current than the neighboring control cell. Interestingly, the NMDA receptor component was also increased. The infected cells showed on average 1.8 $\pm$ 0.1-fold increase (Fig. 5.13A and B). We correlated the AMPA and NMDA EPSCs increase for each pair and for the most of the cells there was a correlation between AMPA and NMDA current increase (Fig. 5.13C). That led us to a hypothesis that a synapse with higher AMPA receptor component would most likely have higher NMDA receptor component. We discussed that further in the section 5.2.4.2.
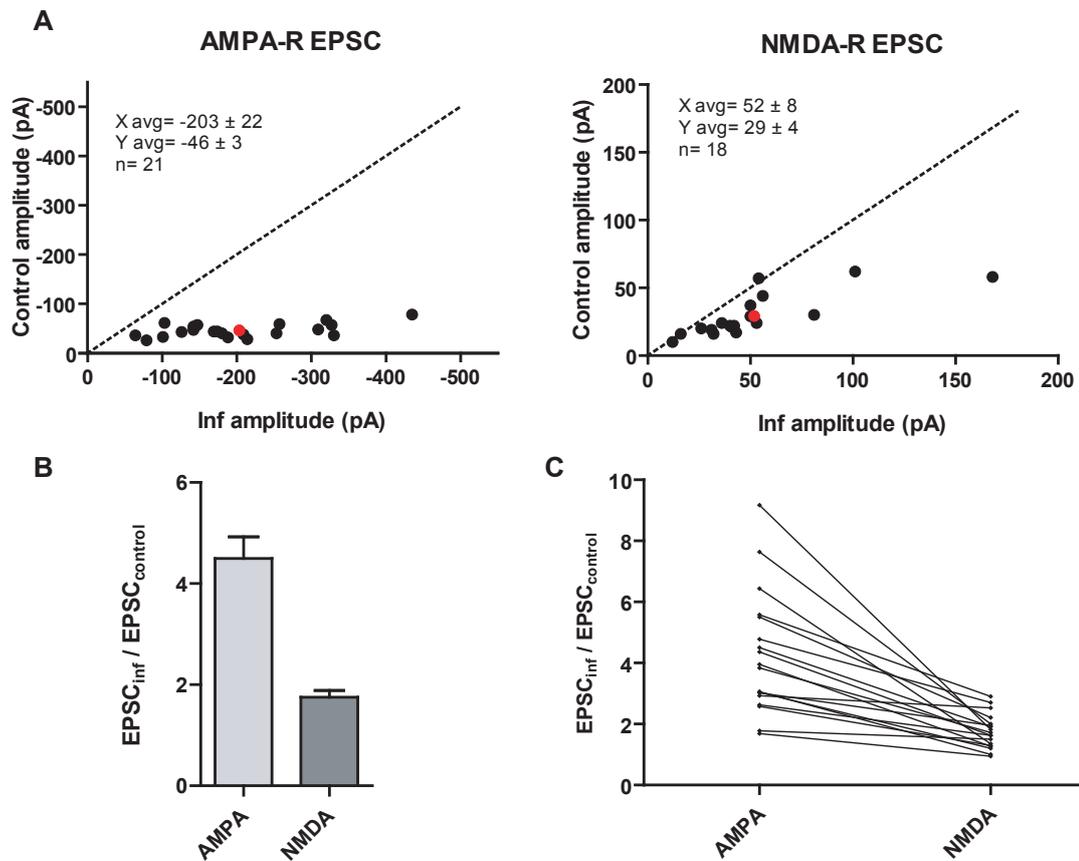
Figure 5.13: A, Distributions of EPSC amplitudes show an increase in AMPA and NMDA currents for PSD-95-infected cell. **B**, Average increase for AMPA and NMDA currents. **C**, Plotted AMPA and NMDA EPSC ratios of each cell pair. AMPA and NMDA ratios of the same pair are connected with a line.

5.2.2.1 Impact of different experimental conditions on the PSD-95 effect

Given that NMDA receptors interact directly with PSD-95, one would expect an increase in NMDA currents upon overexpression of PSD-95. However, most of the previous studies published did not observe such an effect. In order to address the question what could be the possible reason for this difference, we measured AMPA and NMDA currents from PSD-95-overexpressing and control cells under experimental conditions used in the other studies.

First we changed the rat strain we used for obtaining hippocampal slices. Initially, we used Wistar rats whereas all of the previous studies used slices from Sprague Dawley rats. We hypothesized that two strains may differ in the protein expression profiles of either

Figure 5.14: Distributions of EPSC amplitudes show an increase in both AMPA and NMDA currents in PSD-95-infected cell in the Sprague Dawley slices.

members of MAGUK family or NMDA receptors subunits or other proteins involved in NMDA receptors trafficking and function. Therefore we overexpressed PSD-95 in Sprague Dawley slices and tested the effect of PSD-95 on AMPA and NMDA currents. We could still observe an effect on both AMPA and NMDA currents (Fig. 5.14). The ratio between infected and control cell was 5.2 ± 1.1 for AMPA receptor component and 2.3 ± 0.3 for NMDA receptor component. The increase in EPSCs was even slightly larger in Sprague Dawley slices. All the following experiments we performed using slices from the Wistar rats.

Another possible reason for the difference in the PSD-95 effects observed in different labs could be different culturing conditions of slices. Namely, antibiotics like penicillin and streptomycin, are often included in slice media to prevent the slice contamination. Interestingly, effects of these antibiotics on synaptic transmission have been reported. For example, penicillin is GABA-A receptors antagonist that can lead to epileptiform bursting when applied to slice cultures (Schneiderman et al., 1994). This bursting in turn causes NMDA-dependent plastic changes which produce long-lasting network oscillations *in vitro*. On the other hand, aminoglycosides like streptomycin, kanamycin and neomycin, are shown to modulate the agonist response of NMDA receptors in a similar manner that extracellular polyamines do (Harvey and Skolnick, 1999). In particular, they potentiate the agonist responses in a glycin-dependent and voltage-independent manner. Taking these data in consideration, it could be possible that the PSD-95 effect on NMDA receptor component was masked in the previous studies due to the action of penicillin and/or streptomycin.

When we cultured the slices from the Wistar rats in the presence of penicillin and strepto-

Figure 5.15: Distributions of EPSC amplitudes show an increase in both AMPA and NMDA currents in PSD-95-infected cell in Wistar slices cultured in the presence of penicillin and streptomycin.

mycin we could still observe PSD-95-mediated potentiation in both AMPA (5.8 ± 0.5-fold) and NMDA (3.2 ± 0.4-fold) currents (Fig. 5.15). Both AMPA and NMDA receptor component were enhanced more strongly in the presence of antibiotics than in the absence of antibiotics. For the rest of the study we omitted antibiotics in our culturing medium.

Beside the culturing conditions, we also varied some recording conditions. In particular, when rectification of AMPA receptors is measured, the polyamine spermine is included in the patch pippete. Spermine blocks Ca^{2+}-permeable AMPA receptors at positive potentials and makes rectification more pronounced and easier to measure. Interestingly, spermine exhibits an effect also on NMDA receptors. It has been reported that intracellular spermine has a direct inhibitory effect on NMDA receptors by decreasing the open probability of NMDA receptor channels in a dose-dependent manner (Turecek et al., 2004).

When we included 0.1 mM spermine in the intracellular solution the AMPA receptor component was still increased in PSD-95-overexpressing cells (Fig. 5.16), though to lower extent compared to the other conditions (3.3 ± 0.8-fold), whereas the NMDA currents were enhanced in the similar manner (2.3 ± 0.4-fold).

The PSD-95 effect on both AMPA and NMDA currents was therefore consistent in all experimental conditions we used. The summary of the results is shown in figure 5.17. There may be some other causes for the observed differences between us and other labs. For example, the expression level of PSD-95 in the infected cells may be higher under our conditions, therefore leading to more robust effect on AMPA currents, but also enabling the effect on
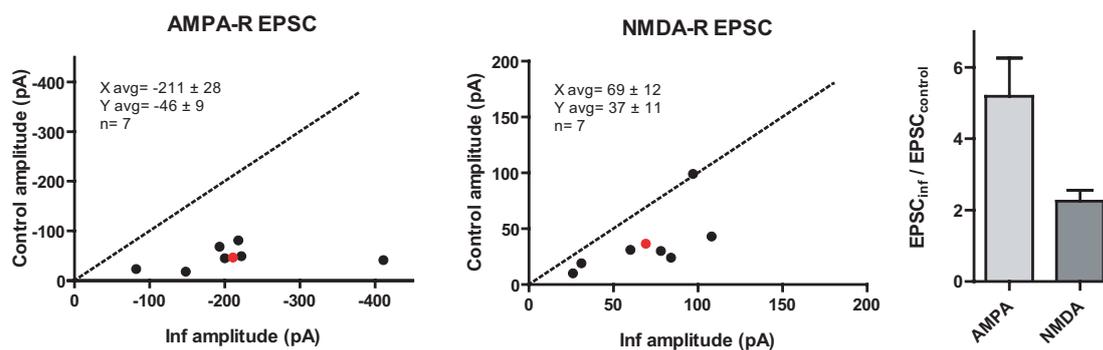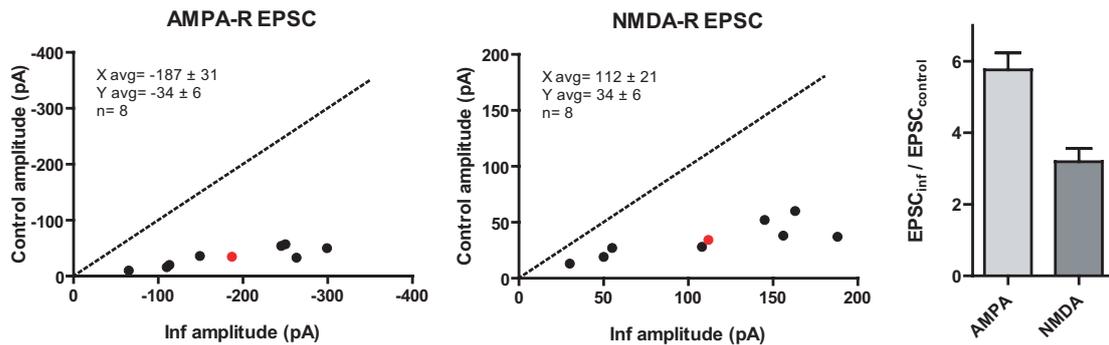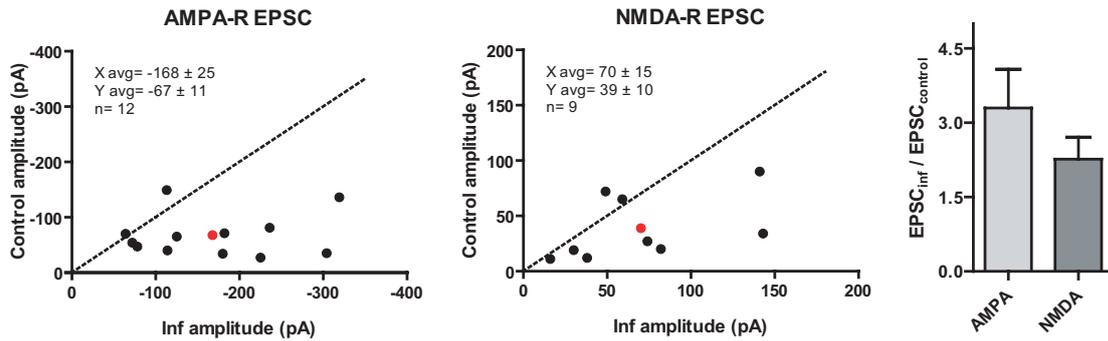
Figure 5.16: Distributions of EPSC amplitudes show an increase in both AMPA and NMDA currents for PSD-95-infected cell recorded in the presence of 0.1 mM spermine in the intracellular solution.
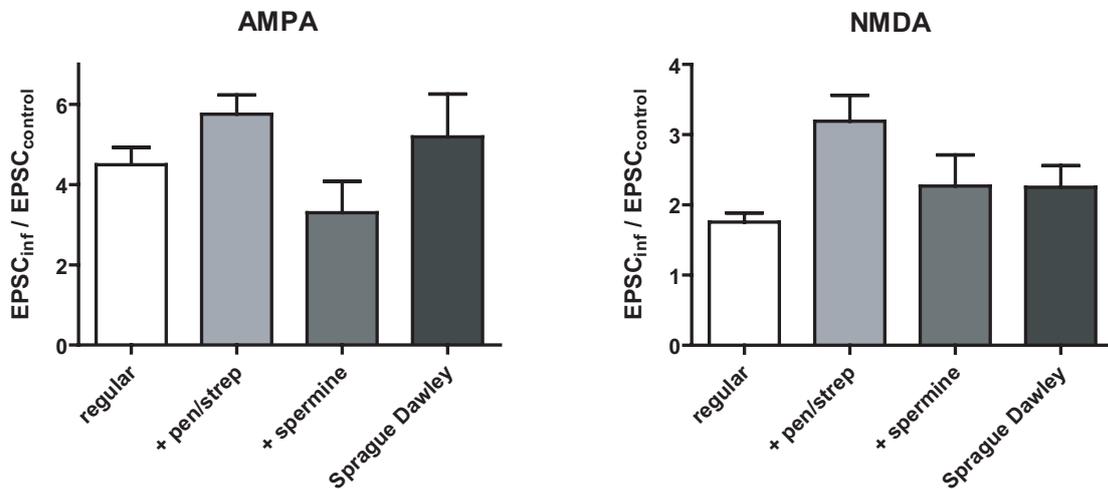
Figure 5.17: Summary of all conditions used and the corresponding AMPA and NMDA ratios between infected and control cells. "Regular" refers to the culturing in the absence of antibiotics and recording with the intracellular solution without spermine.

NMDA currents to be measured. The other factors, such as onset and length of PSD-95 expression, may be important. Alternatively, the number of manipulated neurons in the network may affect the outcome.

5.2.2.2 Measurements of isolated NMDA currents

We measured NMDA current as a late component (70 ms after the stimulus) of the compound current at + 40 mV. To exclude a possibility that our measured NMDA current was
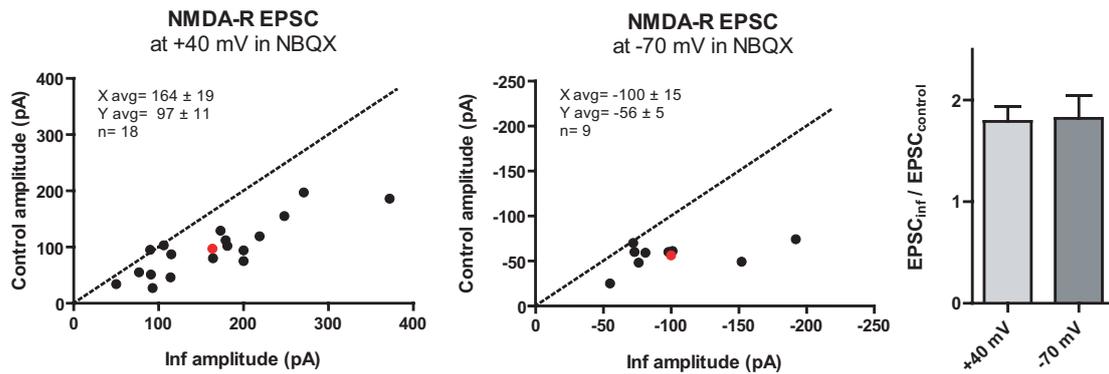
Figure 5.18: NMDA EPSCs distribution measured at +40 mV in the presence of NBQX and at -70 mV in the presence of NBQX and low magnesium concentration.

contaminated by AMPA component that had not fully decayed at 70 ms, we isolated NMDA currents by blocking AMPA currents with 10 μM NBQX included in the recording solution. NMDA EPSC amplitude was measured as a peak current at +40 mV. NMDA currents measured from cells overexpressing PSD-95 showed 1.8 ± 0.1-fold potentiation compared to the control cells, same potentiation we observed when NMDA currents were measured as a late component of compound current without NBQX in the bath (Fig. 5.18).

Another way to measure NMDA currents is to record a cell at -70 mV in a low magnesium concentration (0.1 mM). Under these conditions NMDA receptors are not blocked by Mg^{2+}, so no depolarization is necessary to release the block. Measuring at negative potentials, i.e. being closer to the cell resting potential, leads to the smaller "voltage escape" (Williams and Mitchell, 2008). Namely, the synaptic potentials are progressively attenuated as they spread from the site of origin (dendritic tree) to the soma where they are measured. Therefore, in order to measure the NMDA currents more accurately, we clamped the cell at -70 mV in the presence of low Mg^{2+} and NBQX and compared the amplitudes of PSD-95 overexpressing cell and control cell. Again the PSD-95 cells showed 1.8 ± 0.2-fold increase in NMDA currents, similar to the other measurements (Fig. 5.18).

From these data we concluded that increased NMDA currents we observed were not a measurement artifact.

5.2.3 Presynaptic effects of PSD-95 overexpression

From the data shown above we concluded that overexpression of PSD-95 leads to the robust increase in AMPA receptor component, as reported by others, and milder, but significant increase in NMDA receptor component. The next step was to investigate what underlies this enhancement of synaptic strength in PSD-95-overexpressing cells.

Some studies suggested that PSD-95 might affect the presynapse by a retrograde mechanism and change the release probability of neurons (Migaud et al., 1998; El-Husseini et al., 2000; Futai et al., 2007). To test if PSD-95-infected cells in cultured hippocampal slices have altered release probability, we used several experimental paradigms to monitor for presynaptic changes.
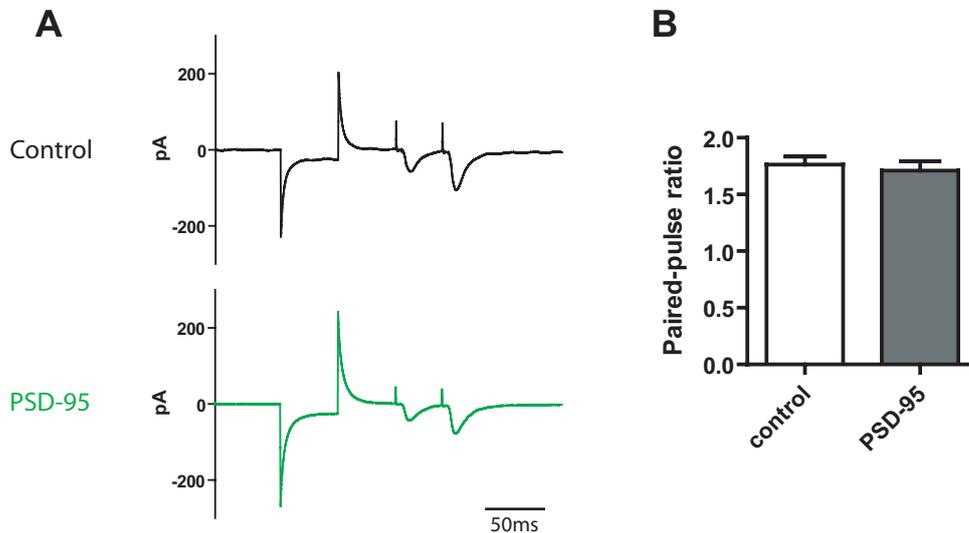
Figure 5.19: A, Example current traces of control and PSD-95-infected neuron as response to successive stimuli (40 ms interval). **B**, Bar graphs representing the average paired-pulse ratio obtained from 19 cells for each condition.

5.2.3.1 Paired-pulse ratio in PSD-95-infected cells

Paired-pulse ratio (PPR) is a measurement of the presynaptic release probability. In this paradigm we delivered two stimuli to a cell in a 40 ms interval and calculated the ratio between the second and the first synaptic response (Fig. 5.19A). At 40 ms inter-stimulus interval the ratio between the second and the first amplitude was larger than 1. This facili-

tation of the second synaptic response can be explained by residual Ca^{2+} in the presynapse after the first stimulus.

As shown in figure 5.19B, the PPR values of control and PSD-95-infected cells were not significantly different (1.8 ± 0.1 and 1.7 ± 0.1, respectively), indicating that PSD-95 does not alter presynaptic release probability.

5.2.3.2 NMDA receptor block by MK-801

To further test for the modulation of presynaptic release by PSD-95, we used MK-801, an open-channel blocker of NMDA receptors. In the presence of MK-801, isolated NMDA currents are blocked in a stimulus-dependent way; this block occurs at a faster rate at synapses with higher release probability and a slower rate at synapses with lower release probability. Decay curves were fit with single exponential function and decay constants were given in the stimulus number. We compared block of control and PSD-95-overexpressing cell in the presence of 40 μM MK-801. The rate of block of NMDA receptors in cells overexpressing PSD-95 was not significantly different from control cells: control: $\tau=$ 25 stimuli, PSD-95: $\tau=23$ stimuli (Fig. 5.20A), indicating that there was no difference in the release probability between the two groups.
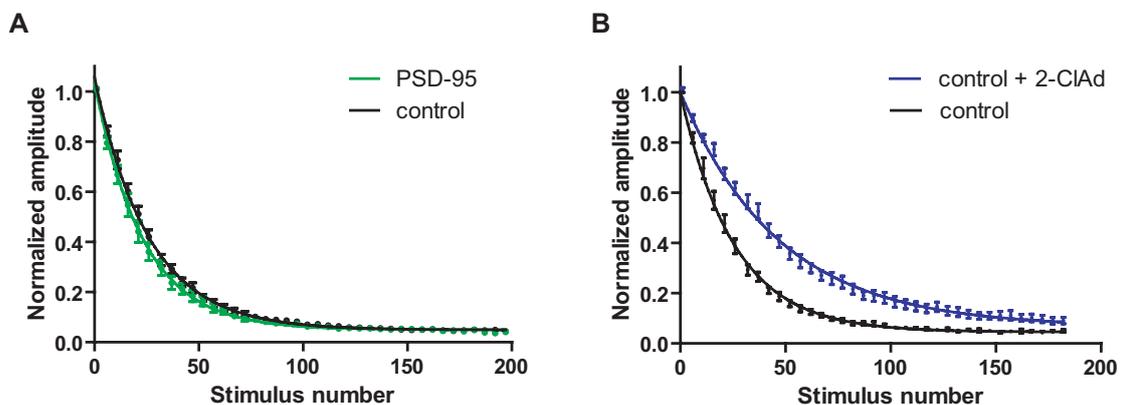
Figure 5.20: A, Averaged normalized NMDA receptor EPSCs during the perfusion with MK-801 for control and PSD-95 overexpressing cell (n=18 pairs). **B**, Control cells from the experiment in (**A**) were compared to 11 control cells measured in the absence of 2-ClAd. Amplitudes are the average of each five consecutive EPSCs normalized to that of the first five averaged EPSC in the presence of MK-801.

In order to test that we could measure the differences in release probability using this method, we compared the decay kinetics of control cell in the absence and in the presence of 2-chloroadenosine (2-ClAd). 2-ClAd decreases release probability by acting on the presynaptic adenosine receptors. As expected, the block of cells by MK-801 was faster in the absence of 2-ClAd than in the presence (Fig. 5.20B). Decay constants for the control cells in the presence of 2-ClAd was $\tau = 47$ stimuli.

5.2.3.3 Sensitivity of release probability to extracellular Ca^{2+}

Futai and co-workers found that overexpression of PSD-95 increases the sensitivity of presynaptic release machinery to extracellular Ca^{2+}, which leads to higher AMPA and NMDA currents in PSD-95-overexpressing cells (Futai et al., 2007). When extracellular concentration of Ca^{2+} was increased to saturating concentration (10 mM, release probability maximal), difference between control and PSD-95 cell was occluded. As another test for presynaptic effects of PSD-95, we compared the NMDA current-ratio between infected and control cell in the presence of 2 mM and 10 mM Ca^{2+} concentrations to the one we already measured in 4 mM Ca^{2+}.
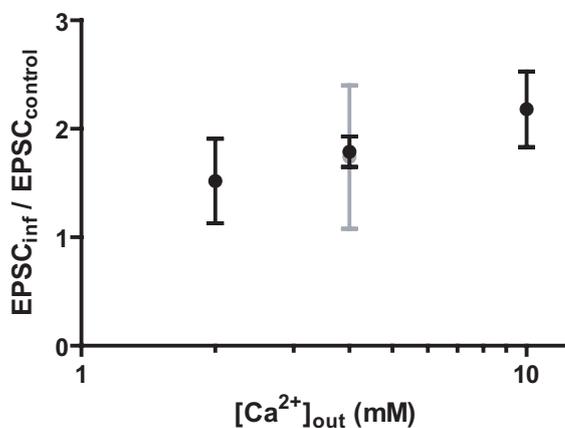
Figure 5.21: NMDA EPSCs ratios of PSD-95-infected to control cells in different extracellular Ca^{2+} concentration. Number of cell pairs: 2 mM, 10; 4 mM, 18; 10 mM, 8; 4 mM w/o 2-ClAd (gray), 7.

If enhancing effect of PSD-95 on NMDA currents resulted from higher release probability in infected cells, the NMDA ratio should be lower at higher Ca^{2+} concentrations. We could

not observe any significant differences (one way ANOVA test) in NMDA EPSCs enhancement in all concentrations tested: 2 mM: 1.5 ± 0.4; 4 mM: 1.8 ± 0.1; 10 mM: 2.2 ± 0.3 (Fig. 5.21). In addition, we measured the infected to control cell NMDA EPSC ratio in 4 mM Ca^{2+} in the absence of 2-ClAd. Under this condition the release probability was higher than in the presence of 2-ClAd, but the ratio we measured was not different from the one in the presence of 2-ClAd (1.7 ± 0.7, Fig. 5.21).

From these data we concluded that overexpression of PSD-95 in the postsynaptic cell did not lead to functional changes in opposing presynaptic boutons.

5.2.4 Postsynaptic effects of PSD-95 overexpression

Overexpression of PSD-95 led to enhanced AMPA and NMDA currents. We concluded that this enhancement was not mediated by the presynaptic changes. What could be the postsynaptic mechanisms that mediated this enhancement? Expression of PSD-95 increases the number of synaptic AMPA receptors by mechanism that requires the interaction of PSD-95 with stargazin (Schnell et al., 2002; Ehrlich et al., 2007). PSD-95, similarly to LTP, increases the amplitude and frequency of mEPSCs and converts silent synapses to functional synapses (Stein et al., 2003). How are the NMDA receptors currents increased upon overexpression of PSD-95? One possibility is that the composition of synaptic NMDA receptors is changed leading to the higher amplitudes or that PSD-95 changes functional properties of existing NMDA receptors. Another possibility is that, similarly to AMPA receptors, the number of synaptic NMDA receptors is increased.

5.2.4.1 PSD-95 overexpression and NMDA receptors subunit composition

NR2B-containing NMDA receptors have a slower decay kinetic compared to NR2A-containing receptors and are selectively blocked by the antagonist ifenprodil (Cull-Candy and Leszkiewicz, 2004). Overexpression of PSD-95 could recruit more NR2B-containing NMDA receptors to synapses. That would result in both slower decay of the currents and higher EPSC amplitudes. We calculated the decay time as previously described (Cathala et al., 2005) (see also Methods) from the traces of isolated NMDA currents measured at +40 mV in the presence of NBQX (Fig. 5.18). The decay constant was not significantly different be-
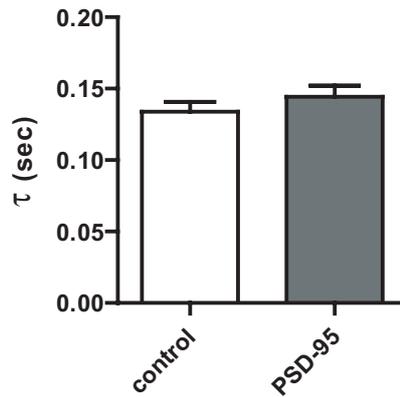
Figure 5.22: Bar graphs of NMDA EPSC decay time constants obtained from 19 cell pairs.

tween PSD-95 overexpressing and control cell: 0.14 ± 0.01 s and 0.13 ± 0.01 s, respectively. This result indicates that overexpression of PSD-95 did not lead to a change in the NMDA receptors subunit composition.

There is evidence that PSD-95 changes some of the channel properties of NMDA receptors. Li and colleagues reported that during development NMDA receptor desensitization is decreased and this was not dependent on the subunit switch but was correlated with synaptic localization of the receptors (Li et al., 2003). The authors showed that overexpession of PSD-95 reduced the NMDA receptor desensitization in immature neurons, whereas uncoupling of the receptors from PSD-95 in mature neurons increased receptors desensitization. In a more recent study Sornarajah and colleagues found that NMDA receptor desensitization is regulated by direct binding of PSD-95 (Sornarajah et al., 2008). We did not follow up this hypothesis, but we could not exclude the possibility that PSD-95 exhibited some effects on NMDA receptor biophysical properties.

5.2.4.2 Coordinated trafficking of AMPA and NMDA receptors

After excluding the presynaptic effect of PSD-95 expression and a change in a subunit-composition of NMDA receptors, we concluded that PSD-95 increases the number of NMDA receptors. This increase was not as robust as increase in AMPA receptors number, even though PSD-95 interacts directly with NMDA receptors and only indirectly with AMPA receptors.

We asked the question whether increased NMDA currents were a direct effect of PSD-95 or an indirect effect, i.e. a consequence of the increased number of AMPA receptors. Trafficking of AMPA receptors and NMDA receptors is mostly considered to be independent, as for example in LTP where AMPA receptors are rapidly and selectively inserted into the synapse. But this raises the question of how a constant AMPA/NMDA ratio is preserved in the synapses with ongoing plasticity. Turrigiano and colleagues reported that upon LTP a rapid and long lasting increase in AMPA receptor component is followed by delayed but also long-lasting potentiation of NMDA receptor component (Watt et al., 2004). It could be that PSD-95, similarly to LTP increases AMPA receptor number, and NMDA receptors follow AMPA receptors in order to restore AMPA/NMDA ratio of synapses. This way the effect of PSD-95 on NMDA receptors would be indirect.
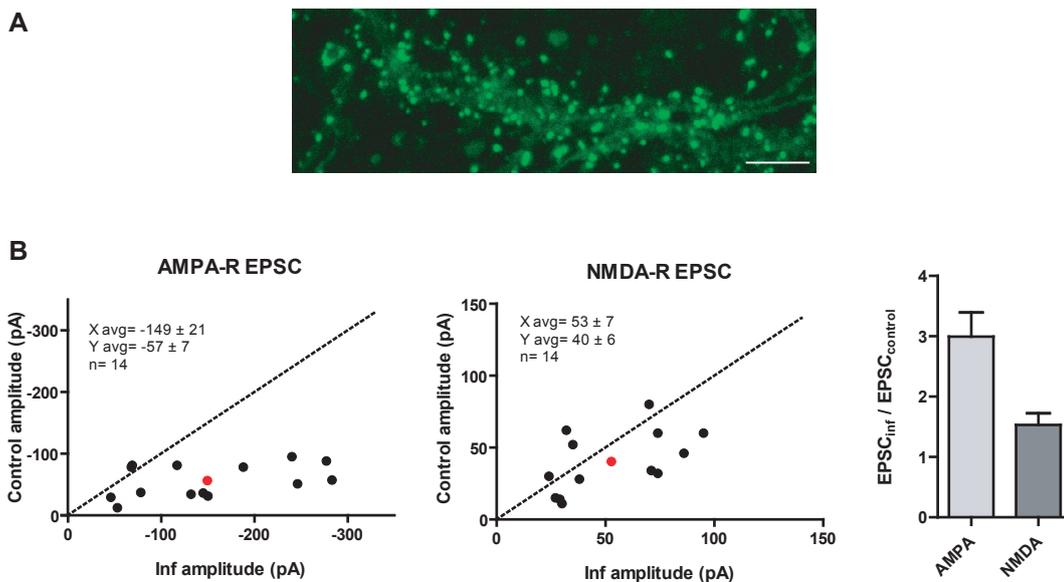
Figure 5.23: A, Spine labeling of cell overexpressing PSD-95-HV:GFP. Scale bar 4.3 μm. **B**, Distributions of AMPA and NMDA EPSC amplitudes for PSD-95-HV-infected and control cell with bar graphs showing average AMPA and NMDA ratios.

We aimed to test whether PSD-95 effect on NMDA receptors is dependent on the effect on AMPA receptors. In other words, would PSD-95 still lead to an increase in NMDA receptor component under conditions where AMPA receptor component is not changed? To this end we used the mutant version of PSD-95 where presumably interaction with stargazin and

therefore with AMPA receptors is disrupted (Schnell et al., 2002). This mutant version of PSD-95 has one point mutation in the PDZ domain 1 (H130V) and one in the PDZ domain 2 (H225V) that converts interaction of PSD-95 from a class I to a class II PDZ/ligand interaction. We overexpressed this PSD-95 mutant (PSD-95-HV) and looked at AMPA and NMDA currents.

The PSD-95-HV mutant showed localization to spines when overexpressed in CA1 cells (Fig. 5.23A). Much to our surprise, PSD-95-HV still showed 3.0 ± 0.4-fold increase in AMPA currents compared to control cell (Fig. 5.23B), suggesting that interaction of PSD-95 with TARPs was not disrupted or PDS-95 interacted directly with AMPA receptors. We could not exclude the possibility that PSD-95-HV interacted with a set of class II ligands (for example, GluR2 or Ephrin B1), that could indirectly lead to increase in AMPA receptors number. NMDA receptor component showed milder, 1.5 ± 0.2-fold increase.

Given that PSD-95-HV mutant has still an effect on AMPA currents, we could not use this construct to dissociate PSD-95 effect on AMPA and NMDA currents.

5.2.5 Mechanism of PSD-95 effect on synaptic AMPA and NMDA receptors

5.2.5.1 Overexpression of PSD-95/PSD-93 chimeras

Next we asked the question whether the effect on synaptic receptors is limited to PSD-95 or the other members of MAGUK family exhibit the similar effect. In the study of Elias and colleagues, when PSD-93 was overexpressed in hippocampal organotypic slices, infected cell showed approximately 2-fold increase in AMPA receptor component and no effect in NMDA receptor component (Elias et al., 2006). We overexpressed PSD-93:GFP in hippocampal slices and similarly to PSD-95, PSD-93 showed spine labeling (Fig. 5.24A). Cells overexpressing PSD-93 showed an 1.6 ± 0.1-fold increase in AMPA currents and 1.6 ± 0.2-fold increase in NMDA currents (Fig. 5.24B), indicating that the effect of PSD-93 on synaptic currents was much milder compared to PSD-95.

What is the reason for the different effect of PSD-95 and PSD-93 on synaptic currents? We compared the protein sequence of the two members of MAGUK family. Even though the overall structure of PSD-95 and PSD-93 is similar, they differ in their N-termini preceding the first PDZ domain (Fig. 5.25). We proceeded with exchanging the N-termini between

A

B
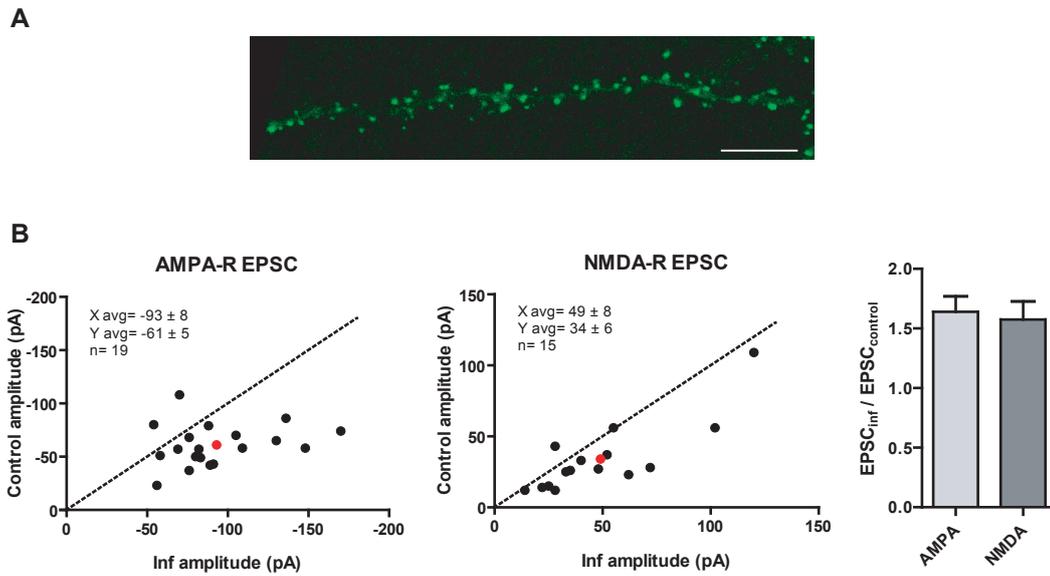
Figure 5.24: **A**, Confocal image of CA1 cell overexpressing PSD-93:GFP showing spine localization of PSD-93. Scale bar 6.8 μm. **B**, Distributions of AMPA and NMDA EPSC amplitudes for PSD-93-infected and control cell with bar graphs showing average AMPA and NMDA ratios.

```
PSD-93 MFFACYCALRTNVKKYRYQDEDG-PHDHSLPRLTHEVRGPELVHVSEKNL
PSD-95 M--DCLCIVTT--KKYRYQDEDTPPLEHSPAHLPNQANSPP-V-------

PSD-93 SQIENVHGYVLQSHISPLKASPAPIIVNTDTLDTIPY---VNGTEIEYEF
PSD-95 ------------------------IVNTDTLEAPGYELQVNGTEGEMEY

PSD-93 EEITLERGNSGLGFSIAGGTDNPHIGDDPGIFITKIIPGGAAAEDGR...
PSD-95 EEITLERGNSGLGFSIAGGTDNPHIGDDPSIFITKIIPGGAAAQDGR...
       |----------------- PDZ1 ----------------------...
```

Figure 5.25: Protein sequence alignment of the PSD-95 and PSD-93 N-termini. The non-homologous amino acids are shown in red. Three amino acids which are phosphorylated by Cdk5 in PSD-95 and corresponding amino acids in PSD-93 are marked with squares.

PSD-95 and PSD-93 to test if the chimeras PSD-95(N93), i.e. PSD-95 with the N-terminus of PSD-93 and PSD-93(N95), i.e. PSD-93 with the N-terminus of PSD-95, still exhibit the observed effects on AMPA and NMDA currents as the wild types. Importantly, both chimeras had normal spine localization as shown in figure 5.26.

PSD-95(N93) led to a 1.9 $\pm$ 0.2-fold increase in AMPA currents and no increase in NMDA currents (1.1 $\pm$ 0.1, Fig. 5.27A). PSD-93(N95) chimera showed 2.5 $\pm$ 0.2-fold increase in
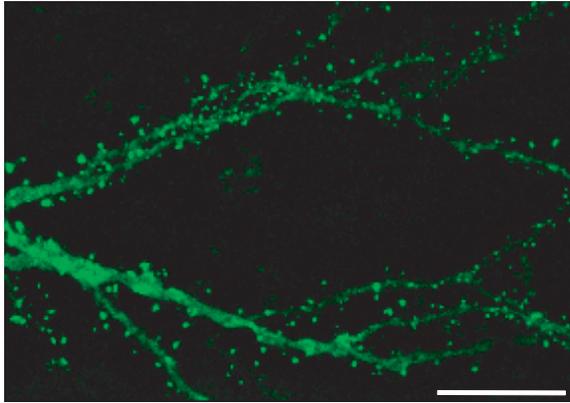
PSD-95 (N93):GFP   PSD-93 (N95):GFP
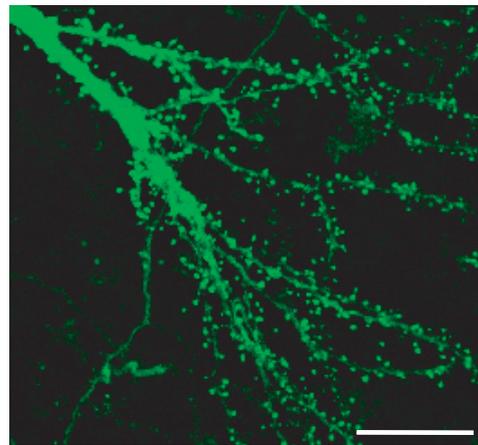
Figure 5.26: Confocal images of CA1 cells overexpressing PSD-95(N93):GFP (scale bar 13.9 μ) and PSD-93(N95):GFP (scale bar 16.5 μm) showing spine localization of the chimeras.

AMPA receptor component and 1.7 ± 0.2-fold increase in NMDA receptor component (Fig. 5.27B). Effects of chimeras and PSD-95 and PSD-93 are summarized in the figure 5.27C.

The results we obtained for the chimeras were not conclusive regarding the protein domain regulating the PSD-95 effect. PSD-95 with the N-terminus of PSD-93 had no effect on NMDA currents, which was not the case in any other condition tested. The effect of PSD-95(N93) on AMPA currents was similar to the effect of PSD-93. On the other hand, PSD-93 with the N-terminus of PSD-95 showed much milder effect on AMPA currents than PSD-95 and similar effect on NMDA currents as both wild types.

From these data we concluded that N-termini did not account alone for the effect of PSD-95 and PSD-93 and they required cooperation with other protein domains.

5.2.5.2 Cdk5-phosphorylation mutants of PSD-95

Cdk5 phosphorylates T19, S25 and S35 of the PSD-95 N-terminus (Morabito et al., 2004). Cdk5-dependent phosphorylation of PSD-95 was proposed to be a mechanism for regulating the clustering of PSD-95: when phosphorylated PSD-95 multimerization and synaptic clustering were reduced (Morabito et al., 2004). Inhibition of Cdk5 increases the binding of Src to PSD-95 and that facilitates the phosphorylation of NR2B that stabilizes NR2B-containing NMDA receptors on the cell surface (Zhang et al., 2008).

A   PSD-95 (N93)

B   PSD-93 (N95)

C
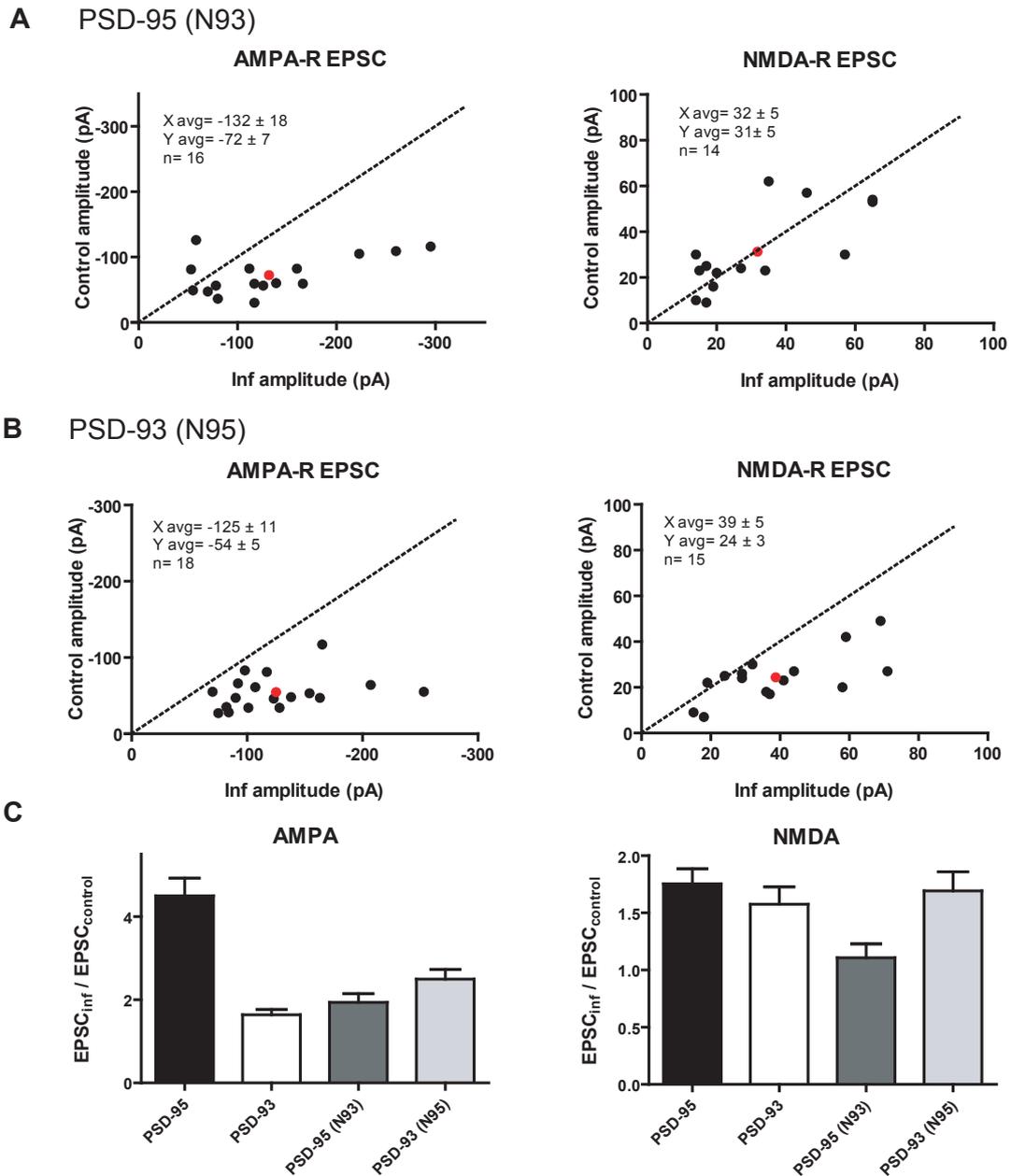
Figure 5.27: AMPA and NMDA EPSC amplitude distribution of PSD-95(N93) (**A**) and PSD-93(N95) (**B**) chimeras. **C**, Summary of the effect of overexpression of PSD-95, PSD-93, PSD-95(N93)and PSD-93(N95).

The N-terminus of PSD-93 is not phosphorylated by Cdk5 (Fig. 5.25). We hypothesized that phosphorylation of PSD-95 by Cdk5 may causes the differential effect of PSD-95 and PSD-93 synaptic transmission. We mutated the phosphorylation sites in PSD-95 to the

PSD-95 (T19A, S25A, S35A):GFP   PSD-95 (T19D, S25D, S35D):GFP
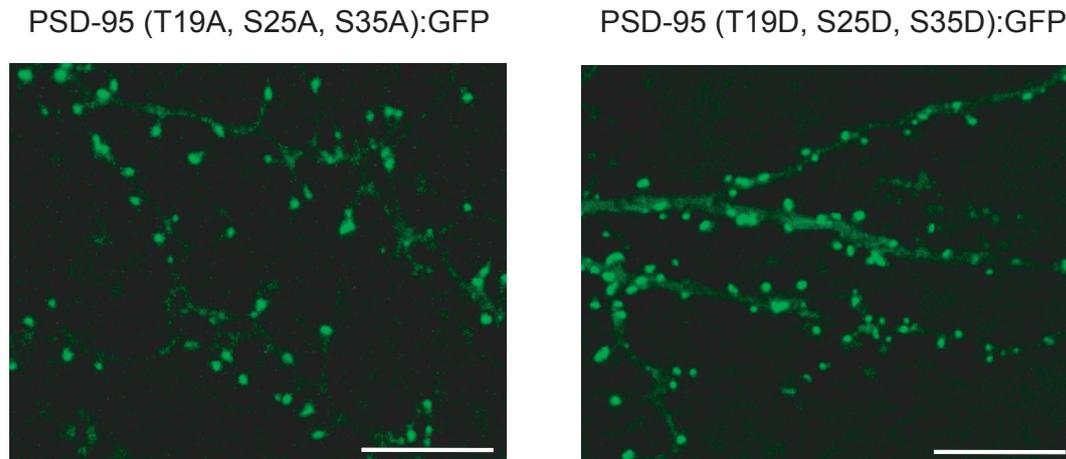
Figure 5.28: CA1 cells overexpressing PSD-95(T19A,S25A,S35A):GFP (scale bar 7.5 μm) and PSD-95(T19D,S25D,S35D):GFP (scale bar 9.6 μm) indicating that Cdk5-phosphorylation mutants are localized to spines.

non-phosphorylatable PSD-95(T19A, S25A, S35A) and to the mutant that mimics phosphorylation, PSD-95(T19D, S25D, S35D). We expected that non-phosphorylated version of PSD-95 may exhibit larger effect on AMPA and/or NMDA receptors by more pronounced clustering of PSD-95 in the synapse and/or by stabilization of NMDA receptors at the cell surface. Firstly, we checked whether the Cdk5 phosphorylation mutants had normal spine localization. As shown in the figure 5.28, both mutants localized to spines.

PSD-95(T19A, S25A, S35A) did not show any larger effect on AMPA receptor component compared to wild type PSD-95 and PSD-95(T19D,S25D,S35D) mutant (Fig. 5.29). In fact, the effect on AMPA receptors was lower than for PSD-95 wild type (3.2 ± 0.4-fold, Fig. 5.29A) and similar to PSD-95(T19D,S25D,S35D) mutant which showed 3.5 ± 0.7-fold increase (Fig. 5.29B). The effect of PSD-95(T19A,S25A,S35A) on NMDA current was same as for wild type PSD-95 (1.8 ± 0.2, Fig. 5.29A), whereas PSD-95(T19D,S25D,S35D) exhibited lower NMDA receptor increase (1.4 ± 0.2, Fig. 5.29B). A summary of these results is shown in figure 5.29C.

From these data we concluded that PSD-95 effect on AMPA and NMDA receptor component was not dependent on Cdk5 phosphorylation of the N-terminus of PSD-95.

A PSD-95 (T19A,S25A,S35A)
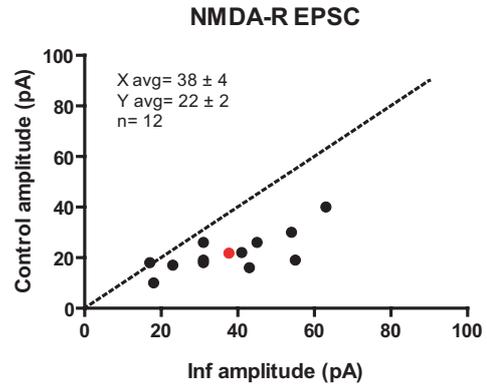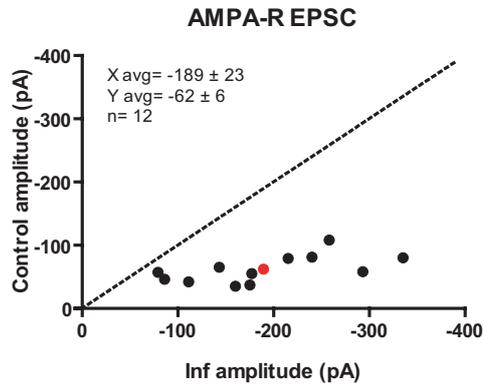
B PSD-93 (T19D,S25D,S35D)
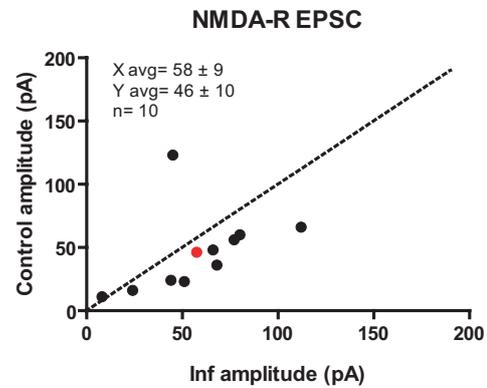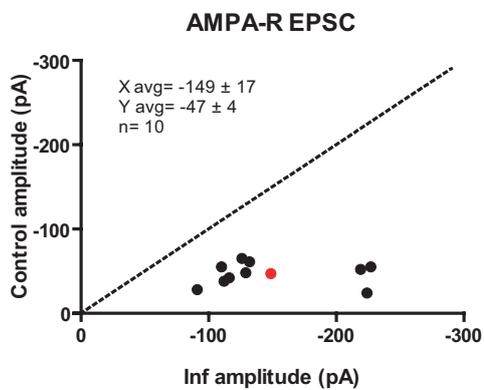
C
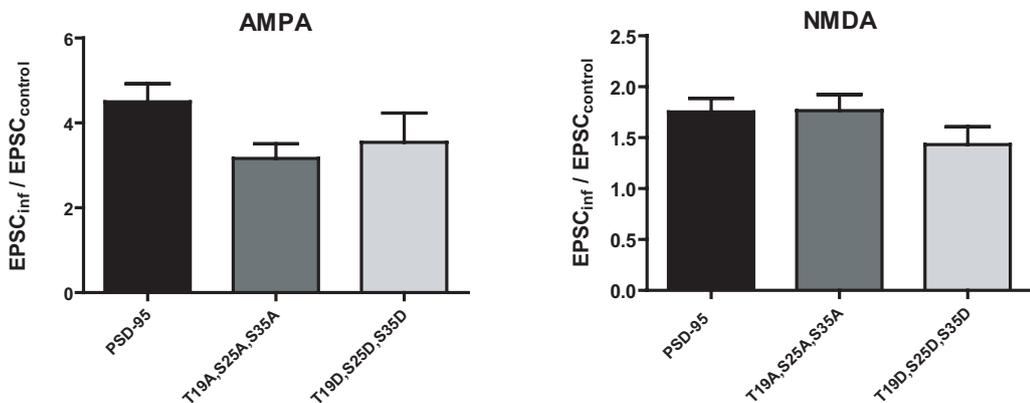
Figure 5.29: AMPA and NMDA EPSC amplitude distribution of posphorylation mutants PSD-95(T19A,S25A,S35A) (**A**) and PSD-95(T19D,S25D,S35D) (**B**) chimeras. **C**, Summary of the effect of overexpression of PSD-95 and the PSD-95 mutants on AMPA and NMDA currents.

5.2.5.3 Activity-dependence of PSD-95 effect

Development of glutamergic synapses requires spontaneous synaptic activity and NMDA receptor activation (Zhu and Malinow, 2002). If PSD-95 shares the same mechanisms for
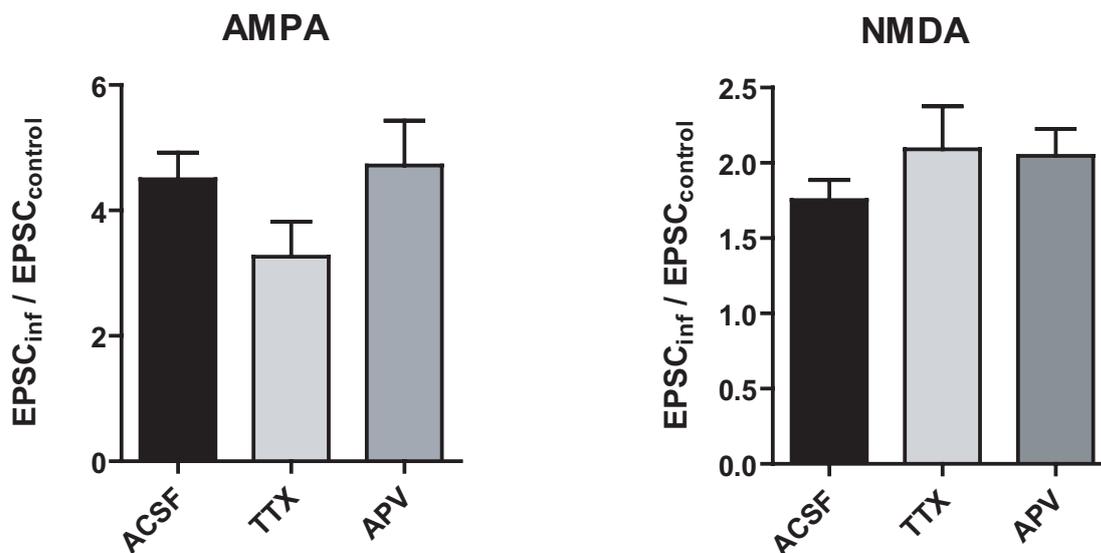
Figure 5.30: AMPA and NMDA EPSCs from the slices incubated overnight with TTX (n=10 pairs) or APV (n=9 pairs)

promoting synapse development as synaptic activity, the prediction would be that the presence of TTX and APV in the slice would block the effect of PSD-95. To test this, we incubated slices with TTX or APV and measured evoked EPSCs. TTX is a sodium channel blocker and prevents cells to fire action potentials, whereas APV is a NMDA receptor antagonist.

In PSD-95-infected cells from the slices incubated with TTX AMPA receptor component was increased 3.3 ± 0.7-fold and NMDA receptor component 2.1 ± 0.3-fold (Fig. 5.30). Therefore, blocking of spontaneous activity in the slice from the time of infection did not prevent PSD-95-mediated synaptic potentiation. Also in the slices incubated with APV, PSD-95 overexpressing cells still showed both AMPA and NMDA currents enhancement (AMPA: 4.7 ± 0.7-fold, NMDA: 2.0 ± 0.2-fold, Fig. 5.30), indicating that NMDA receptor-mediated signaling was not necessary for the PSD-95 effect.

5.2.6 Rectification properties of PSD-95 overexpressing synapses

During the course of our study we observed that ratio of peak outward compound current at +40 mV and peak inward current at -70 mV for infected cell was lower compared to control cell. This suggested that PSD-95-overexpressing cells allowed only a small outward
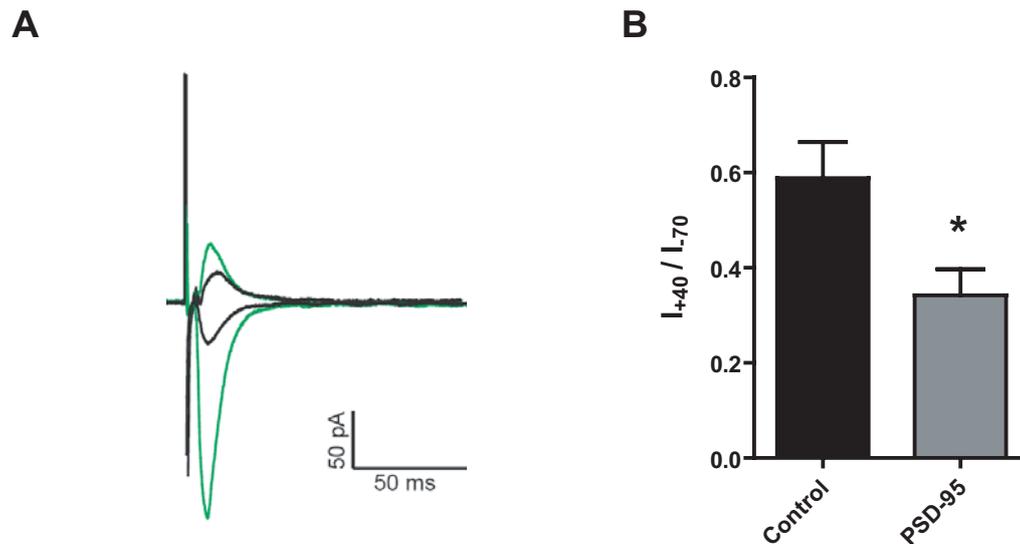
Figure 5.31: **A**, Representative traces of isolated AMPA currents at -70 mV and +40 mV for the control (black traces) and PSD-95-infected cell (green traces). **B**, Rectification index measured in control (n=28) and PSD-95-infected cells (n=28) (p<0.05, unpaired t-test).

current compared to control cells. The likely cause of the small current at positive potentials is the presence of synaptic rectifying AMPA receptors. Namely, AMPA receptors lacking edited GluR2 subunit, are Ca^{2+}-permeable (CP-AMPA receptors) and exhibit inwardly rectifying I-V relationships (see also Introduction). The rectification is caused by intracellular polyamines blocking the receptor pore at positive voltages. The ubiquitous expression of GluR2 in principal neurons ensures that Ca^{2+}-impermeable AMPA receptors (CI-AMPA receptors) dominate synaptic transmission. However, recent studies showed that CP-AMPA receptors are expressed in developing synapses of hippocampus (Ho et al., 2007). Also, AMPA receptor redistribution, leading to an enrichment of CP-AMPA receptors in the synapse, was shown to occur upon PICK1 overexpression (Terashima et al., 2004) and cocaine administration (Bellone and Luscher, 2006).

We aimed to investigate whether overexpression of PSD-95 changed the rectification index of the synapses. To this end, we measured isolated AMPA currents of PSD-95-infected and control cells at -70 mV and +40 mV in the presence of APV. Rectification index was calculated as I_{+40}/I_{-70}. The cells overexpressing PSD-95 showed significantly smaller rectification index than control cells (PSD-95: 0.3 ± 0.1; control: 0.6 ± 0.2, Fig. 5.31). This indicated
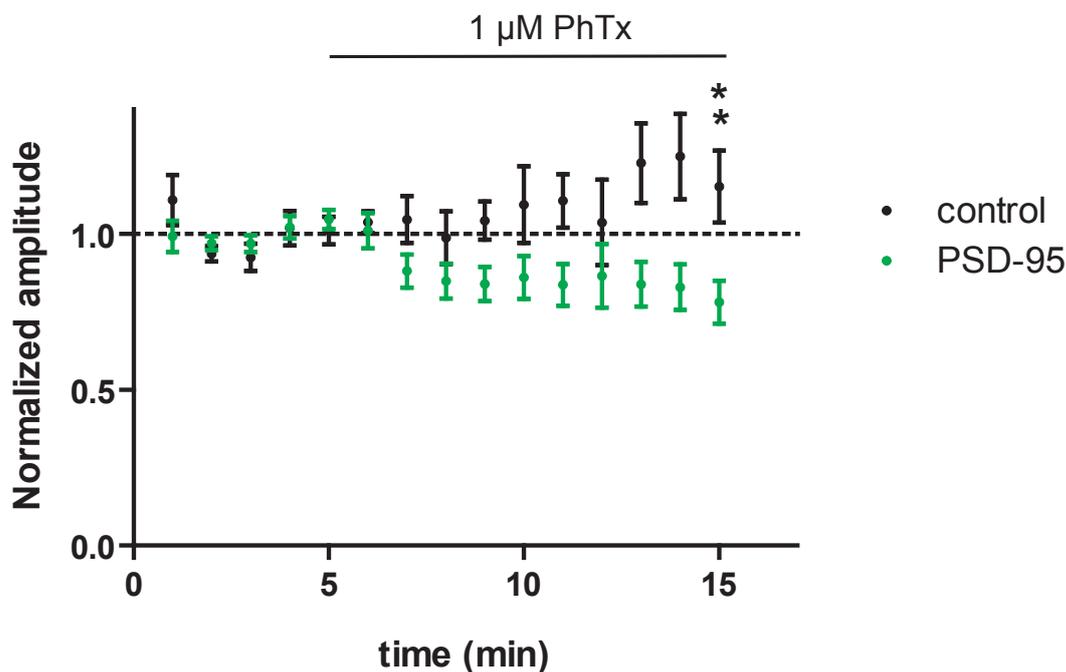
Figure 5.32: Effect of 1μM PhTx on evoked AMPA EPSCs from PSD-95-infected cells (green) and control cells (black). Plotted are averaged 1 min amplitudes normalized to the average response obtained from the first 5 min of recordings before PhTx application. Each data point represents mean±SEM of 5-11 cells recorded in pairs (p<0.05, paired t-test)

that PSD-95 overexpressing synapses had higher content of GluR2-lacking AMPA receptors than control cells.

To further test for this, we used a GluR2-lacking AMPA receptors inhibitor, polyamine philanthotoxin-433 (PhTx) (Koh et al., 1995), to block the rectifying Ca^{2+}-permeable fraction of AMPA receptors. After 10 minutes of 1μM PhTx application PSD-95-overexpressing cells were significantly more sensitive to PhTx than control cell (Fig. 5.32). More specifically, AMPA currents of infected cells were $78 \pm 7\%$ of baseline (n=9), whereas the AMPA currents of control cells exhibited even slight increase during the PhTx application, $115 \pm 12\%$ of the baseline (n=9).

Given the decreased rectification index and higher sensitivity to PhTx we suggest that PSD-95 overexpression leads to an increase in GluR2-lacking receptors content in a synapse. PSD-95 could either selectively mediate trafficking of rectifying receptors from the existing pool or, similarly to PICK1, lead to recomposition of AMPA receptors.

6 Discussion

The goal of this study was to understand how the function and trafficking of AMPA receptors are regulated. The focus was on the interaction of AMPA receptors with stargazin and PSD-95. This study shows that AMPA receptors are functionally modulated by stargazin and that receptors associated with stargazin have different pharmacological properties than the receptors without stargazin. We found that antagonistic effect of CNQX, GYKI-53655 and CP-465,022 on AMPA receptors was changed in the presence of stargazin.

We confirmed the finding that overexpression of PSD-95 dramatically increases the number of AMPA receptors in the synapse, and in addition, we observed an increase in NMDA receptor number. We addressed the possible mechanisms of PSD-95 action and investigated the role of Cdk5 kinase in regulating PSD-95 function. This study shows a novel finding regarding the effect of PSD-95 on rectification properties of synaptic AMPA receptors, suggesting that PSD-95 controls AMPA receptor synaptic localization in a subunit-dependent manner.

6.1 Stargazin modulates AMPA receptors antagonism

TARPs function as auxiliary subunits of AMPA receptors. Similarly to auxiliary subunits of voltage-gated channels, TARPs control the channel properties of AMPA receptors. Stargazin slows AMPA receptor activation, deactivation and desensitization and increases the efficacy of partial agonist kainate (Tomita et al., 2005; Priel et al., 2005; Turetsky et al., 2005). Stargazin increases the efficacy of benzothiadiazides, and increases the potency of cyclothiazide on flop variants of AMPA receptors (Tomita et al., 2006). Stargazin association reduces AMPA receptor affinity for spermine such that GluR2-lacking receptors display only intermediate instead of complete rectification (Soto et al., 2007). Three other members of

TARP family, γ-3, γ-4 and γ-8, regulate AMPA receptors in qualitatively similar manner, although quantitatively they can show great heterogeneity (Cho et al., 2007; Milstein et al., 2007).

We were interested in how stargazin affected the pharmacological properties of AMPA receptors. To study the pharmacology of AMPA receptors, we used the Xenopus oocytes expression system. This system has several advantages compared to other heterologous expression systems. The oocytes have only few endogenous channels (for example Ca^{2+} -activated Cl^- channels) and that permits a particular channel to be studied without contamination currents from other channels. In addition, oocytes are large cells (about 1 mm in diameter) and easy to handle. This system was used in other studies regarding the stargazin effect on AMPA receptors (Tomita et al., 2004; Kott et al., 2007; Chen et al., 2000). We investigated the effects of stargazin on the antagonism of competitive antagonist CNQX and the allosteric inhibitors GYKI-53655 (GYKI) and CP-465,022 (CP).

6.1.1 Stargazin changes CNQX into partial agonist

We compared the sensitivity to CNQX of GluR1 in the presence and absence of stargazin. We observed a higher IC_{50} for CNQX in the presence of stargazin than in the absence (Fig. 5.1B). During the course of our study the work of Menuz and colleagues was published showing that CNQX acts as a partial agonist on AMPA receptors when they were associated with TARPs (Menuz et al., 2007). We tested if we could observe the same phenomena in our system. Indeed, when we measured dose-response curves of CNQX in the absence of glutamate we could observe that CNQX activated AMPA receptors and elicited measurable currents (Fig. 5.1C). These currents were much smaller than those obtained in the presence of full agonist glutamate and reached 9 % $\pm$ 1 % of the currents evoked by 200 μM glutamate (Fig. 5.1B). This effect explains our initial finding that stargazin lowers the affinity of CNQX. More specifically, in the presence of stargazin CNQX competes with glutamate for binding but evokes only small currents, so the outcome effect resembles inhibition.

How does stargazin affect binding of CNQX? When bound to the receptor, glutamate leads to a conformational change within the ligand-binding domain (LBD) caused by rotation of domain 2 toward the domain 1 that leads to subsequent linkers separation and pore opening.

Binding of full agonist, such as glutamate, induces maximal domain closure, whereas CNQX in the absence of TARP led to a partial domain closure (Menuz et al., 2007) (Fig.3.3B, see also Introduction). Association of stargazin could either enhance this domain closure by interacting directly with LBD or it facilitates the transduction of domain closure to channel opening by interacting with the linker domains of the receptor. Our data on stargazin effect on GYKI- and CP-insensitive mutants (Fig. 5.5, see below) strongly suggests that stargazin interacts with the linker domains of the receptor.

6.1.2 Stargazin changes the antagonism of GYKI and CP

We next focused on allosteric inhibitors of AMPA receptors, GYKI and CP. In contrast to the effect on CNQX, co-expression of stargazin increased the affinity of GluR1 homomers for GYKI and CP (Fig. 5.3A and B). The effect on CP binding was milder compared to GYKI. What can explain the difference in the stargazin effect on these two drugs? Menniti and colleagues showed that there is a single binding site for CP on AMPA receptor subunit and that site overlaps with the binding site of GYKI-52466 (Menniti et al., 2000). In addition, Balannik and colleagues showed that in the absence of stargazin the binding sites of these two drugs are located in the linker domains and partly overlap (Balannik et al., 2005). Nevertheless, association of stargazin affected the inhibition by GYKI and CP to a different extent. This could be explained by the structural differences of GYKI and CP (Fig. 3.4). It is still not known what part of GYKI and CP binds directly to the receptors. The methylcarbamyl group at the N-3 position of GYKI-53655 makes it more potent inhibitor than its analog GYKI-52466 (Donevan et al., 1994). The increased affinity of the N-3-substituted analogs related to their increased binding and decreased unbinding rates. The presence of this group could also be important for the increased efficacy of GYKI in the presence of stargazin. Alternatively, allosteric effect of stargazin binding might lead to a formation of additional binding site for GYKI, but not for CP. We cannot exclude the possibility that GYKI but not CP might interact directly with stargazin.

Interestingly, Mayer and colleagues reported in one of the first studies investigating the mechanisms of GYKI that native AMPA receptors expressed from polyA+ mRNA revealed greater sensitivity to GYKI than receptors generated by expression of recombinant AMPA

receptors. They suggested that this might be explained by either an interaction with an unidentified accessory protein or a novel receptor subunit (Partin et al., 1996). Our data suggest that the reported difference might be caused by the associated TARP.

6.1.3 Increased GYKI sensitivity is independent from desensitization

In order to obtain larger glutamate-evoked currents we performed all recordings in the presence of TCM, a positive AMPA receptor modulator similar to CTZ. Some earlier studies suggest that CTZ and GYKI bind in a competitive manner at a common binding site of the receptor, and that GYKI might exhibit its effect by promoting the desensitization of AMPA receptors (Palmer and Lodge, 1993; Zorumski et al., 1993). In order to exclude the interference of TCM on stargazin effect, we measured GYKI dose-response curves in the absence of TCM. Under this condition we still observed lower IC_{50} of GYKI in the presence of stargazin arguing that effect of stargazin on GluR1 affinity for GYKI is independent of desensitization (Fig. 5.4A). However, in case of the non-desensitizing GluR1^{LY} mutant, the effect of stargazin on GYKI antagonism was abolished. In the GluR1^{LY} mutant the aromatic side chain projects into the domain 1 of a partner subunit, increasing the affinity for dimer formation more that 10^5-fold (Weston et al., 2006). Conformation of LY mutant might be more rigid, occluding the effect of stargazin. This is also suggested by the finding that LY mutation perturbed stargazin action on glutamate-evoked currents (Tomita et al., 2007).

Balannik and colleagues suggested that manipulations, which reduce AMPA receptor desensitization, decrease the inhibitory effect of GYKI and CP (Balannik et al., 2005). They measured 10-fold higher IC_{50} of GYKI for GluR3 homomers in the presence of CTZ than in the absence. In the presence of stargazin, we observed only a moderate difference of GYKI IC_{50} in the presence of TCM (-TCM 28 μM; +TCM 38.5 μM). Surprisingly, in the absence of stargazin we saw the opposite effect of TCM: GYKI potency was lower in the absence of TCM ($\approx$200 μM) than in the presence of TCM ($\approx$100 μM). Is TCM/CTZ effect on GYKI potency different for GluR3 homomers compared to GluR1 homomers? Although this possibility does not seem very likely, some subunit-dependence of CTZ action has been reported: CTZ shifted the GYKI-52466 inhibition curve to the right in heteromeric AMPA receptors but not in GluR1 and GluR4 homomers (Johansen et al., 1995). The authors explained

this effect as the lower sensitivity of GluR2-lacking receptors for GYKI-52466 in the absence of CTZ. At present, the allosteric interaction between CTZ/TCM and GYKI and possible AMPA receptor subunit-dependence of this interaction remains poorly understood.

6.1.4 Stargazin restores sensitivity of insensitive mutants

Using receptor mutagenesis, Ballanik and colleagues found that GYKI and CP bind at the S1-M1 and S2-M4 linkers region, thereby disrupting the transduction of agonist binding to channel opening (Balannik et al., 2005). The authors used the Xenopus heterologous system to overexpress GluR subunits in the absence of stargazin. Since there is no evidence for native "TARP-less" AMPA receptors, we reinvestigated this finding by co-expressing stargazin with previously described GYKI- and CP- mutants. Overexpression of stargazin restored the sensitivity to GYKI of GluR1^{GYKI}, whereas GluR1^{CP} co-expressed with stargazin was only mildly blocked by higher concentrations of CP (Fig. 5.5A and B).

There are at least two possible mechanisms of how the introduced mutations lead to the receptor insensitivity: one possibility is that GYKI cannot bind anymore to the receptors and the other is that binding of GYKI is intact but the transduction of LBD conformational change to the pore opening is not prevented by GYKI binding. How could stargazin recover the sensitivity of the "insensitive" mutants? By an allosteric interaction with the linker domains, stargazin could create a new binding site for GYKI. Alternatively, in the presence of stargazin binding of GYKI might block the pore opening of the "insensitive" mutants. Based on these results, we concluded that stargazin interacts with the linker domains of the receptor rather than with the LBD.

We were not able to test GYKI sensitivity of GluR2^{GYKI} and GluR2^{WT}in the absence of stargazin due to the low expression level, but we could see that GluR2^{GYKI} co-expressed with stargazin was sensitive to GYKI in a similar manner that GluR2^{WT} was, implying that qualitatively stargazin effect was not subunit-dependent.

6.1.5 Ectodomain of stargazin modulates antagonist affinity

Different domains of stargazin are involved in trafficking of receptors and changing the channel properties: the cytoplasmic tail of stargazin determines receptors trafficking, whereas

the ectodomain controls channel properties (Tomita et al., 2005). Tomita and colleagues designed a chimeric stargazin protein with the first ectodomain replaced with the one from γ-5 (Ex1 chimera) and this construct had no effect on desensitization and deactivation of AMPA receptors (Tomita et al., 2005). Interestingly, Ex1 did not change CNQX into partial agonist when we co-expressed it with GluR1. It also did not have any effect on CNQX inhibition dose-response curves (Fig. 5.2A and B). In case of GYKI inhibition, both $GluR1^{WT}$ and $GluR1^{GYKI}$ when co-expressed with Ex1 were less sensitive to GYKI than without stargazin. Importantly, Ex1 still trafficked the receptors to the surface, since the currents were much larger than in the absence of Ex1.

This finding suggests that the first ectodomain of stargazin is involved in the process of GluR1 inhibition. This is important finding for understanding the pharmacology of AMPA receptors and also offers a new approach for the therapeutic drug design focusing on the regulation of TARP ectodomain-AMPA receptor interaction.

6.1.6 Insensitive mutants show altered glutamate dose-response curves

During the course of our experiments we observed that mutants of GluR1 showed lower currents than wild type receptors when expressed in oocytes. Although our experiments were design to monitor inhibition of insensitive mutants, we could not exclude the possibility that mutant forms of GluR1 had other receptor properties altered. Therefore, we measured the glutamate dose-response curves of $GluR1^{WT}$ and the insensitive mutants. We observed a 2.7-fold decrease in the EC_{50} for glutamate of GluR1 in the presence of stargazin (Fig. 5.8). In similar studies, the EC_{50} for glutamate was decreased 3.7-fold (Priel et al., 2005) and 2-fold (Yamazaki et al., 2004) when stargazin was co-expressed with GluR1 in oocytes. However, we could not observe the same effect of stargazin on insensitive mutants: EC_{50} of $GluR1^{GYKI}$ was only modestly affected by co-expression of stargazin and EC_{50} of $GluR1^{CP}$ was same in the presence and absence of stargazin. Interestingly, the mutants had higher EC_{50} already when expressed alone. The linkers separation upon glutamate binding in these mutants might be greater than in the wild type and perhaps could not be further enhanced by stargazin.

There are some examples in the literature where point mutations in GluR subunits led

to an increased potency of glutamate. For example, LY mutation in GluR subunits that renders AMPA receptors non-desensitizing showed lower EC_{50} value than wild type GluR (Stern-Bach et al., 1998; Armstrong et al., 2003). Similarly, non-desensitizing GluR6 Y490C L752C mutant had 20-fold lower EC_{50} than wild type GluR6 (Weston et al., 2006). Not only mutations in LBD could lead to increased potency of glutamate. Lurcher mutation located in a hydrophobic region of the M3 domain of GluR subunit showed increased affinity for glutamate and reduced desensitization (Klein and Howe, 2004). Interestingly, stargazin has no effect on glutamate EC_{50} of both LY and Lurcher mutants (Priel et al., 2005; Tomita et al., 2007).

6.1.7 Insensitive mutants show reduced surface expression

Stargazin greatly increased glutamate-evoked currents from Xenopus oocytes when co-injected with limited amount of GluR1 (Tomita et al., 2005). Importantly, this increase was shown to be the effect of both increased number of receptors at the surface and enhanced glutamate efficacy. We measured a 4.2-fold increase in surface expression of GluR1 when co-expressed with stargazin (Fig. 5.9A), which is similar enhancement by stargazin Yamazaki and colleagues observed in HEK cells: 4.1-fold increase for GluR1 and 4.3-fold increase for GluR2 (Yamazaki et al., 2004). The mutants $GluR1^{GYKI}$ and $GluR1^{CP}$ were expressed much less on the oocytes surface in the absence of stargazin compared to wild type. Stargazin potentiation of surface expression was still present (8.5-fold increase for $GluR1^{GYKI}$ and 9.5-fold increase for $GluR1^{CP}$) but the expression levels were still lower than when GluR1 was expressed alone.

AMPA receptors as multimeric proteins are subject to a quality-control system in the ER which verifies whether receptors are folded and assembled properly. The subunits have retention signals that can be masked by heteromeric assembly. For example, the Q/R editing site in the re-entrant loop of GluR2 subunit was shown to be the retention signal. The edited GluR2 could exit the ER only when assembled with other subunits (Greger et al., 2002). There is the evidence that functionality of the receptors can be also verified in the ER. GluR6 mutants with blocked desensitization as well as non-desensitizing GluR2 LY mutant are retained in the ER, pointing to the functional check point in the ER (Priel

et al., 2006; Greger et al., 2006). Similarly, mutations that eliminate glutamate binding in kainate receptors promote the retention of these receptors (Mah et al., 2005; Valluru et al., 2005). Our observation that GluR1^{GYKI} and GluR1^{CP} were also largely retained in the intracellular compartments in the absence of stargazin, suggests further that only receptors with non-altered function can be exported to the surface.

How is the function of the receptors monitored in the ER? What is the quality control mechanism that prevents non-desensitizing receptors and receptors that cannot bind glutamate to exit the ER? Numerous quality control mechanisms exist to retain ER-resident proteins and immature, monomeric, or misfolded proteins. However, most of the mentioned mutations do not lead to a gross change in the receptor conformation. The glutamate is constantly present in the ER implying that oligomeric GluRs would naturally exist in a bound conformation (Meeker et al., 1989). The binding of glutamate lead to the channel opening and subsequent desensitization of the receptors. Priel and colleagues suggest that glutamate binding in the ER might be needed for the presentation of the desensitized conformation to quality control machinery. The quality control machinery could recognize structural signals in the LBD, either the specific motif that is exposed or masked at the desensitized state or global conformational change of the receptor (Priel et al., 2006). In that sense, the GluR1 mutants we used in our study might have altered gating that would lead to their impaired trafficking.

Unlike kainate receptors, AMPA receptors interact with TARPs, therefore the mechanism of their exit from the ER may have some unique features. The recent study shows that GluR4 that cannot bind glutamate can be exported to the surface when co-expressed with stargazin (Coleman et al., 2009). It seems that both glutamate and stargazin make additive contributions to structural stability of AMPA receptor LBD and thereby promote their exit from the ER.

6.2 PSD-95 regulates synaptic function in hippocampal neurons

Members of MAGUK family are scaffolding proteins present at excitatory synapses. PSD-95, the prototypical member of the family, binds to the C-terminus of NR2 subunits of NMDA receptors and cluster them on the membrane surface (Kornau et al., 1995). This proposed that PSD-95 might localize NMDA receptors to the synapse. Since this finding many studies focused on the role of PSD-95 in synaptic function and clear conclusion that emerged from these studies was somewhat surprising: PSD-95 is necessary for synaptic trafficking of AMPA receptors. However, some differences in the observations obtained from different labs accompanied this finding. The role of PSD-95 in the localization of NMDA receptors, as well as the possible role in the presynaptic function have not been established yet.

We used viral overexpression to increase the level of PSD-95 in hippocampal neurons and monitored the consequences of this manipulation on synaptic function. Our study supports the model in which PSD-95 regulates the number of synaptic AMPA receptors but in addition suggests an effect on NMDA receptor number as well as on AMPA receptor subunit-composition.

6.2.1 PSD-95 overexpression enhance both AMPA and NMDA currents

Virally overexpressed PSD-95 localized to spines as it showed punctated staining (Fig. 5.12). Synaptic currents of infected neurons were largely affected: AMPA currents were increased 4.5 ± 0.4-fold, whereas NMDA currents were increased 1.8 ± 0.1-fold compared to a neighboring control cell (Fig. 5.13). The effect of PSD-95 on AMPA receptor-mediated transmission was already reported in several studies (Schnell et al., 2002; Stein et al., 2003; Beique and Andrade, 2003; Ehrlich and Malinow, 2004). Biochemical experiments showed that PSD-95 increased the number of AMPA receptors rather than changing intrinsic biophysical properties of AMPA receptors (El-Husseini et al., 2000). PSD-95 was found to be a critical factor driving AMPA receptors into synapse during LTP and experience-driven synaptic strengthening (Stein et al., 2003; Ehrlich and Malinow, 2004). All these data suggest that PSD-95 is necessary for synaptic trafficking of AMPA receptors.

Does PSD-95 traffic AMPA receptors in native synapses or the increase in AMPA receptors

number we and others observed was overexpression artifact? Studies of PSD-95 and PSD-93 knock-out mice reported normal AMPA and NMDA currents in these mice (Migaud et al., 1998; Elias et al., 2006). This suggests a large redundancy and functional compensation between the members of MAGUK family. When deleted in the germ line, particular MAGUK member can be replaced by other members. When shRNA for either PSD-95 or PSD-93 was used acutely in hippocampal neurons containing fully mature synapses, basal AMPA receptors transmission was reduced 50% (Elias et al., 2006), proving that MAGUKs are necessary for the synaptic localization od AMPA receptors.

The role of PSD-95 in trafficking and synaptic localization of NMDA receptors is less established. PDZ-interaction of NMDA receptors was shown to be important for masking their retention signal and subsequent exit from the ER (Standley et al., 2000). SAP102 was shown to be involved in the NMDA receptors delivery to the cell surface through an interaction with the exocyst complex member, Sec8 (Sans et al., 2003). Transgenic mice expressing NR2A with deleted C terminus showed an absence of NMDA receptors from the synapse, but receptors were expressed at the extrasynaptic sites (Steigerwald et al., 2000). This finding resembles the study of Schnell and colleagues where stargazin overexpression did not lead to an increase in synaptic AMPA currents (Schnell et al., 2002), suggesting that the sheer increase in the receptor number is not sufficient for synaptic potentiation. Instead, the number of synaptic slots is the limiting factor for the postsynaptic strength. All these initial studies pointed to the model that PDZ-interaction of NMDA receptors was necessary for their synaptic localization and MAGUK members were the likely candidates to control this synaptic trafficking.

Given the data described above, it was surprising that in previous studies the overexpression of PSD-95 in the organotypical hippocampal slices did not lead to an increase in NMDA currents (Schnell et al., 2002; Stein et al., 2003). Additional mechanisms controlling the NMDA receptor synaptic number were suggested. We did observe an increase in NMDA receptors currents upon overexpression of PSD-95 (Fig. 5.13 and 5.18) that we could not explain by a change in a subunit composition of NMDA receptors (Fig. 5.22), nor as an effect of different experimental conditions used (Fig. 5.17). We hypothesized that this effect might not be a direct effect of PSD-95 on NMDA receptors but rather indirect, as an gross increase in AMPA receptor number would eventually lead to the insertion of NMDA recep-

tors. Since we were not able to abolish the effect of PSD-95 on AMPA receptors using class II PSD-95 mutation (PSD-95-HV, Fig. 5.23), we could not test whether PSD-95 would still drive NMDA receptors into synapses without a "pre-increase" in AMPA receptors number.

Taken together, our data suggest that increased level of PSD-95 in neurons creates additional synaptic slots enabling more receptors to participate in the synaptic transmission. It is still not clear whether PSD-95 only provides slots or interacts with the AMPA receptor-TARP complexes and NMDA receptors already outside the synapse. In case of the first possibility, PSD-95 could increase the number of slots for both AMPA receptors and NMDA receptors, but since the NMDA receptors are less mobile and/or available at the extrasynaptic sites than AMPA receptors, the probability that they get captured in the PSD is lower.

6.2.2 PSD-95 does not change glutamate release probability

PSD-95 interacts with neuroligin, a transmembrane protein that binds to presynaptic β-neurexins. It was reported that PSD-95 modulated presynaptic release probability via this interaction (Futai et al., 2007). The presynaptic locus of PSD-95 effect would explain both AMPA and NMDA currents enhancement that we observed. We performed several experiments addressing the release probability in the cells overexpressing PSD-95. We could not observe any difference between non-infected and infected cells neither in paired-pulse ratio (Fig. 5.19) nor in the kinetics of MK-801 block (Fig. 5.20). The effect of PSD-95 on NMDA receptors did not show any sensitivity to extracellular Ca^{2+} concentration as NMDA current enhancement was largely constant in all of the concentration tested (Fig. 5.21). Therefore, our data argue for no change in release probability in the cells overexpressing PSD-95.

PSD-95 was suggested to be involved in maturation of presynaptic terminals in dissociated hippocampal neurons as it enhanced presynaptic cluster size and FM4-64 staining (El-Husseini et al., 2000). Hippocampal neurons cultured for 21 days overexpressing PSD-95 had larger and more numerous spines (El-Husseini et al., 2000). What could be the mechanism mediating the possible effect of PSD-95 on synapse formation and number? One of the first step in the synapse formation is the assembly of the presynapse. Discrete pre-assembled packets of presynaptic active-zone are rapidly transported to the site of axodendritic contact

(Ahmari et al., 2000). The assembly sequence of the postsynaptic part is less clear. Most of the studies suggested that PSD-95 is one of the first protein recruited to the synapse. PSD-95 and GKAP (guanylate kinase domain-associated protein) both clustered at synaptic sites in young cultured hippocampal neurons several days before NMDA and AMPA receptors and shortly after the formation of presynaptic specializations (Rao et al., 1998). The filopodia and spines of young cultured cortical neurons bearing PSD-95:GFP clusters were significantly more stable, suggesting that decreased mobility of dendritic filopodia during the development is caused by the presence of PSD-95 clusters (Prange and Murphy, 2001).

In contrast, Washbourne and colleagues found that discrete clusters of NMDA receptors were present in the dendrites from young cortical neurons before synapse formation and that these NMDA receptors clusters were recruited to new synapses within minutes after presynaptic contacts (Washbourne et al., 2002). Surprisingly, recruitment of NMDA receptor clusters could either precede or overlap with PSD-95 recruitment.

How could overexpression of PSD-95 lead to the increased spine size and number? By providing more slots in the postsynaptic density and insertion of more synaptic receptors, PSD-95 could lead to parallel expansion of the presynaptic terminal and release machinery, for example vesicle pool. The presence of more PSD-95 in the cell could lead to stabilization of the initial contacts made by the dendritic filopodia which would result in more spines. Multimerization of SAP97 was associated with increased stability of SAP97 in spines (Nakagawa et al., 2004). It could be that high amount of PSD-95 protein caused by viral overexpression led to more prominent mulitimerization of PSD-95 which would result in lower spine turnover, and subsequently more spines and higher EPSC amplitudes.

We did not observe a change in release probability in infected cells, but we could not exclude that overexpression of PSD-95 led to an increased number of spines and/or lower turnover of existing spines. In that case, an increase in both AMPA and NMDA currents must be expected.

6.2.3 Overexpression of PSD-93 shows modest effect on synaptic currents

We observed much milder effect of PSD-93 overexpression on synaptic currents compared to PSD-95 overexpression. Cells overexpressing PSD-93 showed 1.6 ± 0.1-fold increase in

AMPA currents and 1.6 ± 0.2-fold in NMDA currents (Fig. 5.24). What could account for the different effect of different MAGUK members?

Beside the PSD-95 and PSD-93, overexpression of SAP102 also led to the selective increase in AMPA EPSCs (Schnell et al., 2002). In PSD-95/PSD-93 double knockout mice SAP102 expression was upregulated and accounted for the remaining AMPA receptor-mediated current (Elias et al., 2006). However, acute knockdown of SAP102 with shRNA did not alter the basal synaptic transmission indicating that SAP102 is not necessary for the receptors localization in mature synapses (Elias et al., 2006).

The role of the fourth member of MAGUK family, SAP97 is less well understood. SAP97 is distinct from the other MAGUK members in a way that interacts directly with the C-terminus of GluR1 (Leonard et al., 1998) and has no palmitoylation signal necessary for the synaptic localization. Schnell and colleagues did not observe any effect of SAP97 over-expression on AMPA and NMDA currents, but when they overexpressed a chimera where the PSD-95 palmitoylation motif was inserted on SAP97 both AMPA and NMDA components were increased (Schnell et al., 2002). In contrast, other studies showed that SAP97 overexpression in hippocampal slices led to an increase in AMPA EPSCs (Nakagawa et al., 2004). Using the negative-stain electron microscopy, the authors showed surprisingly different shapes of monomeric PSD-95 and SAP97, and whereas PSD-95 was mainly monomeric SAP97 tended to dimerize (Nakagawa et al., 2004). In addition, it was shown that the C-terminal of GluR1 was essential for bringing SAP97 to the plasma membrane, where it acted to promote dendrite growth (Zhou et al., 2008). The difference in the shape and multimerization between SAP97 and PSD-95 suggests that even though the molecular structure of the MAGUK proteins may be the same, they can serve different roles as scaffolds. Also given the role of SAP97 in dendrite growth, it could be that some of the MAGUKs have additional roles in neurons.

It was shown previously that PSD-95 and PSD-93 control the number of AMPA receptors at non-overlapping subsets of excitatory synapses (Elias et al., 2006). The shRNA knockdown of both PSD-95 and PSD-93 led to the same ($\approx$50%) decrease in AMPA EPSC, although the overexpression of PSD-93 gave $\approx$2-fold increase in AMPA EPSC, less than it was observed for PSD-95 (Elias et al., 2006; Schnell et al., 2002). PSD-95 and PSD-93 differ in their N-terminal sequence (Fig. 5.25). From the data obtained for PSD-95/PSD-93 chimera-

overexpression we could conclude that the N-terminus did not solely account for the PSD-95 and PSD-93 effect, so the downstream protein parts also take part in determining MAGUKs specificity. The milder PSD-93 effect on basal synaptic transmission we observed could be caused by a lower protein level expression of PSD-93, different potential of PSD-93 to make synaptic slots or smaller population of synapses affected by PSD-93 overexpression.

6.2.4 Cdk5-dependent phosphorylation does not control the effect of PSD-95

Cdk5 is a serine-threonine kinase with diverse functions both in normal and pathological processes in mammalian CNS and it has been implicated in the processes of learning and memory. Genetic deletion of Cdk5 causes perinatal lethality with severe defects in cortico-genesis and neuronal positioning (Ohshima et al., 2005). Conditional Cdk5 knock-out adult mice had normal AMPA receptor-mediated fields and increased NMDA receptor-mediated transmission due to a direct effect of Cdk5 on NR2B-containing NMDA receptors degradation (Hawasli et al., 2007). Namely, deletion of Cdk5 reduced degradation of NR2B-receptors by calpain, leading to improved spatial memory and lower threshold for LTP compared to the wild type (Hawasli et al., 2007).

The N-terminus of PSD-95 contains consensus phosphorylation sites for Cdk5 kinase. The Cdk5-phosphorylation status of PSD-95 regulates its clustering in the synapse (Morabito et al., 2004). A non-phosphorylatable mutant version of PSD-95 had bigger cluster size compared to wild type. Also cultured cortical neurons from Cdk5 knock-out mice showed larger clusters of PSD-95 compared to the wild type cells (Morabito et al., 2004). Cdk5 was also reported to have an indirect effect on NR2B-containing NMDA receptors via PSD-95 phosphorylation, where phosphorylation of PSD-95 affected NR2B receptors internalization (Zhang et al., 2008). We tested if the non-phosphorylatable mutant led to higher AMPA and NMDA currents compared to wild type, but we could not observe such an effect (Fig. 5.29A). Also PSD-95 mutant that mimicked the Cdk5 phosphorylation did not show any significantly different effect on AMPA and NMDA currents compared to wild type PSD-95 (Fig. 5.29). Importantly, both mutants localized to spines (Fig. 5.28).

What could explain the absence of differential effects of PSD-95 phosphorylation mutants? Both above described effects of Cdk5 on PSD-95 were demonstrated in dissociated neuronal

cultures and it could be that the phosphorylation of PSD-95 does not affect the clustering in more physiological preparations, such as cultured slices. On the other hand, Cdk5-mediated phosphorylation of PSD-95 might play a role in PSD-95 clustering only during the period of synaptogenesis and not once synapses are established. Alternatively, it could be that PSD-95 cluster size does not necessarily affect the synaptic strength.

6.2.5 PSD-95 effect on synaptic currents is not activity-dependent

Spontaneous activity of neurons is of great importance for their normal development. Changes in network activity are sensed by the neurons and they response by triggering the activity-dependent signaling. We hypothesized that some of these activity-dependent mechanisms might be important for PSD-95 to exhibit its effect. We incubated slices in TTX, which prevented the cells to fire the action potentials, but PSD-95 still enhanced AMPA and NMDA EPSCs (Fig. 5.30). The effect on AMPA currents was somewhat lower in the presence of TTX, which could be explained by the upregulated insertion of AMPA receptors in the presence of TTX ("synaptic scaling") therefore occluding the effect of PSD-95. Namely, when the activity of neurons is chronically blocked by prolonged incubation with TTX there is an upregulation of the number of synaptic AMPA receptors. This process is believed to be a homeostatic mechanism evolved to compensate for the decreased excitation of the neuron.

Activation of NMDA receptors during the spontaneous activity and subsequent influx of Ca^{2+} plays also a role in development of neuronal circuits. For example, NMDA receptors activated during miniature synaptic events, actively inhibit dendritic GluR1 synthesis, tonically suppressing the synaptic expression of GluR1 homomers (Sutton et al., 2006). Importantly, NMDA-induced internalization of AMPA receptors was shown to be mediated by NMDA receptor-activation dependent PSD-95 ubiquitination (Colledge et al., 2003). Pharmacological blockade of NMDA receptors in hippocampal slices did not affect synapse formation and dendritic spine growth but did increase the motility of spines (Alvarez et al., 2007). When we blocked NMDA receptors by incubating slices by APV, both AMPA and NMDA currents were enhanced similarly to the control conditions (Fig. 5.30). This result suggests that Ca^{2+} influx through NMDA receptors is not necessary for the PSD-95 effect on synaptic currents.

6.2.6 PSD-95 overexpression and AMPA receptor-subunit composition

AMPA receptors in hippocampus are usually composed of GluR2/3 and GluR1/2 (Wenthold et al., 1996). The presence of edited GluR2 subunit determines the key properties of AMPA receptors, such as Ca^{2+}-permeability and rectification. Unlike interneurons which have significant portion of GluR2-lacking receptors, pyramidal neurons express GluR2-lacking receptors only early in the development (Pickard et al., 2000). However, some studies suggested that pyramidal neurons may have a significant pool of GluR2-lacking receptors that might get incorporated in the synapse under certain circumstances (Kumar et al., 2002; Ju et al., 2004; Terashima et al., 2004). A recent study shows that LTP induction in CA1 hippocampal neurons causes the rapid incorporation of GluR2-lacking AMPA receptors at synapses, but these are only present transiently and are replaced by GluR2-containing receptors after 20 min of LTP expression (Plant et al., 2006).

PSD-95 overexpression occludes LTP implying that they utilize the same cellular mechanism for regulating the synaptic strength (Stein et al., 2003). We tested whether PSD-95 overexpression also inserted GluR2-lacking receptors into the synapses. Indeed, we observed significant decrease in the rectification index in cells overexpressing PSD-95 (Fig. 5.31). The increased content of GluR2-lacking receptors was further confirmed by partial sensitivity of infected cells to PhTx (Fig. 5.32).

The remaining question is where the GluR2-lacking receptors come from and how PSD-95 selectively inserts them into a synapse. It could be that there is a pre-existing pool of GluR2-lacking receptors but it can be recruited to the synapses only under certain conditions, for example during LTP (Plant et al., 2006). PSD-95 may trigger the same signaling mechanisms in neurons as LTP which would result in an increased portion of synaptic GluR2-lacking receptors. The time point of developmental switch from GluR2-lacking to GluR2-containing AMPA receptors may vary between different preparations and different culturing conditions. In acute cortical slices this switch occurred around the postnatal day 16 (Kumar et al., 2002) and in dissociated hippocampal cultures around 14 DIV (Pickard et al., 2000). We performed our experiments in slices that corresponded to the postnatal day 14-18, indicating that some CP-AMPA receptors might still be present in the CA1 neurons.

Another exciting possibility is that PSD-95 may lead to a recomposition of AMPA re-

ceptors. A change in the AMPA receptor subunit composition has been already observed under following conditions. PICK1, a protein that regulates surface expression of GluR2 subunit, was overexpressed in acute hippocampal slices from 7-12 days old rats and 20-48 hours later the GluR2 content in the synapses was decreased without the change in GluR1 levels (Terashima et al., 2004). This effect of PICK1 on GluR2 was accompanied with the change in the rectification index. AMPA receptor redistribution dependent on PICK1-GluR2 interaction was also observed in neurons of ventral tagmental area upon cocaine administration (Bellone and Luscher, 2006). Testing whether the effect of PSD-95 on AMPA receptor rectification is sensitive to PICK1-GluR2 interaction could answer the question of the mechanism behind the increased portion of CP-AMPA receptor in the PSD-95 overexpressing cells.

Ju and colleagues observed that activity-block in cultured neurons led to an increased dendritic synthesis of GluR1 but not GluR2 (Ju et al., 2004). PSD-95 overexpression might affect de novo dendritic synthesis of GluR1 subunit, resulting in higher content of GluR2-lacking receptors in the synapses.

GluR2 subunit is critical in determining mammalian AMPA receptor function. Thus, understanding the mechanisms that regulate abundance of GluR2-lacking AMPA receptors is of great importance. Emerging role of PSD-95 as one of these mechanisms might be of particular significance.

6.3 Conclusions and Outlook

In my thesis I addressed several aspects of AMPA receptor physiology. More specifically, I investigated how AMPA receptor antagonism is modulated by stargazin, the AMPA receptor auxiliary subunit of the TARP family, and how AMPA receptor synaptic localization is regulated by PSD-95, the main scaffolding protein of excitatory synapse.

In the first part of my thesis I assessed the effect of stargazin association on the inhibition of AMPA receptors by commonly used antagonists CNQX, GYKI-53655 and CP-465,022. To that end, I employed the Xenopus oocyte expression system to express GluR1 AMPA receptor subunit with and without stargazin. I found that GluR1 homomers associated with stargazin had different pharmacological properties than receptors without stargazin. In addition, my study reveals differential effect of stargazin on competitive and non-competitive inhibitors. Co-expression of stargazin decreased the sensitivity of AMPA receptors to competitive antagonist CNQX. In fact, CNQX was a partial agonist and not an antagonist of AMPA receptors in the presence of stargazin. In contrast, stargazin increased sensitivity of AMPA receptors to a non-competitive inhibitor GYKI-53655 and had the same, but milder, effect on another non-competitive inhibitor, CP-465,022. Interestingly, stargazin recovered the sensitivity of previously described GYKI-53655-insensitive mutant. Given that the mutations of this mutant are located in the linker domains of AMPA receptor subunit, this finding strongly suggests that stargazin interacts with the linker domains of the receptors, instead, or in addition, to the ligand-binding domain as it was previously suggested. The insensitive mutant showed also impaired surface trafficking to the membrane surface, supporting the idea that only receptors without altered function are exported to the cell surface.

This study also shows that extracellular domain of stargazin regulates the AMPA receptor antagonism. That finding is important for both understanding the AMPA receptor-TARP interaction and future therapeutic approach when AMPA receptor blockers are concerned. Another important implication of these study is that stargazin co-expression is necessary when pharmacology of AMPA receptors is studied in the heterologous systems, given that probably all native AMPA receptors are associated with TARPs.

There are still many open questions regarding the interaction of AMPA receptors with TARPs. For instance, the number of TARP molecules that bind to a AMPA receptor

tetramer is not known. It would be interesting to see whether this number is constant over the whole population of AMPA receptors, or is dynamically regulated, for example in the receptor subunit-dependent manner. Another open question is whether all AMPA receptors are associated with TARPs. To date, there is a lack of evidence for "TARP-less" AMPA receptors, but the possibility that certain populations of neurons or even subsets of synapses of the same neuron might not have TARPs, cannot be excluded.

In the second part of my thesis I focused on PSD-95, the most studied synaptic scaffolding protein of the MAGUK family. I aimed to understand how overexpression of PSD-95 in neurons of cultured hippocampal slices affects their synaptic currents. There were some discrepancies in the data obtained by the different labs regarding the effect of PSD-95 on synapse. I addressed the question of what accounts for these different observation and performed some measurements under different experimental conditions. I further discussed the caveats accompanying overexpression approach, suggesting that different protein levels, onset and length of expression may alter the outcome of the experiments.

My study confirms that PSD-95 regulates trafficking of AMPA receptors in the synapse, but also emphasizes on the effect of PSD-95 on synaptic NMDA receptor number, an effect which was not observed in the previous studies or it was neglected. The significance of this finding is the implication of PSD-95 as a general synaptic slot protein and a new view on NMDA receptor dynamics in the synapse. I could also show that the effect of PSD-95 on the synaptic currents is not mediated by changes in the presynaptic release probability but that the locus of the PSD-95 effect is postsynaptic. In order to compare the effect of PSD-95 with other MAGUK family members, I overexpessed PSD-93 in hippocampal neurons and observed much milder effect on the synaptic currents. This suggests that different MAGUKs can serve differential role as scaffolds.

I examined the effect of PSD-95 on the rectification properties of synaptic AMPA receptors and observed that PSD-95 overexpression led to an increased portion of GluR2-lacking receptors. It is debated in the field whether GluR2-lacking receptors are present in the CA1 neurons after the synapses are formed, and my work supports the findings that GluR2-lacking receptors can be found in the synapse under certain conditions. It will be interesting to further investigate what are the possible mechanisms underling this apparent selectivity of PSD-95 for GluR2-lacking receptors.

Bibliography

Ahmari, S. E., Buchanan, J., and Smith, S. J. (2000). Assembly of presynaptic active zones from cytoplasmic transport packets. *Nat Neurosci*, 3(5):445–51.

Alvarez, V. A., Ridenour, D. A., and Sabatini, B. L. (2007). Distinct structural and ionotropic roles of NMDA receptors in controlling spine and synapse stability. *J Neurosci*, 27(28):7365–76.

Armstrong, N. and Gouaux, E. (2000). Mechanisms for activation and antagonism of an AMPA-sensitive glutamate receptor: crystal structures of the GluR2 ligand binding core. *Neuron*, 28(1):165–81.

Armstrong, N., Jasti, J., Beich-Frandsen, M., and Gouaux, E. (2006). Measurement of conformational changes accompanying desensitization in an ionotropic glutamate receptor. *Cell*, 127(1):85–97.

Armstrong, N., Mayer, M., and Gouaux, E. (2003). Tuning activation of the AMPA-sensitive GluR2 ion channel by genetic adjustment of agonist-induced conformational changes. *Proc Natl Acad Sci U S A*, 100(10):5736–41.

Balannik, V., Menniti, F. S., Paternain, A. V., Lerma, J., and Stern-Bach, Y. (2005). Molecular mechanism of AMPA receptor noncompetitive antagonism. *Neuron*, 48(2):279–88.

Beique, J. C. and Andrade, R. (2003). PSD-95 regulates synaptic transmission and plasticity in rat cerebral cortex. *J Physiol*, 546(Pt 3):859–67.

Bellone, C. and Luscher, C. (2006). Cocaine triggered AMPA receptor redistribution is reversed in vivo by mGluR-dependent long-term depression. *Nat Neurosci*, 9(5):636–41.

Bellone, C. and Nicoll, R. A. (2007). Rapid bidirectional switching of synaptic NMDA receptors. *Neuron*, 55(5):779–85.

Cantallops, I. and Cline, H. T. (2000). Synapse formation: if it looks like a duck and quacks like a duck. *Curr Biol*, 10(17):R620–3.

Cathala, L., Holderith, N. B., Nusser, Z., DiGregorio, D. A., and Cull-Candy, S. G. (2005). Changes in synaptic structure underlie the developmental speeding of AMPA receptor-mediated EPSCs. *Nat Neurosci*, 8(10):1310–8.

Chen, L., Chetkovich, D. M., Petralia, R. S., Sweeney, N. T., Kawasaki, Y., Wenthold, R. J., Bredt, D. S., and Nicoll, R. A. (2000). Stargazin regulates synaptic targeting of AMPA receptors by two distinct mechanisms. *Nature*, 408(6815):936–43.

Chen, L., El-Husseini, A., Tomita, S., Bredt, D. S., and Nicoll, R. A. (2003). Stargazin differentially controls the trafficking of alpha-amino-3-hydroxyl-5-methyl-4-isoxazolepropionate and kainate receptors. *Mol Pharmacol*, 64(3):703–6.

Cho, C. H., St-Gelais, F., Zhang, W., Tomita, S., and Howe, J. R. (2007). Two families of TARP isoforms that have distinct effects on the kinetic properties of AMPA receptors and synaptic currents. *Neuron*, 55(6):890–904.

Cho, K. O., Hunt, C. A., and Kennedy, M. B. (1992). The rat brain postsynaptic density fraction contains a homolog of the drosophila discs-large tumor suppressor protein. *Neuron*, 9(5):929–42.

Coleman, S. K., Moykkynen, T., Cai, C., von Ossowski, L., Kuismanen, E., Korpi, E. R., and Keinanen, K. (2006). Isoform-specific early trafficking of AMPA receptor flip and flop variants. *J Neurosci*, 26(43):11220–9.

Coleman, S. K., Moykkynen, T., Jouppila, A., Koskelainen, S., Rivera, C., Korpi, E. R., and Keinanen, K. (2009). Agonist occupancy is essential for forward trafficking of AMPA receptors. *J Neurosci*, 29(2):303–12.

Colledge, M., Snyder, E. M., Crozier, R. A., Soderling, J. A., Jin, Y., Langeberg, L. K., Lu, H., Bear, M. F., and Scott, J. D. (2003). Ubiquitination regulates PSD-95 degradation and AMPA receptor surface expression. *Neuron*, 40(3):595–607.

Cull-Candy, S. G. and Leszkiewicz, D. N. (2004).

Role of distinct NMDA receptor subtypes at central synapses. *Sci STKE*, 2004(255):re16.

Donevan, S. D. and Rogawski, M. A. (1993). GYKI 52466, a 2,3-benzodiazepine, is a highly selective, noncompetitive antagonist of AMPA/kainate receptor responses. *Neuron*, 10(1):51–9.

Donevan, S. D., Yamaguchi, S., and Rogawski, M. A. (1994). Non-N-methyl-D-aspartate receptor antagonism by 3-N-substituted 2,3-benzodiazepines: relationship to anticonvulsant activity. *J Pharmacol Exp Ther*, 271(1):25–9.

Ehrlich, I., Klein, M., Rumpel, S., and Malinow, R. (2007). PSD-95 is required for activity-driven synapse stabilization. *Proc Natl Acad Sci U S A*, 104(10):4176–81.

Ehrlich, I. and Malinow, R. (2004). Postsynaptic density 95 controls AMPA receptor incorporation during long-term potentiation and experience-driven synaptic plasticity. *J Neurosci*, 24(4):916–27.

El-Husseini, A. E., Schnell, E., Chetkovich, D. M., Nicoll, R. A., and Bredt, D. S. (2000). PSD-95 involvement in maturation of excitatory synapses. *Science*, 290(5495):1364–8.

El-Husseini Ael, D., Schnell, E., Dakoji, S., Sweeney, N., Zhou, Q., Prange, O., Gauthier-Campbell, C., Aguilera-Moreno, A., Nicoll, R. A., and Bredt, D. S. (2002). Synaptic strength regulated by palmitate cycling on PSD-95. *Cell*, 108(6):849–63.

Elias, G. M., Funke, L., Stein, V., Grant, S. G., Bredt, D. S., and Nicoll, R. A. (2006).

Synapse-specific and developmentally regulated targeting of AMPA receptors by a family of MAGUK scaffolding proteins. *Neuron*, 52(2):307–20.

Elias, G. M. and Nicoll, R. A. (2007). Synaptic trafficking of glutamate receptors by MAGUK scaffolding proteins. *Trends Cell Biol*, 17(7):343–52.

Funke, L., Dakoji, S., and Bredt, D. S. (2005). Membrane-associated guanylate kinases regulate adhesion and plasticity at cell junctions. *Annu Rev Biochem*, 74:219–45.

Futai, K., Kim, M. J., Hashikawa, T., Scheiffele, P., Sheng, M., and Hayashi, Y. (2007). Retrograde modulation of presynaptic release probability through signaling mediated by PSD-95-neuroligin. *Nat Neurosci*, 10(2):186–95.

Gardoni, F. (2008). MAGUK proteins: new targets for pharmacological intervention in the glutamatergic synapse. *Eur J Pharmacol*, 585(1):147–52.

Greger, I. H., Akamine, P., Khatri, L., and Ziff, E. B. (2006). Developmentally regulated, combinatorial RNA processing modulates AMPA receptor biogenesis. *Neuron*, 51(1):85–97.

Greger, I. H., Khatri, L., Kong, X., and Ziff, E. B. (2003). Ampa receptor tetramerization is mediated by Q/R editing. *Neuron*, 40(4):763–74.

Greger, I. H., Khatri, L., and Ziff, E. B. (2002). RNA editing at arg607 controls AMPA receptor exit from the endoplasmic reticulum. *Neuron*, 34(5):759–72.

Groc, L., Heine, M., Cognet, L., Brickley, K., Stephenson, F. A., Lounis, B., and Choquet, D. (2004). Differential activity-dependent regulation of the lateral mobilities of AMPA and NMDA receptors. *Nat Neurosci*, 7(7):695–6.

Harvey, S. C. and Skolnick, P. (1999). Polyamine-like actions of aminoglycosides at recombinant N-methyl-D-aspartate receptors. *J Pharmacol Exp Ther*, 291(1):285–91.

Hawasli, A. H., Benavides, D. R., Nguyen, C., Kansy, J. W., Hayashi, K., Chambon, P., Greengard, P., Powell, C. M., Cooper, D. C., and Bibb, J. A. (2007). Cyclin-dependent kinase 5 governs learning and synaptic plasticity via control of NMDAR degradation. *Nat Neurosci*, 10(7):880–6.

Hayashi, Y., Shi, S. H., Esteban, J. A., Piccini, A., Poncer, J. C., and Malinow, R. (2000). Driving AMPA receptors into synapses by LTP and CaMKII: requirement for GluR1 and PDZ domain interaction. *Science*, 287(5461):2262–7.

Ho, M. T., Pelkey, K. A., Topolnik, L., Petralia, R. S., Takamiya, K., Xia, J., Huganir, R. L., Lacaille, J. C., and McBain, C. J. (2007). Developmental expression of Ca2+-permeable AMPA receptors underlies depolarization-induced long-term depression at mossy fiber CA3 pyramid synapses. *J Neurosci*, 27(43):11651–62.

Hollmann, M. and Heinemann, S. (1994).

Cloned glutamate receptors. *Annu Rev Neurosci*, 17:31–108.

Johansen, T. H., Chaudhary, A., and Verdoorn, T. A. (1995). Interactions among GYKI-52466, cyclothiazide, and aniracetam at recombinant AMPA and kainate receptors. *Mol Pharmacol*, 48(5):946–55.

Ju, W., Morishita, W., Tsui, J., Gaietta, G., Deerinck, T. J., Adams, S. R., Garner, C. C., Tsien, R. Y., Ellisman, M. H., and Malenka, R. C. (2004). Activity-dependent regulation of dendritic synthesis and trafficking of AMPA receptors. *Nat Neurosci*, 7(3):244–53.

Kakegawa, W., Tsuzuki, K., Yoshida, Y., Kameyama, K., and Ozawa, S. (2004). Input- and subunit-specific AMPA receptor trafficking underlying long-term potentiation at hippocampal CA3 synapses. *Eur J Neurosci*, 20(1):101–10.

Kato, A. S., Siuda, E. R., Nisenbaum, E. S., and Bredt, D. S. (2008). AMPA receptor subunit-specific regulation by a distinct family of type ii TARPs. *Neuron*, 59(6):986–96.

Kim, E. and Sheng, M. (2004). PDZ domain proteins of synapses. *Nat Rev Neurosci*, 5(10):771–81.

Kim, M. J., Futai, K., Jo, J., Hayashi, Y., Cho, K., and Sheng, M. (2007). Synaptic accumulation of PSD95 and synaptic function regulated by phosphorylation of serine-295 of PSD-95. *Neuron*, 56(3):488–502.

Klein, R. M. and Howe, J. R. (2004). Effects of the lurcher mutation on GluR1 desensiti-

zation and activation kinetics. *J Neurosci*, 24(21):4941–51.

Koh, D. S., Burnashev, N., and Jonas, P. (1995). Block of native Ca(2+)-permeable AMPA receptors in rat brain by intracellular polyamines generates double rectification. *J Physiol*, 486 (Pt 2):305–12.

Kornau, H. C., Schenker, L. T., Kennedy, M. B., and Seeburg, P. H. (1995). Domain interaction between NMDA receptor subunits and the postsynaptic density protein PSD-95. *Science*, 269(5231):1737–40.

Kott, S., Werner, M., Korber, C., and Hollmann, M. (2007). Electrophysiological properties of AMPA receptors are differentially modulated depending on the associated member of the TARP family. *J Neurosci*, 27(14):3780–9.

Kumar, S. S., Bacci, A., Kharazia, V., and Huguenard, J. R. (2002). A developmental switch of AMPA receptor subunits in neocortical pyramidal neurons. *J Neurosci*, 22(8):3005–15.

Leonard, A. S., Davare, M. A., Horne, M. C., Garner, C. C., and Hell, J. W. (1998). SAP97 is associated with the alpha-amino-3-hydroxy-5-methylisoxazole-4-propionic acid receptor GluR1 subunit. *J Biol Chem*, 273(31):19518–24.

Letts, V. A., Felix, R., Biddlecome, G. H., Arikkath, J., Mahaffey, C. L., Valenzuela, A., Bartlett, F. S., n., Mori, Y., Campbell, K. P., and Frankel, W. N. (1998). The mouse stargazer gene encodes a neuronal

Ca2+-channel gamma subunit. *Nat Genet*, 19(4):340–7.

Li, B., Otsu, Y., Murphy, T. H., and Raymond, L. A. (2003). Developmental decrease in NMDA receptor desensitization associated with shift to synapse and interaction with postsynaptic density-95. *J Neurosci*, 23(35):11244–54.

Lorenz, C., Pusch, M., and Jentsch, T. J. (1996). Heteromultimeric CLC chloride channels with novel properties. *Proc Natl Acad Sci U S A*, 93(23):13362–6.

Lundstrom, K. (2003). Semliki forest virus vectors for rapid and high-level expression of integral membrane proteins. *Biochim Biophys Acta*, 1610(1):90–6.

Mah, S. J., Cornell, E., Mitchell, N. A., and Fleck, M. W. (2005). Glutamate receptor trafficking: endoplasmic reticulum quality control involves ligand binding and receptor function. *J Neurosci*, 25(9):2215–25.

Malenka, R. C. and Nicoll, R. A. (1993). NMDA-receptor-dependent synaptic plasticity: multiple forms and mechanisms. *Trends Neurosci*, 16(12):521–7.

Malinow, R. and Malenka, R. C. (2002). AMPA receptor trafficking and synaptic plasticity. *Annu Rev Neurosci*, 25:103–26.

Meeker, R. B., Swanson, D. J., and Hayward, J. N. (1989). Light and electron microscopic localization of glutamate immunoreactivity in the supraoptic nucleus of the rat hypothalamus. *Neuroscience*, 33(1):157–67.

Menniti, F. S., Chenard, B. L., Collins, M. B., Ducat, M. F., Elliott, M. L., Ewing, F. E., Huang, J. I., Kelly, K. A., Lazzaro, J. T., Pagnozzi, M. J., Weeks, J. L., Welch, W. M., and White, W. F. (2000). Characterization of the binding site for a novel class of noncompetitive alpha-amino-3-hydroxy-5-methyl-4-isoxazolepropionic acid receptor antagonists. *Mol Pharmacol*, 58(6):1310–7.

Menuz, K., Stroud, R. M., Nicoll, R. A., and Hays, F. A. (2007). TARP auxiliary subunits switch AMPA receptor antagonists into partial agonists. *Science*, 318(5851):815–7.

Migaud, M., Charlesworth, P., Dempster, M., Webster, L. C., Watabe, A. M., Makhinson, M., He, Y., Ramsay, M. F., Morris, R. G., Morrison, J. H., O'Dell, T. J., and Grant, S. G. (1998). Enhanced long-term potentiation and impaired learning in mice with mutant postsynaptic density-95 protein. *Nature*, 396(6710):433–9.

Milstein, A. D., Zhou, W., Karimzadegan, S., Bredt, D. S., and Nicoll, R. A. (2007). TARP subtypes differentially and dose-dependently control synaptic AMPA receptor gating. *Neuron*, 55(6):905–18.

Mitchell, N. A. and Fleck, M. W. (2007). Targeting AMPA receptor gating processes with allosteric modulators and mutations. *Biophys J*, 92(7):2392–402.

Monyer, H., Burnashev, N., Laurie, D. J., Sakmann, B., and Seeburg, P. H. (1994). Developmental and regional expression in the

rat brain and functional properties of four NMDA receptors. *Neuron*, 12(3):529–40.

Monyer, H., Seeburg, P. H., and Wisden, W. (1991). Glutamate-operated channels: developmentally early and mature forms arise by alternative splicing. *Neuron*, 6(5):799–810.

Morabito, M. A., Sheng, M., and Tsai, L. H. (2004). Cyclin-dependent kinase 5 phosphorylates the N-terminal domain of the postsynaptic density protein PSD-95 in neurons. *J Neurosci*, 24(4):865–76.

Mosbacher, J., Schoepfer, R., Monyer, H., Burnashev, N., Seeburg, P. H., and Ruppersberg, J. P. (1994). A molecular determinant for submillisecond desensitization in glutamate receptors. *Science*, 266(5187):1059–62.

Nakagawa, T., Futai, K., Lashuel, H. A., Lo, I., Okamoto, K., Walz, T., Hayashi, Y., and Sheng, M. (2004). Quaternary structure, protein dynamics, and synaptic function of SAP97 controlled by L27 domain interactions. *Neuron*, 44(3):453–67.

Nehring, R. B., Wischmeyer, E., Doring, F., Veh, R. W., Sheng, M., and Karschin, A. (2000). Neuronal inwardly rectifying K(+) channels differentially couple to PDZ proteins of the PSD-95/SAP90 family. *J Neurosci*, 20(1):156–62.

Noebels, J. L., Qiao, X., Bronson, R. T., Spencer, C., and Davisson, M. T. (1990). Stargazer: a new neurological mutant on chromosome 15 in the mouse with prolonged cortical seizures. *Epilepsy Res*, 7(2):129–35.

O'Brien, R. J., Kamboj, S., Ehlers, M. D., Rosen, K. R., Fischbach, G. D., and Huganir, R. L. (1998). Activity-dependent modulation of synaptic AMPA receptor accumulation. *Neuron*, 21(5):1067–78.

Ohshima, T., Ogura, H., Tomizawa, K., Hayashi, K., Suzuki, H., Saito, T., Kamei, H., Nishi, A., Bibb, J. A., Hisanaga, S., Matsui, H., and Mikoshiba, K. (2005). Impairment of hippocampal long-term depression and defective spatial learning and memory in p35 mice. *J Neurochem*, 94(4):917–25.

O'Keefe, J. and Dostrovsky, J. (1971). The hippocampus as a spatial map. preliminary evidence from unit activity in the freely-moving rat. *Brain Res*, 34(1):171–5.

Palmer, A. J. and Lodge, D. (1993). Cyclothiazide reverses AMPA receptor antagonism of the 2,3-benzodiazepine, GYKI 53655. *Eur J Pharmacol*, 244(2):193–4.

Partin, K. M., Fleck, M. W., and Mayer, M. L. (1996). AMPA receptor flip/flop mutants affecting deactivation, desensitization, and modulation by cyclothiazide, aniracetam, and thiocyanate. *J Neurosci*, 16(21):6634–47.

Penzes, P., Johnson, R. C., Sattler, R., Zhang, X., Huganir, R. L., Kambampati, V., Mains, R. E., and Eipper, B. A. (2001). The neuronal Rho-GEF kalirin-7 interacts with PDZ domain-containing proteins and regulates dendritic morphogenesis. *Neuron*, 29(1):229–42.

Pickard, L., Noel, J., Henley, J. M., Collingridge,

G. L., and Molnar, E. (2000). Developmental changes in synaptic AMPA and NMDA receptor distribution and AMPA receptor subunit composition in living hippocampal neurons. *J Neurosci*, 20(21):7922–31.

Plant, K., Pelkey, K. A., Bortolotto, Z. A., Morita, D., Terashima, A., McBain, C. J., Collingridge, G. L., and Isaac, J. T. (2006). Transient incorporation of native GluR2-lacking AMPA receptors during hippocampal long-term potentiation. *Nat Neurosci*, 9(5):602–4.

Prange, O. and Murphy, T. H. (2001). Modular transport of postsynaptic density-95 clusters and association with stable spine precursors during early development of cortical neurons. *J Neurosci*, 21(23):9325–33.

Priel, A., Kolleker, A., Ayalon, G., Gillor, M., Osten, P., and Stern-Bach, Y. (2005). Stargazin reduces desensitization and slows deactivation of the AMPA-type glutamate receptors. *J Neurosci*, 25(10):2682–6.

Priel, A., Selak, S., Lerma, J., and Stern-Bach, Y. (2006). Block of kainate receptor desensitization uncovers a key trafficking checkpoint. *Neuron*, 52(6):1037–46.

Rao, A., Kim, E., Sheng, M., and Craig, A. M. (1998). Heterogeneity in the molecular composition of excitatory postsynaptic sites during development of hippocampal neurons in culture. *J Neurosci*, 18(4):1217–29.

Sans, N., Petralia, R. S., Wang, Y. X., Blahos, J., n., Hell, J. W., and Wenthold, R. J. (2000). A developmental change in NMDA receptor-associated proteins at hippocampal synapses. *J Neurosci*, 20(3):1260–71.

Sans, N., Prybylowski, K., Petralia, R. S., Chang, K., Wang, Y. X., Racca, C., Vicini, S., and Wenthold, R. J. (2003). NMDA receptor trafficking through an interaction between PDZ proteins and the exocyst complex. *Nat Cell Biol*, 5(6):520–30.

Schneiderman, J. H., Sterling, C. A., and Luo, R. (1994). Hippocampal plasticity following epileptiform bursting produced by GABAA antagonists. *Neuroscience*, 59(2):259–73.

Schnell, E., Sizemore, M., Karimzadegan, S., Chen, L., Bredt, D. S., and Nicoll, R. A. (2002). Direct interactions between PSD-95 and stargazin control synaptic AMPA receptor number. *Proc Natl Acad Sci U S A*, 99(21):13902–7.

Scoville, W. B. and Milner, B. (1957). Loss of recent memory after bilateral hippocampal lesions. *J Neurol Neurosurg Psychiatry*, 20(1):11–21.

Sekiguchi, M., Fleck, M. W., Mayer, M. L., Takeo, J., Chiba, Y., Yamashita, S., and Wada, K. (1997). A novel allosteric potentiator of AMPA receptors: 4–2-(phenylsulfonylamino)ethylthio–2,6-difluoro-phenoxyaceta mide. *J Neurosci*, 17(15):5760–71.

Shi, S. H., Hayashi, Y., Petralia, R. S., Zaman, S. H., Wenthold, R. J., Svoboda, K., and Malinow, R. (1999). Rapid spine delivery and redistribution of AMPA receptors after

synaptic NMDA receptor activation. *Science*, 284(5421):1811–6.

Sommer, B., Keinanen, K., Verdoorn, T. A., Wisden, W., Burnashev, N., Herb, A., Kohler, M., Takagi, T., Sakmann, B., and Seeburg, P. H. (1990). Flip and flop: a cell-specific functional switch in glutamate-operated channels of the CNS. *Science*, 249(4976):1580–5.

Sommer, B., Kohler, M., Sprengel, R., and Seeburg, P. H. (1991). RNA editing in brain controls a determinant of ion flow in glutamate-gated channels. *Cell*, 67(1):11–9.

Sornarajah, L., Vasuta, O. C., Zhang, L., Sutton, C., Li, B., El-Husseini, A., and Raymond, L. A. (2008). NMDA receptor desensitization regulated by direct binding to PDZ1-2 domains of PSD-95. *J Neurophysiol*, 99(6):3052–62.

Soto, D., Coombs, I. D., Kelly, L., Farrant, M., and Cull-Candy, S. G. (2007). Stargazin attenuates intracellular polyamine block of calcium-permeable AMPA receptors. *Nat Neurosci*, 10(10):1260–7.

Standley, S., Roche, K. W., McCallum, J., Sans, N., and Wenthold, R. J. (2000). PDZ domain suppression of an ER retention signal in NMDA receptor NR1 splice variants. *Neuron*, 28(3):887–98.

Steigerwald, F., Schulz, T. W., Schenker, L. T., Kennedy, M. B., Seeburg, P. H., and Kohr, G. (2000). C-terminal truncation of NR2A subunits impairs synaptic but not extrasy-naptic localization of NMDA receptors. *J Neurosci*, 20(12):4573–81.

Stein, V., House, D. R., Bredt, D. S., and Nicoll, R. A. (2003). Postsynaptic density-95 mimics and occludes hippocampal long-term potentiation and enhances long-term depression. *J Neurosci*, 23(13):5503–6.

Steiner, P., Alberi, S., Kulangara, K., Yersin, A., Sarria, J. C., Regulier, E., Kasas, S., Dietler, G., Muller, D., Catsicas, S., and Hirling, H. (2005). Interactions between NEEP21, GRIP1 and GluR2 regulate sorting and recycling of the glutamate receptor subunit GluR2. *EMBO J*, 24(16):2873–84.

Steiner, P., Higley, M. J., Xu, W., Czervionke, B. L., Malenka, R. C., and Sabatini, B. L. (2008). Destabilization of the postsynaptic density by PSD-95 serine 73 phosphorylation inhibits spine growth and synaptic plasticity. *Neuron*, 60(5):788–802.

Stern-Bach, Y., Russo, S., Neuman, M., and Rosenmund, C. (1998). A point mutation in the glutamate binding site blocks desensitization of AMPA receptors. *Neuron*, 21(4):907–18.

Stoppini, L., Buchs, P. A., and Muller, D. (1991). A simple method for organotypic cultures of nervous tissue. *J Neurosci Methods*, 37(2):173–82.

Sutton, M. A., Ito, H. T., Cressy, P., Kempf, C., Woo, J. C., and Schuman, E. M. (2006). Miniature neurotransmission stabilizes synaptic function via tonic suppression

of local dendritic protein synthesis. *Cell*, 125(4):785–99.

Tarnawa, I., Farkas, S., Berzsenyi, P., Pataki, A., and Andrasi, F. (1989). Electrophysiological studies with a 2,3-benzodiazepine muscle relaxant: GYKI 52466. *Eur J Pharmacol*, 167(2):193–9.

Terashima, A., Cotton, L., Dev, K. K., Meyer, G., Zaman, S., Duprat, F., Henley, J. M., Collingridge, G. L., and Isaac, J. T. (2004). Regulation of synaptic strength and AMPA receptor subunit composition by PICK1. *J Neurosci*, 24(23):5381–90.

Tomita, S., Adesnik, H., Sekiguchi, M., Zhang, W., Wada, K., Howe, J. R., Nicoll, R. A., and Bredt, D. S. (2005). Stargazin modulates AMPA receptor gating and trafficking by distinct domains. *Nature*, 435(7045):1052–8.

Tomita, S., Chen, L., Kawasaki, Y., Petralia, R. S., Wenthold, R. J., Nicoll, R. A., and Bredt, D. S. (2003). Functional studies and distribution define a family of transmembrane AMPA receptor regulatory proteins. *J Cell Biol*, 161(4):805–16.

Tomita, S., Fukata, M., Nicoll, R. A., and Bredt, D. S. (2004). Dynamic interaction of stargazin-like TARPs with cycling AMPA receptors at synapses. *Science*, 303(5663):1508–11.

Tomita, S., Sekiguchi, M., Wada, K., Nicoll, R. A., and Bredt, D. S. (2006). Stargazin controls the pharmacology of AMPA receptor potentiators. *Proc Natl Acad Sci U S A*, 103(26):10064–7.

Tomita, S., Shenoy, A., Fukata, Y., Nicoll, R. A., and Bredt, D. S. (2007). Stargazin interacts functionally with the AMPA receptor glutamate-binding module. *Neuropharmacology*, 52(1):87–91.

Turecek, R., Vlcek, K., Petrovic, M., Horak, M., Vlachova, V., and Vyklicky, L., J. (2004). Intracellular spermine decreases open probability of N-methyl-D-aspartate receptor channels. *Neuroscience*, 125(4):879–87.

Turetsky, D., Garringer, E., and Patneau, D. K. (2005). Stargazin modulates native AMPA receptor functional properties by two distinct mechanisms. *J Neurosci*, 25(32):7438–48.

Turrigiano, G. G. and Nelson, S. B. (1998). Thinking globally, acting locally: AMPA receptor turnover and synaptic strength. *Neuron*, 21(5):933–5.

Valluru, L., Xu, J., Zhu, Y., Yan, S., Contractor, A., and Swanson, G. T. (2005). Ligand binding is a critical requirement for plasma membrane expression of heteromeric kainate receptors. *J Biol Chem*, 280(7):6085–93.

Washbourne, P., Bennett, J. E., and McAllister, A. K. (2002). Rapid recruitment of NMDA receptor transport packets to nascent synapses. *Nat Neurosci*, 5(8):751–9.

Watt, A. J., Sjostrom, P. J., Hausser, M., Nelson, S. B., and Turrigiano, G. G. (2004). A proportional but slower NMDA potentia-

tion follows AMPA potentiation in LTP. *Nat Neurosci*, 7(5):518–24.

Wenthold, R. J., Petralia, R. S., Blahos, J., I., and Niedzielski, A. S. (1996). Evidence for multiple AMPA receptor complexes in hippocampal CA1/CA2 neurons. *J Neurosci*, 16(6):1982–9.

Weston, M. C., Schuck, P., Ghosal, A., Rosenmund, C., and Mayer, M. L. (2006). Conformational restriction blocks glutamate receptor desensitization. *Nat Struct Mol Biol*, 13(12):1120–7.

Williams, S. R. and Mitchell, S. J. (2008). Direct measurement of somatic voltage clamp errors in central neurons. *Nat Neurosci*, 11(7):790–8.

Yamada, K. A. and Tang, C. M. (1993). Benzothiadiazides inhibit rapid glutamate receptor desensitization and enhance glutamatergic synaptic currents. *J Neurosci*, 13(9):3904–15.

Yamazaki, M., Ohno-Shosaku, T., Fukaya, M., Kano, M., Watanabe, M., and Sakimura, K. (2004). A novel action of stargazin as an enhancer of AMPA receptor activity. *Neurosci Res*, 50(4):369–74.

Zerangue, N., Schwappach, B., Jan, Y. N., and Jan, L. Y. (1999). A new ER trafficking signal regulates the subunit stoichiometry of plasma membrane K(ATP) channels. *Neuron*, 22(3):537–48.

Zhang, S., Edelmann, L., Liu, J., Crandall, J. E., and Morabito, M. A. (2008). Cdk5 regulates the phosphorylation of tyrosine 1472 NR2B

and the surface expression of NMDA receptors. *J Neurosci*, 28(2):415–24.

Zhao, J., Peng, Y., Xu, Z., Chen, R. Q., Gu, Q. H., Chen, Z., and Lu, W. (2008). Synaptic metaplasticity through NMDA receptor lateral diffusion. *J Neurosci*, 28(12):3060–70.

Zhou, W., Zhang, L., Guoxiang, X., Mojsilovic-Petrovic, J., Takamaya, K., Sattler, R., Huganir, R., and Kalb, R. (2008). GluR1 controls dendrite growth through its binding partner, SAP97. *J Neurosci*, 28(41):10220–33.

Zhu, J. J. and Malinow, R. (2002). Acute versus chronic NMDA receptor blockade and synaptic AMPA receptor delivery. *Nat Neurosci*, 5(6):513–4.

Ziff, E. B. (2007). TARPs and the AMPA receptor trafficking paradox. *Neuron*, 53(5):627–33.

Zorumski, C. F., Yamada, K. A., Price, M. T., and Olney, J. W. (1993). A benzodiazepine recognition site associated with the non-NMDA glutamate receptor. *Neuron*, 10(1):61–7.

7 Acknowledgments

I would like to thank my supervisor Dr. Valentin Stein for his support and help throughout this project, teaching me all the techniques I used in my study and for patient discussions. I am thankful to all the Stein lab members for a great time in the lab and enjoyable lunch and coffee breaks.

I want to thank to Prof. Tobias Bonhoeffer and all the members of his group for the lovely atmosphere and valuable scientific input on my project. I thank Volker Scheuss for motivating discussions and support. I am thankful to Prof. Walter Stühmer for introducing the world of science to me, his constant support and keeping in touch with me. Thanks to Boehringer Ingelheim Fonds for funding all the conferences and courses I went. Without them many things would not be possible for me.

I owe a lot to Helmut Kessels for his huge support in critical moments of my study, for motivating discussions and teaching me to have fun in what I do. Thanks to Ilka Rinke, Miriam Mann, Nadine Becker, Tara Keck and Judith Artmann for long conversations and support. Thanks to Matthias Traut for being such a great, caring friend, for his everyday help with the experiments, inspiring discussions and making me laugh. Parsimoniously, you made my time in the lab relaxing and enjoyable.

Above all I want to thank to my family for their quiet support and love, and to my friends (Kaca, Viki, Jeca, Jole, Dragana) for sharing happiness and sadness with me.

All my thanks and love to Bojan for his support and patience.

8 Curriculum vitae

PERSONAL DATA

Name	Barbara Cokic
Date of birth	July 13th, 1980
Place of birth	Zajecar, Serbia
Citizenship	Serbian

EDUCATION

09/2005-present	Ph.D. research under the supervision of Dr. Valentin Stein, Max Planck Institute of Neurobiology, Martinsried, Germany
2004-2005	Member of the International Max Planck Research School, Program of Neuroscience, Göttingen, Germany
1999-2004	Undergraduate study in Biology at the University of Belgrade, Serbia. Major subject: Molecular Biology and Physiology
	Diploma thesis research with Prof. Walter Stühmer, Max Planck Institute for Experimental Medicine, Göttingen, Germany: "Imaging of putative EAG potassium channel interaction with calmodulin using FRET microscopy"
1999	High-School Diploma, Negotin Gymnasium, Serbia

GRANTS

2006-2008	Boehringer Ingelheim Fonds Scholarship
2004-2005	International Max Planck Research School Scholarship
1999-2004	Scholarship of Ministry of Science and Technology, Serbia

Publication based on the work in this thesis:

Cokić, B. and Stein, V. (2008). Stargazin modulates AMPA receptor antagonism. *Neuropharmacology*, 54(7):1062-70.